Wesleyan University Astronomy Department

Guiding Light in the Shadow of Distant Worlds: An Autoguider for the 0.6m Perkin Research Telescope

by

Jakob Schaeffer
Advisor: Dr. Seth Redfield

A thesis submitted to the
faculty of Wesleyan University
in partial fulfillment of the requirements for the
Degree of Master of Arts
in Astronomy

Middletown, Connecticut May 2012

Acknowledgements

First and foremost I would like to thank my advisor Seth Redfield who allowed me to play with and investigate topics about which I had no idea and come out the other end much wiser, who helped push me to 'geek out', who allowed me to follow my passions, and whose guidance can never be automated. Thank you for a fantastic two years.

I would also like to thank Miroslaw Koziol for his tireless help building the autoguider connections, repairing the 24" telescope and troubleshooting just about any problem or question I may have had. The autoguider would not be where it is today if it were not for his help. Additionally I would like to thank Dave and Bruce Strickland for building and extending the autoguider and guidescope mounts, along with letting me build a bit in their shop. For the optics used in my fake guide star setup I would like to thank Christina Othon and for the temporary clamp used for the autoguider camera I'd like to thank Vacek Miglus.

In addition, I'd like to thank Roy Kilgard, Ed Moran, Bill Herbst and Adam Jensen for their knowledge, help and joviality over these past two years. It has been a great joy being part of this department; out of this world, stellar even.

I would like to thank my family for all their support over the past two years, along with always checking to make sure I ate well.

A hearty thanks to all my fellow astronomy grad students and basement dwelling undergrads, for your great camaraderie through thin and very thick, in our journey through time and space.

A special thanks to DM (Ariel, Jana, Mark, Carrie, Casey, Alex & Noah) for your creativity, spontaneity, affection, friendship and humor. You have never failed to raise my spirits, expectations and abilities. Thank you for being my first time. Beep.

I would also like to thank all you wonderful people out there in the dark, who have observed for this thesis or otherwise. May the skies be clear and ever in your favor.

And finally, I would like to thank you, dear reader of the near-, regular- or distant future, for taking the time to look over these acknowledgements and this thesis. I hope you find what you are looking for, whether reading this by paper, hologram or hippocampal memory implant.

Enjoy.

"These are some of the things that hydrogen atoms do, given fifteen billion years of cosmic evolution."

—Carl Sagan *Cosmos* 1980

Contents

Acknowledgements **i**

1 Introduction **1**

1.1 Astronomical Observation 1

1.1.1 Guiding 4

1.2 Exoplanets 5

1.2.1 Transits 7

1.3 Observing with the 24" Perkin Telescope 8

1.3.1 A Brief History of Richard S. Perkin and his Telescope . . 8

2 Autoguider: Trials and Tribulations **12**

2.1 Motivation 12

2.2 Initial Testing 13

2.3 Piggy-Back Telescope vs. Pick-Off Mirror 14

2.4 6" Finder vs. New Piggy-Back Telescope 16

2.5 Guide Signals 17

2.6 Drive Hysteresis 20

2.7 Autoguider Flexure: Clamp vs. Unclamped 21

2.8 Ice Crystals 22

2.9 Hour Angle Dependence 23

2.10 Wires and Drift 24
2.11 PhD Guiding vs. MaxImDL 30
2.12 Guide Signals: Revisited 31

3 Autoguider: Final Setup **32**
3.1 Instrument Setup 32
3.2 Instrument Parameters 36
3.3 Final Guiding Precision and Issues 41
3.4 Autoguider Operating Procedure 43
3.4.1 Step-by-Step: Autoguider Operation 44
3.4.2 Troubleshooting 46

4 Exoplanet Transits **48**
4.1 Data Reduction & Analysis 48
4.1.1 Previous Work 48
4.1.2 Current Work 48
4.2 Results: WASP-33b 49
4.2.1 Previous Work 49
4.2.2 Current Work 50
4.3 Other Observed Transits 64

5 Conclusions and Future Work **67**
5.1 Conclusions 67
5.2 Future Work 68

A Autoguider Manual **71**

B Guidescope Manual **83**

C WesTEP Data Reduction & Analysis **87**

C.1 Introduction 88

C.2 Downloading the Data 88

C.3 Reducing the Data 90

C.4 Creating a Normalized Lightcurve 91

C.5 Analyzing the Lightcurve 98

C.5.1 Fitting Multiple Transits 101

C.6 Creating an $O - C$ Diagram 102

C.7 How to Do Other Things 104

C.7.1 Data Formatted for TAP and ETD 104

C.7.2 Renaming Many Files 105

C.7.3 Installing the reduceI script 105

C.7.4 Viewing consecutive images in ds9 106

Bibliography **108**

List of Tables

3.1 Properties of the autoguiding system 38

3.2 Stars in field about M57 41

4.1 Properties of the WASP-33 system 50

4.2 Comments on observed WASP-33b transits for the 2011-2012 observing season 54

4.3 Transits of WASP-33b during the 2011-2012 observing season visible from VVO 63

4.4 Observations of other transits during the 2011-2012 season 65

C.1 Limb-darkening parameters for observed systems 99

Chapter 1

Introduction

Welcome, dear reader, to my thesis. Here I shall discuss two distinct but connected areas of research. One is the implementation of an autoguider for the 24-inch (24" or 0.6m) Perkin Telescope here at Van Vleck Observatory (VVO); the other is looking for timing variations in transits of the exoplanet WASP-33b. Therefore my thesis is split broadly into the areas of observational astronomy and exoplanets, and it is with these general fields of study that I shall begin.

1.1 Astronomical Observation

The field of observational astronomy, in the broadest sense, has been around for millennia, ever since someone decided to look up at the sky and wonder. Across many cultures and epochs people have built a bounty of instruments to calculate, predict and measure the sky. For example astrolabes, armillaries, quadrants and even the simple sundial were all instruments built to codify the heavens (DeVorkin 2002). Despite these many practical, and at times gorgeous, devices people were still stuck using the same fundamental tool: their eye. This instrument, though millions of years old and quite versatile overall, has its limitations in the dark[1] (Freeman 2005). This would all come to change in 1609 when Galileo famously turned his telescope to the sky and began an era of telescopic astronomy in which

[1]The human eye is only able to see down to an apparent visual magnitude of $m_V \sim 6$, a resolution of 1 arcmin and changes slower than 20 Hz (Carroll & Ostlie 2006; Andersen 2006).

we are still engaged. Later, Newton replaced lenses with mirrors and from then it has been a steady march to bigger and better telescopes (Andersen 2006).

A typical rule of thumb in telescope technology is that bigger is better and have as little atmosphere between you and what you want to see. Such rules have brought about telescopes like the 1.0-meter refractor at Yerkes Observatory in Wisconsin[2], the 9.82-meter Keck telescopes on Mauna Kea in Hawaii[3] at an altitude of approximately[4] 1000-meters, the 2.4-meter *Hubble Space Telescope* orbiting at an altitude of 1 million meters (Andersen 2006), the 0.95-meter *Kepler* space telescope which is roughly 10 billion meters from Earth (Koch et al. 2010; Werner et al. 2004), and the upcoming 6.5-meter *James Webb Space Telescope*[5] with a planned distance of about 1 billion meters from Earth.

Even with the ability to launch telescopes into space, much productive research can be done from the ground and there are many interesting and clever ways in which ground-based observatories get their best possible view of the sky. The first major advance in telescope technology, aside from building bigger and higher, was replacing the human eye with photographic film. The first recorded photograph was taken in 1826, with the first one taken through a telescope made in 1842 (Hecht 2001; Andersen 2006). The ability to take extended exposures opened whole new avenues of discovery, allowing observers to see objects much fainter than could ever be detected with the naked eye. Throughout the 19th century and well into the 20th century photographic plates and film reigned supreme. Then in 1969 the charge-coupled device (CCD) was invented and shortly thereafter was put to use for astronomical imaging (Smith 2011; Andersen 2006). Since then the CCD has

[2]http://astro.uchicago.edu/yerkes/

[3]http://www.ifa.hawaii.edu/mko/

[4]For this and the following altitude measures, only precision to the nearest order-of-magnitude is given.

[5]http://www.jwst.nasa.gov/

replaced film as the primary means of astronomical imaging, our observatory is no exception.

With great power comes great responsibility, and as telescopes grew more and more sensitive they also required new technologies to compensate for aberrations which before were too small to be of issue. The first and most fundamental of these was tracking, the ability for a telescope to counteract Earth's rotation and thus stay pointed at the same object in the sky over the course of a night. When simply using one's eye it is not too big an issue to adjust the telescope, however for long exposures it is crucial that the telescope track properly, lest the image be full of star streaks instead of stars. Even so, this tracking is typically not perfect and slight imperfections in the speed of the tracking or the alignment of the telescope can cause a star to drift over the course of an observation. To correct for this an observer would be required to actively keep the telescope pointed precisely at the object of interest. Typically this was done by looking through a second smaller 'guidescope', mounted on and aligned with the primary telescope, and moving the telescopes as necessary to keep the object centered. Later, with the advent of CCDs, people guiders were replaced with autoguiders, instruments which were capable of performing all the guiding corrections automatically. Guiding and autoguiders are discussed further in the next section.

In 1897, the aforementioned Yerkes observatory 1.0-meter refractor became the last major refracting telescope built for research (Andersen 2006). This was due largely to the fact that lenses were becoming so large as to be physically unfeasible to be used in telescopes, along with suffering from issues such as chromatic aberration. In its stead, the lens was replaced with reflecting telescopes which did not suffer from chromatic aberration and did not have the same issues when scaled to large sizes. With tracking issues resolved, the larger and larger size of reflecting

telescopes required and enabled their own types of aberration corrections. For example, active optics are used to slowly change the shape of the primary mirror to counteract gravitational and thermal distortions of the mirror while adaptive optics change the shape of a deformable mirror in the light path to counteract the affects of atmospheric seeing, allowing for extremely high resolution images (Chromey 2010).

1.1.1 Guiding

The basic idea of guiding is simple: stay pointed at exactly the same object or spot in the sky. Easier said than done, guiding has many forms, varieties and nuances, a few of which are discussed here. As mentioned in the previous section, early forms of guiding involved telescope tracking and human guiders, however nowadays the primary means of guiding is through autoguiders. These are typically cameras which provide feedback and automatically guide the telescope to correct its pointing, hence 'autoguider'.

The general form of an autoguider is this: a camera sees a star, if the image of that star moves then the autoguider makes the telescope adjust its pointing to get the star back to its original position. The two major ways in which this is done is either with a separate telescope which 'piggy-backs' on the primary telescope or a pick-off mirror which uses some of the light from the primary telescope for guiding. The piggy-back telescope is advantageous as it can provide a large field-of-view, allowing plenty of guide stars to choose from. However, being mounted on the primary scope means that it must be very sturdy to avoid differential flexure, where due to its changing position in space the body of the primary telescope can flex causing the guidescope and main telescope to become misaligned. The movement

of the either telescope's optics can also cause misalignment between the two. The pick-off guider on the other hand does not have to worry about differential flexure and is typically able to detect smaller motions of the star because it is looking through the primary telescope's optics resulting in a finer platescale. However, because it is only using part of the field-of-view of the primary telescope it may not have many possible guide stars in its field.

Richmond (1990) mentions a key factor in autoguiding: the trade-off between image scale and field-of-view. Image scale is important because the guide camera must be able to reliably detect and correct movement of its guide star small enough that there is no movement seen in the primary telescope. Field-of-view is important because even with an infinitely fine image scale, you must be able to find a bright enough star to guide off of in your starfield of interest. In some ways the piggy-back and pick-off guiders exemplify the trade-off between field-of-view and image scale.

The use of an autoguider is advantageous and is standard fare for any modern observatory, e.g. Keck Observatories[6] and *Hubble Space Telescope*[7], because it allows for longer exposures of the night sky as well as, ideally, reducing the movement of a target to about one pixel, removing any noise which may arise from pixel-to-pixel sensitivity variations.

1.2 Exoplanets

We have known about planets other than our own for thousands of years. Their discovery, exploration and even demotion have captured the attention, imagination and ire of the public. They have often sparked ideas of life and worlds vaguely

[6] http://www.keckobservatory.org/
[7] http://hubblesite.org/the_telescope/nuts_and_bolts/instruments/fgs/

similar, yet wholly different than our own. This notwithstanding, the knowledge and discovery of planets which orbit a star(s) other than our own Sun is a very recent phenomenon.

The first confirmed planet outside of our solar system ('exoplanet') came in 1992 when Wolszczan & Frail (1992) discovered a planet sized body orbiting the millisecond pulsar PSR1257+12. As amazing as this discovery was, there is a bit of an elephant in the room, namely that the search for planets is often and deeply entwined with the search for life in our Galaxy. This pulsar planet, orbiting the throbbing remains of a dead star, would likely be a very foreign locale and if it contained any life at all, it would surely be very different from our own. However, in 1995, not three years later, an announcement came from Mayor & Queloz (1995) about a planet discovered around a Sun-like star. The planet orbited the star 51 Peg, was the size of Jupiter and orbited closer to its star than Mercury does to our Sun. At once this was both relatable and disconcerting. We knew and could relate to what it was like to orbit a Sun-like star, but how a planet the size of Jupiter orbiting closer than Mercury could form was not understood (Mayor & Queloz 1995)[8]. This was among the first steps in the many discoveries made about the nature and variety of planets in our Galaxy. In 2000, the first planet which transited its host star was discovered by Charbonneau et al. (2000). There is much that can be learned from transits, and they shall be discussed in the next section. In 2008, the first direct images of planets orbiting other stars were released by Marois et al. (2008) and Kalas et al. (2008). To date there are over 700 known planets[9] in our Galaxy with current and future missions promising to show us the panoply and variety of planets to whom we are but celestial neighbors. With any

[8]Interestingly, the idea to look for hot Jupiters was briefly suggested by Struve (1952).
[9]http://exoplanet.eu/, accessed 30 Apr 2012

luck we may yet find a twin of Earth or even signs of life, be they similar or wholly different from our own; some company out there in the vastness.

1.2.1 Transits

After Charbonneau et al. (2000) observed the first transiting planet, many new avenues were open for understanding the physical nature of exoplanets. Using only photometry one can discern the ratio of stellar to planetary radius. In addition, if the transits can be observed with precise enough timing, variations of when the transits occur can be measured (Agol et al. 2005; Holman & Murray 2005). These variations, more formally known as 'transit timing variations' (TTVs), if periodic, can be signs of another planet in that system. Currently about 10% of known exoplanet systems have multiple planets (Seager 2011) with NASA's *Kepler* mission having found possible TTVs around ∼11% of its planet candidates (Ford et al. 2011). *Kepler* has conclusively observed TTVs in multiple transit systems (Holman et al. 2010; Lissauer et al. 2011) as well as one with only a single transiting body (Ballard et al. 2011). Transit timing variations have been observed from the ground (Maciejewski et al. 2010, 2011), and even from a telescope the same diameter and model[10] as our very own 24" telescope (Fukui et al. 2011). In addition, TTVs can also be useful in the search for possible moons around exoplanets (Kipping 2009). Finally, from photometry alone one can discern, if observing many transits of a planet, the presence of spots or dimmer regions on the host star (Pont et al. 2007).

Moving away from simple photometry if one can take a spectrum of the system much more can be known. If the spectrum, or at least color, of the star can be observed then the orbital inclination of the planet relative to its host star can be

[10]http://bollerandchivens.com/?page_id=558

inferred via the Rossiter-McLaughlin effect (Gaudi & Winn 2007). Spectroscopy can also reveal the composition of the atmosphere of the planet, by looking for absorption lines in the stellar spectrum during transit, either from space (Charbonneau et al. 2002) or the ground (Redfield et al. 2008).

1.3 Observing with the 24" Perkin Telescope

1.3.1 A Brief History of Richard S. Perkin and his Telescope[11]

Richard S. Perkin (Figure 1.1) was born in Brooklyn, New York on October 17, 1906. At the age of nine Dick received his first telescope, from his father, which he would look through often. Not two years after that, he began building his first telescopes out of cardboard tubes and old glasses lenses. By about age 13 he had ground and polished his own 6" refractor. By this point he had been bitten and smitten with astronomy. Throughout his schooling Dick would hold a fascination with the subject.

In 1936 he went to the Tercentenary Celebration at Harvard where there would be meetings involving amateur and professional astronomers. There he bumped into Charles Elmer, the two had a mutual love of astronomy and agreed on the dearth of optics production in the United States. This spark culminated, after several more meetings with Elmer, in the formation of the Perkin-Elmer Corporation in 1937, which would produce precision optics. In 1941 the company opened a Connecticut plant in Stamford, later it would relocate to one in Norwalk. In

[11]Based on Fahy (1987). Wesleyan's library now has a copy of this text, for those interested in the man whose telescope we now use. The text itself focuses mostly on Dick Perkin in relation to his company.

1949 Dick Perkin moved into a house on over seven acres of land in New Canaan, Connecticut, about an hours drive from Middletown. He would live in this house for the rest of his life.

In 1965 Perkin-Elmer acquired Boller & Chivens, another precision optics company, which he would soon task in building a 24" Cassegrain telescope to his specifications for an observatory he had built on his property[12]. It is this very telescope which we now house at Van Vleck Observatory. Fahy (1987) mentions that the "optics were of such perfection that Dick became the envy of every astronomy enthusiast who had the occasion to use the instrument." In the years leading up to his death in 1969, Dick would use "the telescope to ponder developments in the Milky Way, flights of astronauts into space, probes of Mars and Venus, and the new mysterious quasars and pulsars." (Fahy 1987). The telescope itself was maintained, among others, by a master optician for Perkin-Elmer. A picture of the telescope can be seen in Figure 1.2, sending a laser beam to the Moon in 1968 (a year before anyone landed there!). Interesting things to note in this picture are the step ladder, hand paddle and 6" finder scope which remain in roughly the same condition as they appear there.

After Dick Perkin's death in 1969 he was honored by many. In 1970 the International Astronomical Union (IAU) honored him, Richard Scott Perkin, with an eponymous crater on the far side of the Moon. His company, in 1977 would be selected as the primary contractor for the Optical Telescope Assembly of the *Hubble Space Telescope*, which included the 2.4m (∼8ft) primary mirror[13]. However, most important to us is that in 1971[14], after "Dick's death, the telescope that he had made for the observatory at his New Canaan home was sought by several

[12]http://bollerandchivens.com/?page_id=558
[13]http://hubblesite.org/the_telescope/nuts_and_bolts/optics/optics2.php
[14]http://www.wesleyan.edu/astro/research/facilities.html#24inch

Figure 1.1: A photo of Richard S. Perkin later in life. This same picture is framed in the 24" dome, and may even be the original as written on the back in pencil are the words 'front piece', the very location of this image in the source text. Image from Fahy (1987).

deserving universities. Wanting to keep it as close as possible to New Canaan and Dick's astronomer friends, Gladys [his wife] arranged for the telescope to go to Wesleyan University in Middletown, Connecticut." (Fahy 1987).

Along with the Optical Telescope Assembly, Perkin-Elmer also built the Fine Guidance Sensors on the *Hubble Space Telescope*[15]. So in a nice bit of historical connect-the-dots, the *Hubble Space Telescope*'s autoguiders, essential for its operation, were built by a company founded by a man whose personal telescope I have now equipped with its very own autoguider.

[15]http://hubblesite.org/the_telescope/nuts_and_bolts/instruments/fgs/

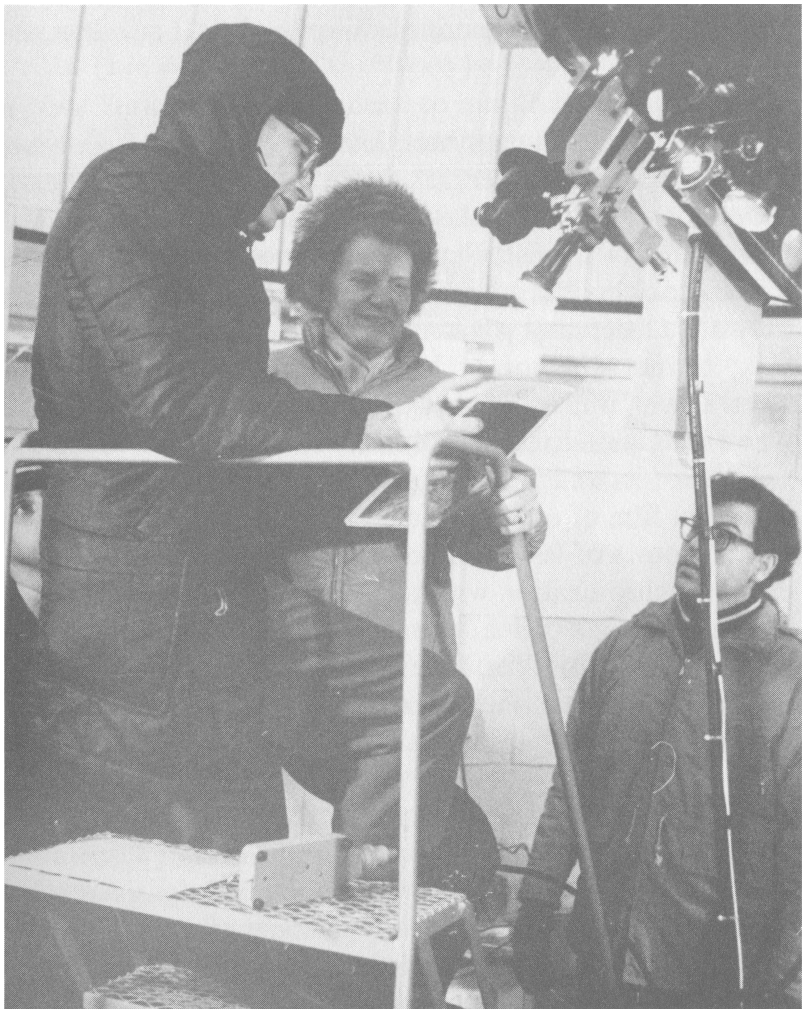

Figure 1.2: "Richard F. Kinnaird and Gladys T. Perkin at the Perkin Observatory, Sending a Laser Beam to the Moon 1968". Image and quoted caption from Fahy (1987). See text for further discussion.

Chapter 2

Autoguider: Trials and Tribulations

In this chapter I shall discuss the many considered possibilities for the setup of our autoguider as well as issues which arose during its testing. The following sections are laid out in chronological order and are intended to lead one from the drawing board to our final autoguider setup, discussed in the following chapter.

2.1 Motivation

It seems natural to begin this discussion of the autoguider with a simple question: "Why does the 24" telescope even need an autoguider?" As with most telescopes, the 24" has various imprecisions in its polar alignment (Johnson 2011) as well as natural imprecisions of the machinery, e.g. tracking speed, slight shifts in the telescope mounting. These imprecisions cause stars to drift and move in the telescope's field-of-view (FOV) over the course of a night. To remedy this, one is required to manually recenter objects. This drift also precludes any single exposures longer than about 20 minutes without noticeable blurring or streaking. For our purposes an autoguider on the 24" would hopefully reduce noise caused by pixel-to-pixel sensitivity variations, resulting in better photometric data for our exoplanetary transits as well as Professor Herbst's stellar variability observations. In addition, this reduced noise could also allow us to observe shallower transits and therefore possibly detect and observe smaller planets. The ability to take

long exposures could be used to look at optical counterparts to X-ray binaries, research currently not able to be done on the 24" due to the imprecision of its tracking (Roy Kilgard, personal communication 2012). For these reasons, some after the fact, it was decided to implement the installation of an autoguider for the 24" telescope.

2.2 Initial Testing

Our first step in the process of the setting up an autoguider was to purchase an autoguiding camera. The autoguider we use, and have since the very start, is an Orion® StarShoot^{TM} Autoguider (Product #52064), see Appendix A, which was received 11 April 2011. This autoguider has both a CCD for detecting the guide stars as well as a port for guide outputs to recenter the telescope, discussed later. The autoguider's camera was initially tested on 16 April 2011 to ensure it worked properly. Attached to the 10" Fiducia telescope, a Schmidt-Cassegrain, the autoguider was moved into the Van Vleck Observatory library and pointed towards Olin Memorial Library, on a particularly overcast day. This produced the autoguider's 'first light', Figure 2.1. This initial image showed that the CCD in the autoguider was working properly, with no major aberrations, technical issues or software problems[1].

Knowing then that the autoguider CCD worked, we had to check that the unit could guide. On the night of 2 May 2011 the autoguider was mounted at the Cassegrain focus of the 16" Schmidt-Cassegrain telescope on the roof of the observatory. The 16" has a guide port which is designed specifically for this type of autoguider output, and vice versa. That night it was able to guide off of Arcturus

[1]PhD Guiding was the software interface initially used with the autoguider.

and Saturn. To ensure that the guiding was actually working, the guide star (or planet) was displaced from its initial position using the telescope's hand paddle. I was then able to see (and hear) the autoguider return the guide star back to its initial position.

These two tests confirmed that the autoguider we had was working properly. It could see guide stars and use them to recenter a telescope. Now that we had the autoguider, it was time to decide how to mount it on the 24" telescope.

2.3 Piggy-Back Telescope vs. Pick-Off Mirror

It was decided quite early on to mount the autoguider on a piggy-back telescope instead of a pick-off mirror for one main reason, field-of-view. With the 24" telescope's CCD having an approximate FOV of $11.6' \times 11.6'$ (Konon 2008), a pick-off mirror of this would likely have had an even smaller field of view. As mentioned earlier, the smaller the field-of-view the more difficult it is, on average, to find a sufficiently bright guide star (Richmond 1990). Therefore it was decided to use a piggy-back scope for its ability to have a larger FOV than the 24" telescope, allowing for a higher chance of always having a sufficiently bright guide star in view; it would also allow us to use the guidescope as a digital finderscope affording a larger view of the sky from inside the warm room.

With the decision made to mount the autoguider on a piggy-back scope, the next step was to consider whether to use the existing 6" finderscope on the 24" or buy a new telescope.

Figure 2.1: First light for the autoguider. Viewing a potted plant outside Olin Memorial Library from inside the Van Vleck Observatory Library using the autoguider attached to a 10" Schmidt-Cassegrain telescope.

2.4 6" Finder vs. New Piggy-Back Telescope

To see whether the 6" finderscope would work for our autoguider, I began by determining its field-of-view. On 22 April 2011, I placed the autoguider in the focal plane of the 6" finder scope (sans eyepiece), which is mounted on the 24" telescope. The FOV of the autoguider in the 6" was about $13' \times 16'$ as determined via imaging of Mizar A and B, Figure 2.2.[2] This FOV, barely larger than that of the 24" CCD, was not large enough that it would provide a significantly larger view of the sky than a pick-off mirror. We likely could have achieved a larger FOV by using a proper array of lenses with the 6" finderscope (as well as a proper focus, cf. Figure 2.2). However, the design, creation and assembly of such an array would have been much more hassle and possibly more cost than just buying a new telescope which fit our needs. Therefore it was decided that we would buy a new telescope to mount on the body of the 24" telescope for use with the autoguider.

The new piggy-back telescope eventually chosen and used in the final setup was an Orion® Deluxe 100mm f/6 Refractor (Product #7338), see Appendix B. This telescope, hereafter known as the 'guidescope', was chosen because its aperture was very close to that of the 6" ($\sim$150 mm) finderscope. This similarity in aperture size meant that very little was being lost in terms of light gathering ability. The guidescope was also higher speed than the 6" (f/6 v. f/10), which meant it could provide a larger field-of-view. The guidescope also has a limiting optical magnitude of 12.6 mag, as given by the manufacturer, which generally should provide enough guide stars in view even with a FOV of $10' \times 10'$ (Richmond 1990). The use of a CCD will likely push this limit to even dimmer stars, see the

[2] Because the angular distance between Mizar A and B is known one can physically measure their distance on the image and determine how this compares to the full measurements of the CCD's field-of-view.

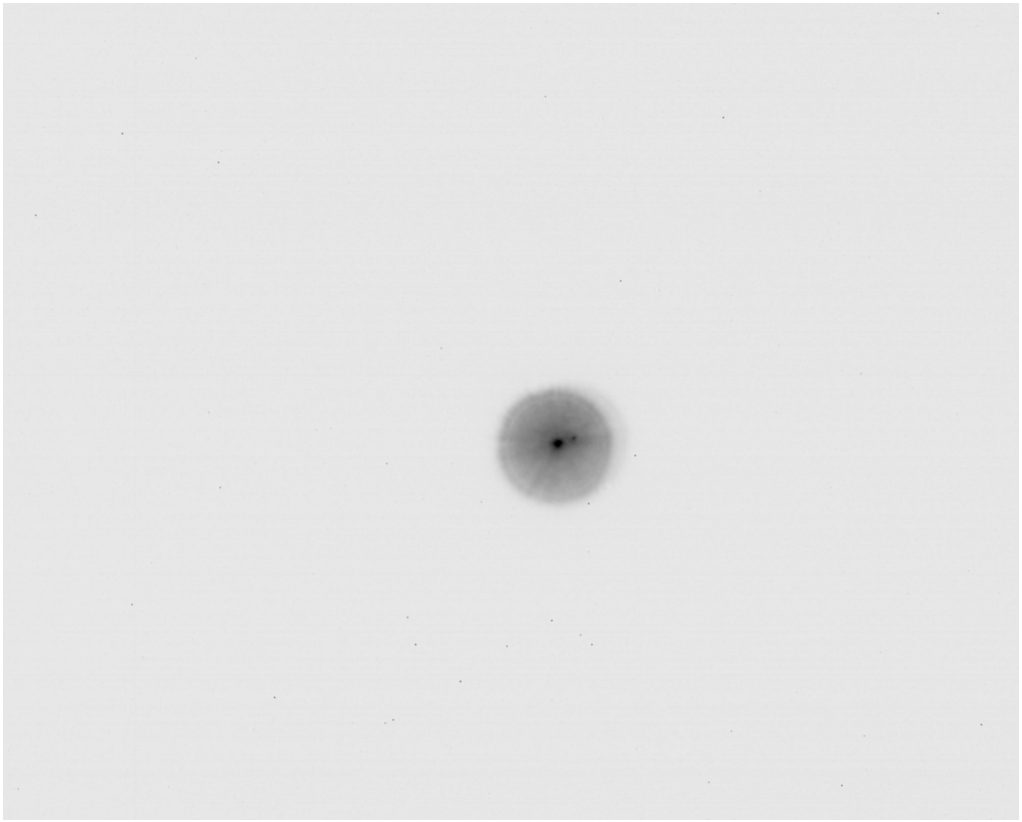

Figure 2.2: Mizar A and B as seen with the autoguider attached to the 6" finderscope. The haze around Mizar A and B is due to the autoguider only being near, not exactly in, the focal plane of the 6". Out-focus required in order to fully focus image. Angular distance between Mizar A and B is $\sim 14''$ (Levy & O'Byrne 2002).

next chapter for the observational results.

With the guidescope and autoguider now chosen, it was time to determine a way for the autoguider to communicate its drive signals to the 24" telescope.

2.5 Guide Signals

Due to the large age difference between the 24" telescope and our autoguider, about 45 years, there was no ready way to connect the two. My non-expertise in electronics and inexperience with the specific circuitry of the 24" telescope

necessitated the assistance of Miroslaw Koziol (Senior Electronics Technician for the Scientific Support Services at Wesleyan University) to determine a means by which the autoguider and 24" telescope could communicate.

The first thing we needed to know was the specific means by which the autoguider sent its guide signal, i.e. what is the voltage of a given guide pulse and is the signal intensity represented by a change in the pulse voltage or its length. In order to measure and test this in a situation similar to our night sky, our guidescope/mount not yet ready, I created a fake guide star assembly, Figure 2.3. In this setup a white-light LED ($\leq$3 W) was used as an illumination source and was pointed perpendicular to the aperture of the autoguider's CCD. Some of the light was led to the autoguider using a plastic fiber optic ($\sim$0.07 cm diameter) from a toy. This arrangement helped to reduce stray light and produce as distinct and clean a point source from the fiber optic as possible. The light was then focused onto the autoguider's CCD using a $\sim$2 cm focal length plano-convex lens. All of this was done in the 24" dome with a cardboard box covering the assembly to reduce ambient light levels and not overexpose the autoguider CCD. This testing was done on 27 June 2011 and the resulting images are shown in Figure 2.4. Guide outputs were checked by gently moving the fiberoptic tip and both listening in the dome for the 24" telescope drive motors as well as observing the movement of the telescope as measured on the warm room control box counters. This testing allowed Mr. Koziol to observe what specific form of signal was used for the drive motors of the 24" telescope, and also that the autoguider outputs responded appropriately for a given displacement of the guide star.

The next day, 28 June 2011, the autoguider was mounted to the 24" telescope and we could begin guiding off the real night sky.

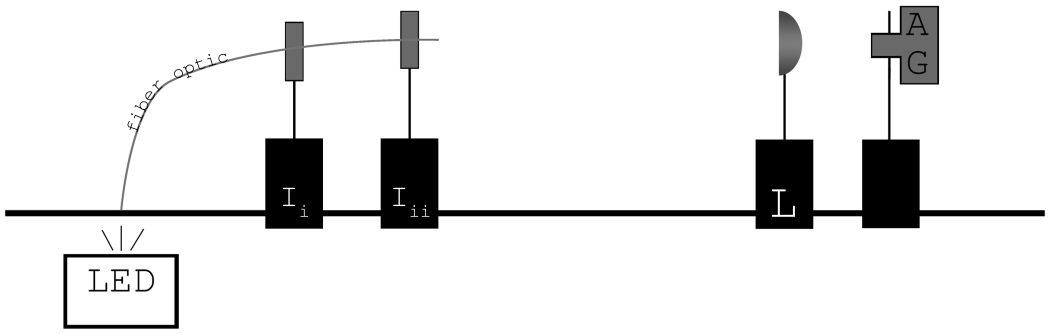

Figure 2.3: A white LED headlamp ($\leq$3 W) was used to illuminate a fiber optic ($\sim$0.07 cm diameter) held by two small irises (I_{i-ii}). Light from the fiber optic was focused onto the autoguider (AG) using a $\sim$2 cm focal length, plano-convex lens (L). The irises, lens and autoguider were all mounted on an optical rail. The distance from the fiber optic tip (I_{ii}) to the autoguider (AG) was $\sim$6.5 cm, with the total apparatus $\sim$15 cm in length.

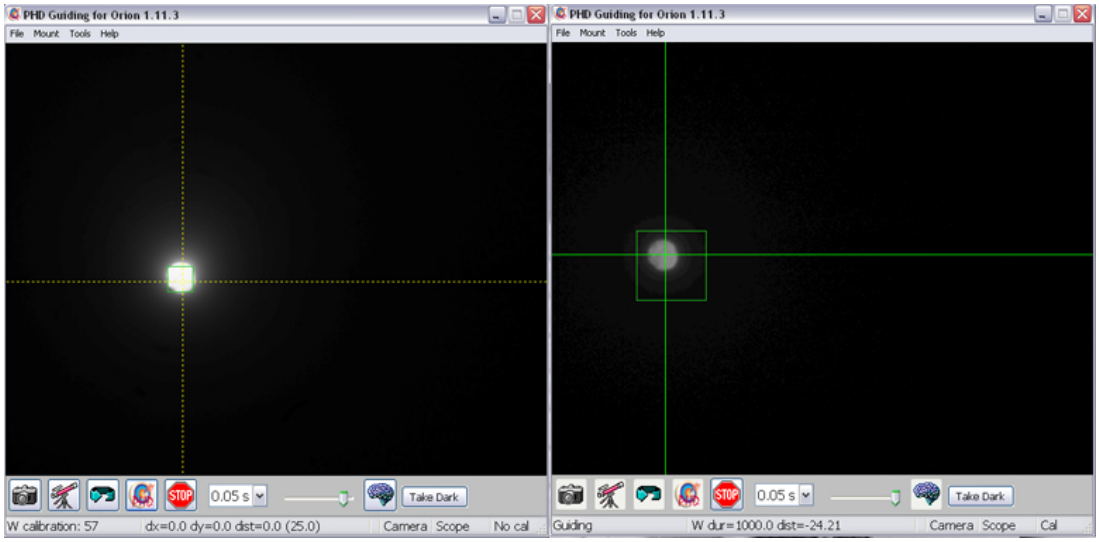

Figure 2.4: *Left*: The autoguider calibrating off the fake guide star, i.e. fiber optic; exposure of 0.05 sec with gain of 5%. *Right*: Guiding off the fake guide star; exposure of 0.05 sec with gain of 0%.

2.6 Drive Hysteresis

With the autoguider and guidescope mounted and working for some time, there was still significant drift seen when observing the sky, even with the autoguider enabled. One possible culprit might have been drift caused by drive signals which were slightly delayed in starting or ending, resulting in an under- or over-shot guide star. Another was hysteresis or backlash in the gears when changing from one direction to another. In order to test these I observed stars by eye through the 24" telescope using an eyepiece with illuminated reticle and carefully watched the stars move using the hand paddles at 'guide' speed. This took place on the night of 9 July 2011 using targets of varying hour angle. In declination I found a delay of approximately 1 second when changing directions, regardless whether north to south or vice versa. In addition there was no detectable delay going from north to north or south to south. In right ascension (RA) there was a drift seen eastward after I had been moving in that direction for a bit; no such drift seen when going westward. This eastward drift lasted on average 1.5 ± 0.2 seconds after I released the hand paddle button. If this drift occurred at the same speed as 'guide' mode ($0.06''$/sec, from 24" Instruction Manual) then it would correspond to a drift of about 15 ± 2 pixels eastward, cf. Figure 2.7–2.8. This drift in RA was found to not be related to a balancing issue with the telescope in RA, as the same eastward drift was still seen when the telescope was intentionally unbalanced so as to make it heavier in the westward direction.

It was determined that even though there may be these drifts and hystereses, the autoguider should correct for them by moving back if overshot or, if undershot, moving until backlash had cleared and movement resumed. Therefore, in theory there should be no net drift from these sources alone, so there was probably

another cause of the observed drift. The next step was to check the autoguider assembly for any flexure.

2.7 Autoguider Flexure: Clamp vs. Unclamped

While it seemed that the drive hysteresis should not contribute to the drift we observed, it was found that the autoguider camera was, in fact, able to flex relative to the guidescope, causing some significant observed drift. This was discovered by having the 24" guide on a target (for sets of 30 $\times$ 1 sec exposures) while the autoguider camera was gently tapped, pushed and moved by hand, in each the N-S and E-W direction. It was found that the perturbations of the autoguider camera caused significant drift in the observed stars, Figure 2.5. A clamp to stabilize the autoguider camera was made, at first temporarily with a clamp and claw borrowed from Vacek Miglus (Lab Technician/Curator for Wesleyan U. Physics Department) to show proof of concept, before having the machine shop build a proper extension to our mount. The proof of concept claw reduced the observed drift by half, Figure 2.6. The machine shop then made a proper extension and clamp to hold the autoguider camera and the autoguider was placed in its new extended mount on 18 Aug 2011, see Figure 3.2. With the new mount the drift showed the same reduction as the proof of concept clamp, i.e. reduction by a factor of 2. With the new mount, similar lean and tap tests were done, and no significant movement of the guide star was observed. It should also be noted that the focusing knob on the autoguider telescope had to be temporarily removed in order for the scope to fit into its new mount, it was properly put back on when the guide scope was in place.

However, even with this issue resolved there was still drift observed. I decided

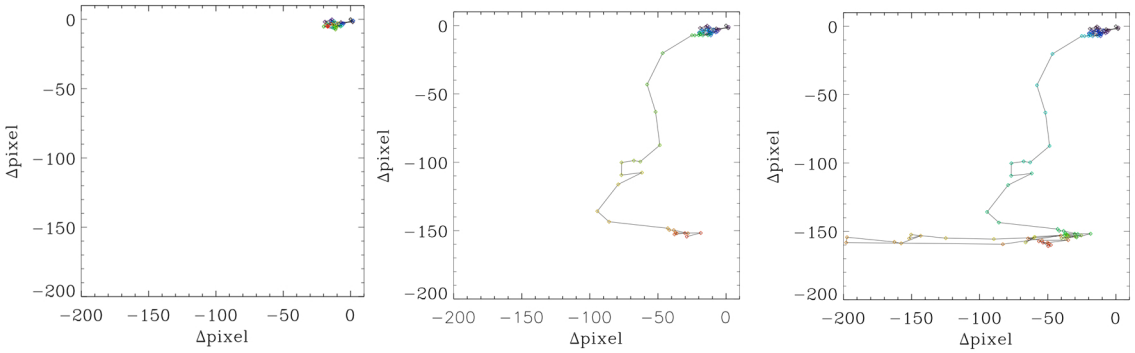

Figure 2.5: *Left*: A control exposure showing the movement of a guide star in the 24" CCD when the autoguider camera was not touched. Collection of 30 × 1 sec exposures. The order of exposures is shown in color: purple is earliest and red the latest. *Center*: The same set of exposures as the left image now with an additional 30 × 1 sec exposures where I gently pushed and tapped against the autoguider camera in the N-S direction. Color scheme is the same as before. *Right*: The same set of exposures as the previous two images now with an additional 30 × 1 sec exposures where I gently pushed and tapped against the autoguider camera in the E-W direction. Color scheme is the same as before.

then to see if there was any correlation between the remaining drift and the hour angle of the telescope, maybe a hint at possible differential flexure between the telescopes.

2.8 Ice Crystals

A brief, but important side note: though not directly involved with the autoguider it is worthy to note a recurring issue with the 24" CCD which had resurfaced. Over the course of the summer ice crystals formed most nights in the 24" telescope's CCD when it was cooled down. This is a recurring problem which has happened several times, even since the CCD's installation (Konon 2008). This time the CCD was sent to Apogee to be fixed in early September 2011. It was returned and reinstalled on the 24" telescope on 14 Oct 2011.

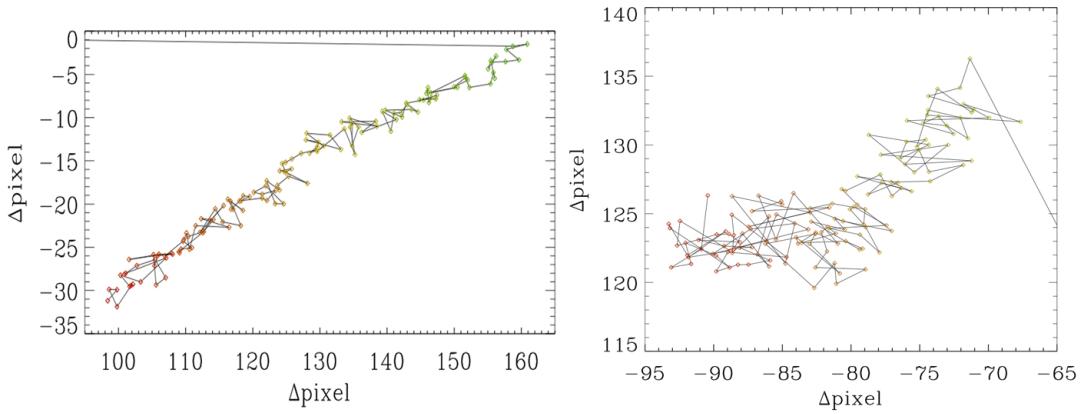

Figure 2.6: *Left*: A one hour observation with the autoguider camera unclamped as it had been from the start. *Right*: The same as the left image though now with the autoguider camera clamped. Notice the drift gets cut in half. Color code: green/yellow is earlier in the observation; red is later.

2.9 Hour Angle Dependence

With drift still seen even after the autoguider camera was clamped, the dependence of drift on the telescope's hour angle was examined. Using one hour increments of time, the drift was observed for all data taken using similar, if not identical, autoguider parameters at varying hour angles, Figure 2.7–2.8. Drifts were measured by averaging the position of the first and last 10% of the points in an observation, and then taking their difference. A drift of zero would imply no movement in the average position of the star over the course of an hour. What was found was that targets seemed to drift in the westward direction an average of about 10 pixels per hour, Figure 2.7, while drifting from 15 pixels per hour northward at low hour angle to 15 pixels per hour southward at high hour angle, with roughly zero pixel per hour drift in declination near the meridian, Figure 2.8.

For right ascension, there does not seem to be any large or distinct relation between hour angle and drift, as it remains fairly constant through a wide range

of hour angles. In declination however, there is a distinct correlation between hour angle and drift. For declination, as the telescope points more westward it drifts more southward. Good examples of this drift are the observations taken at declinations +14° 15m 45s and +89° 16m, where both sets of observations are roughly 7.5 hours each and together span an hour angle range from –4 to 4, where negative hour angles are east of meridian and positive are west. It should be noted that even over a declination range going from +07° to +89° the observations all seem to follow the same aforementioned trend, ruling out any major declination relation to drift.

The spread as a function of hour angle was also measured, Figure 2.9–2.10. The spread was calculated by taking the standard deviation for the first and last 10% of points for each hour long observation, then averaging them. A spread value of zero would imply that the star never moved from a given pixel. No major trends were seen as a function of hour angle in either right ascension or declination. Both coordinates showed an average spread of about 1 pixel. This is likely a bit of an underestimate due to only sampling the first and last tenth of each hour observation chunk, however this sampling helps to eliminate any confounding factors due to drift. For comparison, the average seeing at VVO is about 3″, and the 24” telescope has a plate scale of about 0.34″/pixel (Konon 2008).

2.10 Wires and Drift

Because the aforementioned drift, especially in declination, seems to be affected by hour angle it was considered that maybe the additional weight of wires hanging from the back of the telescope could cause a movement in the pointing

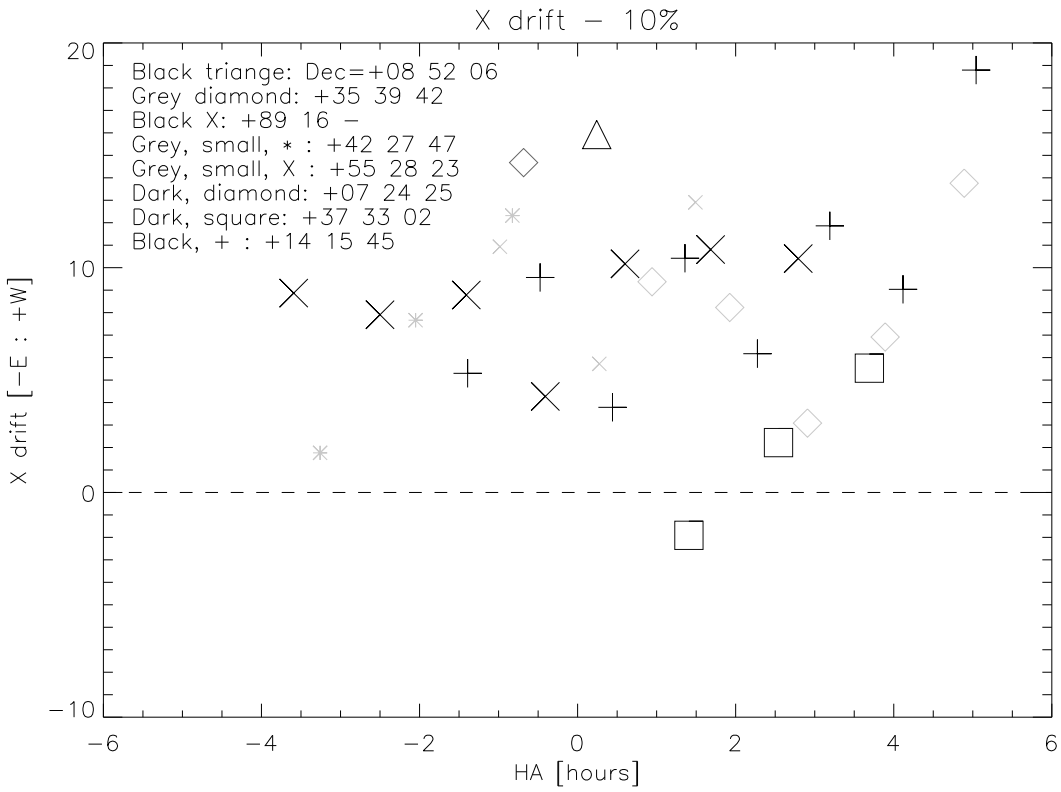

Figure 2.7: Drift seen in RA as a function of hour angle. Negative hour angles correspond to east of the meridian, positive correspond to west. Drift measured from first and last 10% of data points in a given hour of observation. Black points have identical autoguider settings in the software; grey points have settings similar, but not identical, to the black points.

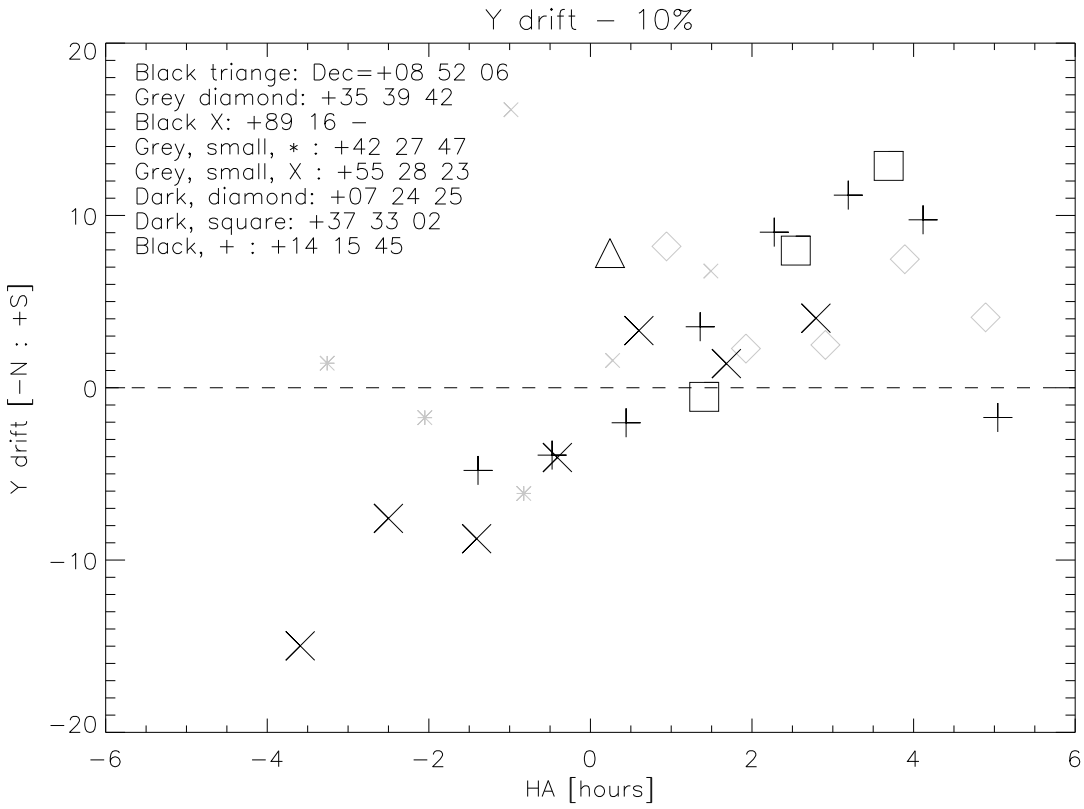

Figure 2.8: Drift seen in declination as a function of hour angle. Negative hour angles correspond to east of the meridian, positive correspond to west. Drift measured from first and last 10% of data points in a given hour of observation. Black points have identical autoguider settings in the software; grey points have settings similar, but not identical, to the black points.

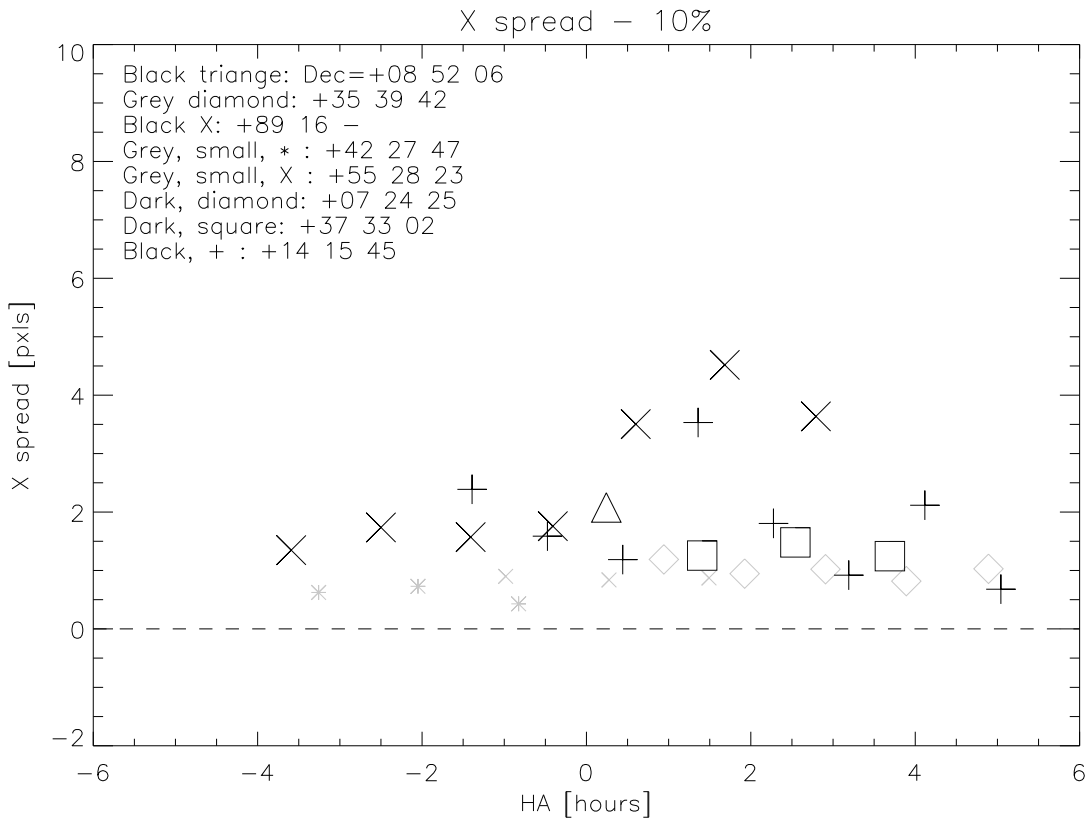

Figure 2.9: Spread seen in RA. Spread measured from first and last 10% of data points in a given hour of observation. Negative hour angles correspond to east of the meridian, positive correspond to west. Black points have identical autoguider settings in the software; grey points have settings similar, but not identical, to the black points.

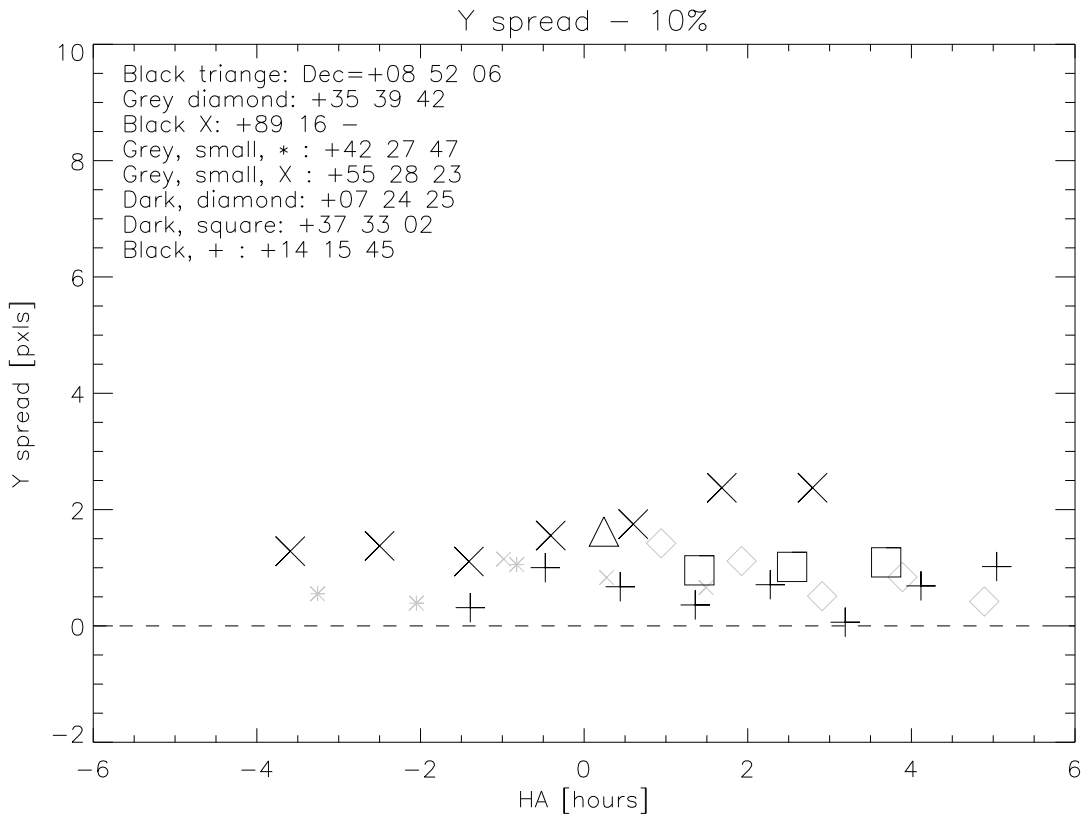

Figure 2.10: Spread seen in declination Spread measured from first and last 10% of data points in a given hour of observation. Negative hour angles correspond to east of the meridian, positive correspond to west. Black points have identical autoguider settings in the software; grey points have settings similar, but not identical, to the black points.

of the telescope or even differential flexure of the 24" and autoguider telescopes. Therefore on the night of 20 March 2012 several sets of 30 images were taken, about five minutes per set, with no autoguiding. For one set the telescope was not touched and was allowed to operate as normal, for the other set the weight of the wires beneath the telescope were adjusted during observation. This adjustment was done by removing and putting back the hand paddles, clustering the hand paddles on one hook, lifting the bulk of the wires connected to the telescope up towards the bottom of the scope, resting the dead-weight of my arms on the wires. These adjustments to the weight of the wires showed distinct influence on the pointing of the telescope, Figure 2.11.

With the weight of the wires being a possible cause of drift in our observations, on the night of 22 March 2012, the hand paddles were placed on the removable ladder and the remaining wires that hang off from the bottom of the 24" telescope were supported and zip-tied to the rolling ladder in the dome so that as the telescope observed for $\sim$3 hours that night, the weight of the wires which the telescope had to support would not change, as determined by hand. However, even with the wires well supported and the telescope not having to pull or move any additional weight of wires as it tracked across the sky, the same type of drift as before was still observed. Therefore it seems that the changing weight of wires as the telescope tracks across the sky does not influence the long term drift we had been observing, even though short timescale adjustments to the weight of the wires do disturb the telescope's pointing.

The changing weight of wires not being an issue, it was decided to check if the software used for guiding might be causing or influencing this drift.

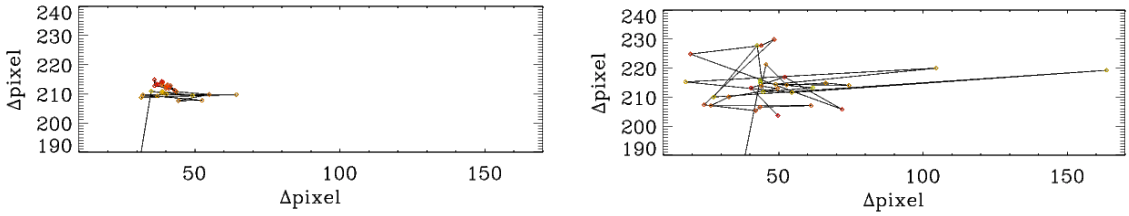

Figure 2.11: Movement of Pollux during consecutive ∼5 minute observing sets with no autoguiding. *Left:* No adjustment of wiring. *Right:* Adjustment of wiring.

2.11 PhD Guiding vs. MaxImDL

With this drift still persisting it was decided to see if the software used might be a factor. Therefore on several nights in March 2012, I used MaxImDL to guide the 24" telescope, whereas before PhD Guiding was the only software used. In these observations the same type of drift was seen. Additionally a displacement in the guide star after calibration, namely more south and west of the original start location, was seen in both programs, and had been seen in PhD since we started using it. With both showing similar issues in drift and calibration displacement, I chose to switch to MaxIm DL as it better integrates the guiding with the taking of data images, as the 24" CCD uses this software. In addition it has many more adjustable parameters for the autoguider, e.g. backlash time added to each guide pulse if guiding switches directions.

With it found that the observed drift and calibration displacements were independent of software used, it can be stated that these issues are likely not a software based one but instead a mechanical or electronic one, the latter of which was tested next.

2.12 Guide Signals: Revisited

With the observed drift being independent of software it was decided to recheck the signals being sent to the telescope by the autoguider. This was done to ensure that each signal being sent from the autoguider was equal for each direction in both RA and Dec and that uneven guide pulses were not causing the observed drift. On 10 April 2012, with Mr. Koziol, the autoguider pulse lengths were tested in both MaxIm DL and PhD Guiding. Using the manual guide modes in each, pulses of a given length were sent to the telescope and observed in the electronics. The lengths programmed to be sent by PhD guiding did not match those observed in the electronics, therefore we switched to using MaxIm DL where the lengths did match. It was shown that the pulse lengths sent in all directions of RA and Dec (i.e. north, south, east, west) were equal. In other words if Maxim DL was told to send a 1 second pulse then a 1 second pulse was observed in the electronics regardless of which direction the telescope was moved.

Therefore it seems that this drift and calibration displacement issue is neither software nor electronics based but instead is based in the mechanics and electro-mechanical interfaces of the 24" telescope. These mechanical problems can be expensive to fix and may not be able to be remedied directly.

Chapter 3

Autoguider: Final Setup

With some longterm drift issues still remaining I lay out here the current state of the autoguider, some technical specifications, details on remaining issues and instructions on its use.

3.1 Instrument Setup

The current arrangement of the autoguider is shown in Figure 3.1–3.3. The guidescope rests in two ring mounts each with three equally spaced mounting screws holding it in place; a third ring mount, with equally spaced screws, holds the autoguider camera in place. The mount itself is bolted to the side of the 24" telescope tube near the guidescope ring mounts, with a region wrapping around the base weights of the 24" telescope held in place by set screws to stabilize the autoguider ring mount, Figure 3.2. The autoguider camera is connected to the guidescope via a metal focal extension and adapter (1.25" to 2"). All focus screws on the telescope and those in the ring mounts were fully tightened to ensure minimal movement or shifting of the guidescope assembly. The autoguider is connected via USB to the computer in the 24" dome and by an RJ-12 cable to the telescope via the warm room control box, see Figure 3.3. The autoguider functions, in a basic sense, as follows: the autoguider takes an image of a star, this image is sent to the computer where the software determines whether it has moved

Figure 3.1: The final setup of the autoguider.

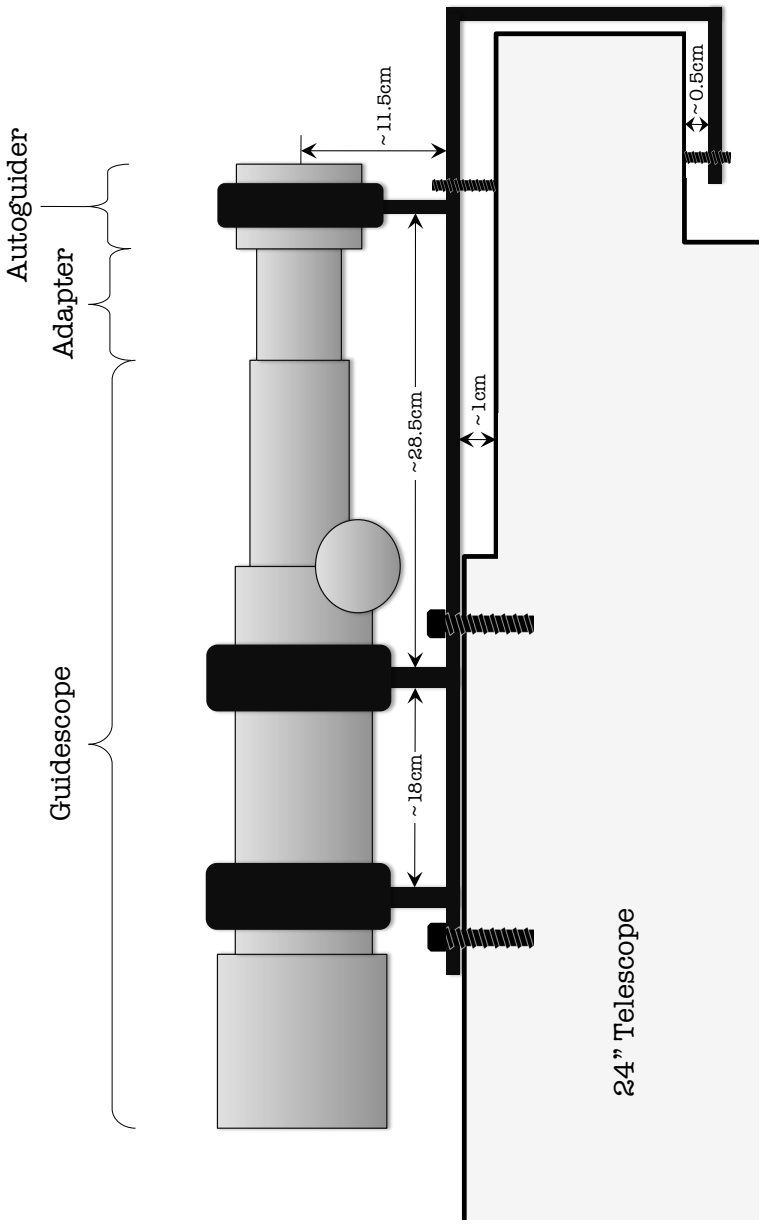

Figure 3.2: The final setup of the autoguider and guidescope. The aperture of the 24" telescope is to the left in this image. Two ring mounts each with three equally spaced set screws in them hold the guidescope in place, a third ring mount with three equally spaced set screws also holds the autoguider camera in place. Two set of bolts near the guidescope ring mounts hold the entire mount to the 24" telescope body. Two pairs of set screws near the autoguider ring mount prevent the mount from flexing or moving at that end. From the tip of the guidescope to the end of the autoguider camera is about 66 cm, or about 2 ft 2 in.

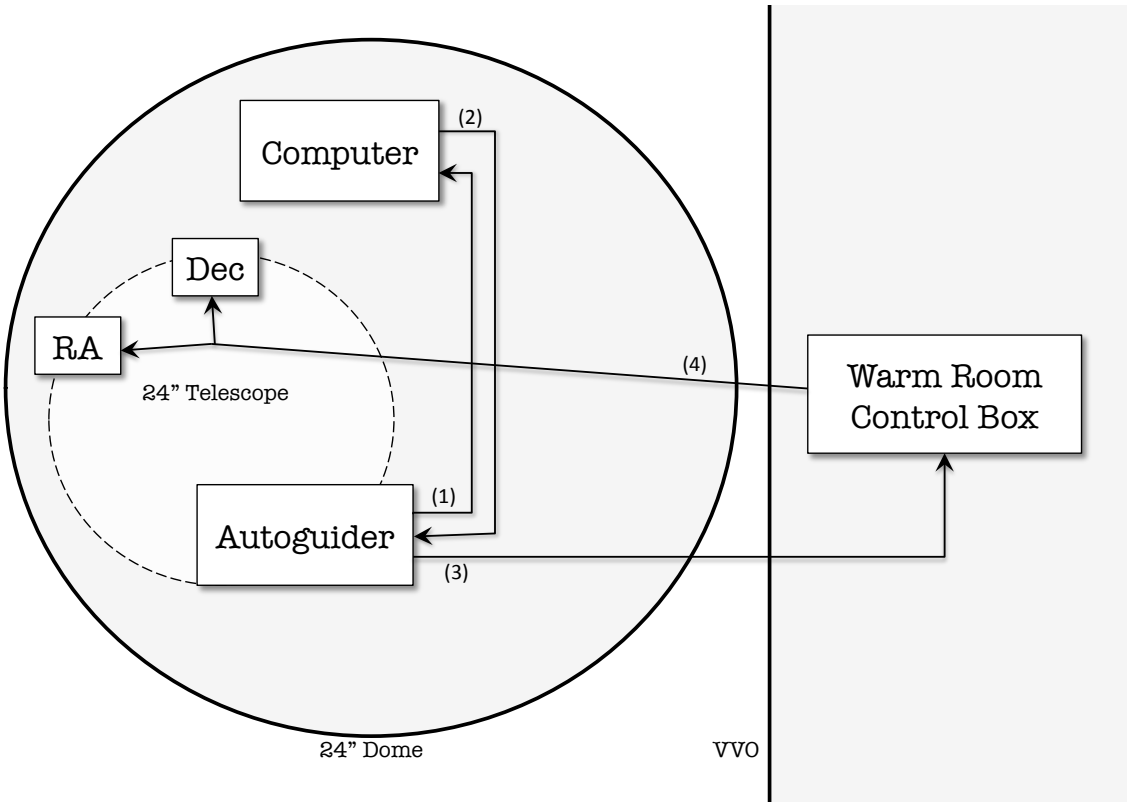

Figure 3.3: A general schematic of the autoguider connections. 1) The autoguider camera observers a star then sends the image to the computer. 2) The computer determines the star's position and whether guide signals need to be sent to adjust the telescope. 3) If necessary, the autoguider sends its guide signals to the warm room control box which then 4) sends signals to the 24" telescope's RA and Dec motors to adjust the telescope. Note: Steps 1) & 2) are done through a single USB connection to the computer.

from its initial position. If it has not then no action is taken, on the other hand if the star has moved from its initial position then the computer tells the autoguider to send out appropriate guide pulses to recenter the star. The autoguider then sends these pulses to the warm room control box where signals are sent to the 24" telescope's RA and Dec motors which adjust the telescope so as to recenter the star. This operation is diagramed in Figure 3.3. The autoguider camera is aligned with the 24" telescope's CCD. In both cameras, as seen in MaxIm DL, up is north, left is east, down is south, right is west. In other words, vertical motion of the star in both CCDs corresponds to movement in declination while horizontal motion corresponds to movement in right ascension.

3.2 Instrument Parameters

An overview of parameters for the autoguiding system can be found in Table 3.1. The field-of-view of the autoguider, through the guidescope, was first estimated to be about $30' \times 30'$ using the full Moon, Figure 3.4. The full Moon is about $30'$ in diameter (Levy & O'Byrne 2002), therefore since nearly all of it fits in the field-of-view, we can roughly estimate that the size of the autoguider field-of-view is about $30'$ on a side, a bit larger horizontally (RA) and a bit smaller vertically (Dec). This estimate was later refined, and the field-of-view along with plate scale of the autoguider CCD was more properly determined using two sets of stars with known angular separation, Figure 3.5 and Table 3.2. The starfield about M57 was chosen because, due to the Ring Nebula, it was unique and easy to identify. The angular distance between each set of stars was calculated using the GCIRC utility in the IDL library, with coordinates from SIMBAD[1]. A physical scale was

[1]SIMBAD (Set of Identifications, Measurements and Bibliography for Astronomical Data): http://simbad.u-strasbg.fr/

then made where the angular distance between each star pair was converted into a physical length, as measured on a printout of this field with a ruler, giving a measure of mm/arcsec. To get the field-of-view from the physical length, each side was measured and then converted into an angular quantity. This technique yielded a field-of-view of $37.7' \times 28.9'$, in agreement with the initial estimate made with the Moon (Figure 3.4). Dividing by the amount of pixels on each side of the detector (Table 3.1) gave a vertical and horizontal plate scale, which were then averaged to give an overall plate scale of $1.73''$/pixel.

Now with the amount of sky that the autoguider can see determined, let us see if this is sufficient to observe, on average, three to five stars, as suggested by Richmond (1990). From the labeled stars in Figure 3.5 we can see stars down to a magnitude of nearly $m_V \approx 13$. The box in Figure 3.5 shows the autoguider able to lock on to a guide star of magnitude $m_V = 11.56$. Allen (1973) gives the number of stars brighter than a given magnitude for a certain field-of-view[2] at certain galactic latitudes, as well as an average count over all galactic latitudes. Using the autoguider's field-of-view for stars $m_V \leq 11.0$ there are about 16 stars visible at the Galactic equator, about three (3) at the Galactic poles and about seven (7) stars on average over all Galactic latitudes. This is a fairly conservative estimate since it has already been shown that the autoguider can lock onto a star dimmer than $m_V = 11.0$. In addition, the image (Figure 3.5) was taken during a full Moon so less moonlight may allow the autoguider to lock on to dimmer stars. For comparison, the number of stars visible in the autoguider's field-of-view for $m_V \leq 12.0$ is about 46 stars at the Galactic equator, seven (7) at the Galactic poles and 17 stars on average over all Galactic latitudes (Allen 1973). Averaging

[2]Allen (1973) provides star counts for one square degree, so the counts that I use are scaled to match our field-of-view: $\frac{\text{autoguider FOV}}{\text{1 sq. degree}} = \frac{37.7' \times 28.9'}{60' \times 60'} \approx 0.302$.

Table 3.1. Properties of the autoguiding system

Field-of-view	$37.6' \times 28.9'$
Plate scale	$1.73''$/pixel
CCD dimensions	1280×1024
Guidescope aperture & speed	100 mm, f/6
Avg. No. Stars Visible ($m_V \leq 11.5$)	~ 12
Current Drift	∼10 pxls/hr north & east

Note. — Further information on the autoguider and guidescope can be found in Appendix A and B, respectively.

the star counts for these two magnitudes, I can interpolate to get the star counts for $m_V \lesssim 11.5$: about 31 stars at the Galactic equator, five (5) at the Galactic poles and about 12 stars on average over all Galactic latitudes.

Therefore, on average, there should be enough guide stars in view to meet the suggestion by Richmond (1990), to have three to five stars in view at all times, over all Galactic latitudes. However, this is simply an average, and any given field-of-view may vary in number of visible stars. More specifically, these star counts can be described with a Poisson distribution, which have standard deviations of $\sqrt{\#\text{ of counts}}$ (Taylor 1997). For $m_V \lesssim 11.5$, this gives 31 ± 6 stars[3] at the Galactic equator; 5 ± 2 stars at Galactic pole; 12 ± 3 stars on average over all Galactic latitudes. Therefore, when observing near the Galactic poles there may be regions where three or less stars are visible. Overall this means that for most regions of the sky the autoguider should have more than three guide stars visible, with only regions around the Galactic pole possibly having less than that. In other words, the autoguider is usable over nearly all the night sky and therefore does not greatly restrict the number of targets for which autoguiding can be used.

[3]Standard deviations are rounded to the nearest integer.

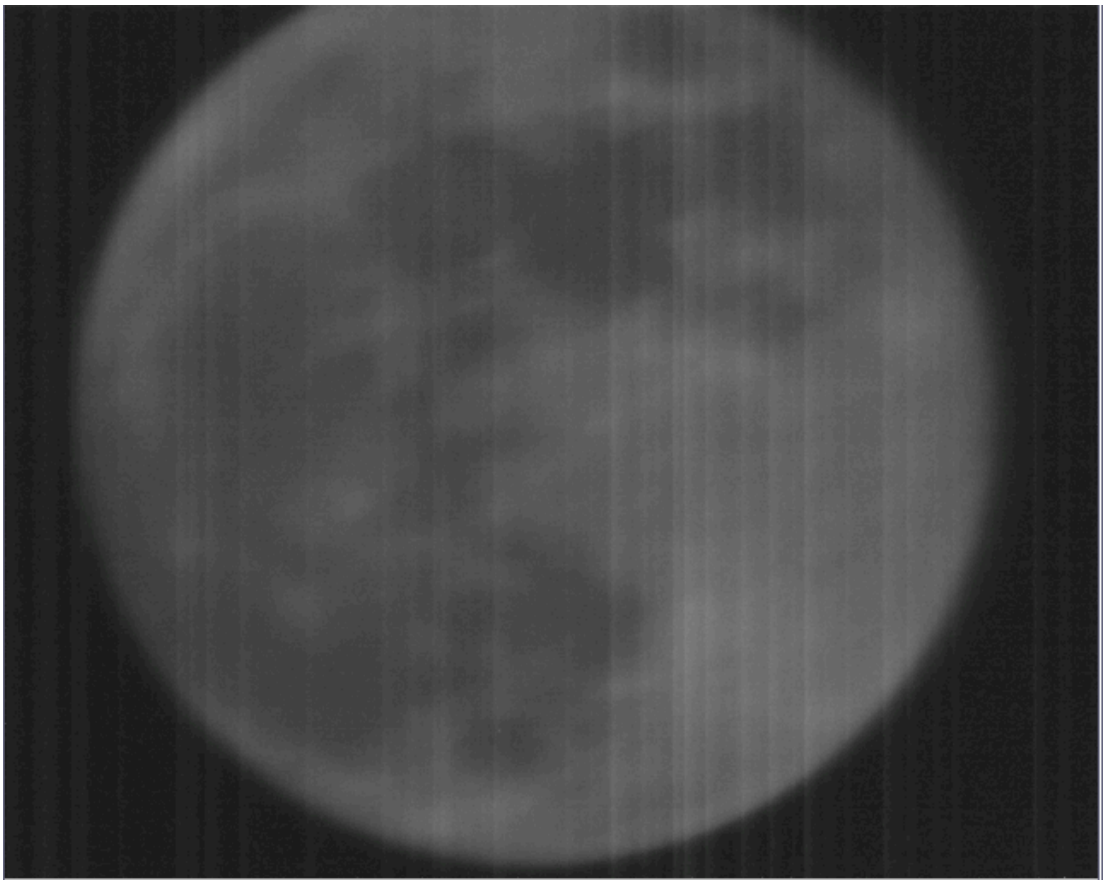

Figure 3.4: Field-of-view of the autoguider CCD through the guidescope, showing a full Moon. This gives a rough approximation of the FOV of the autoguider and guidescope assembly to be $\sim 30' \times 30'$.

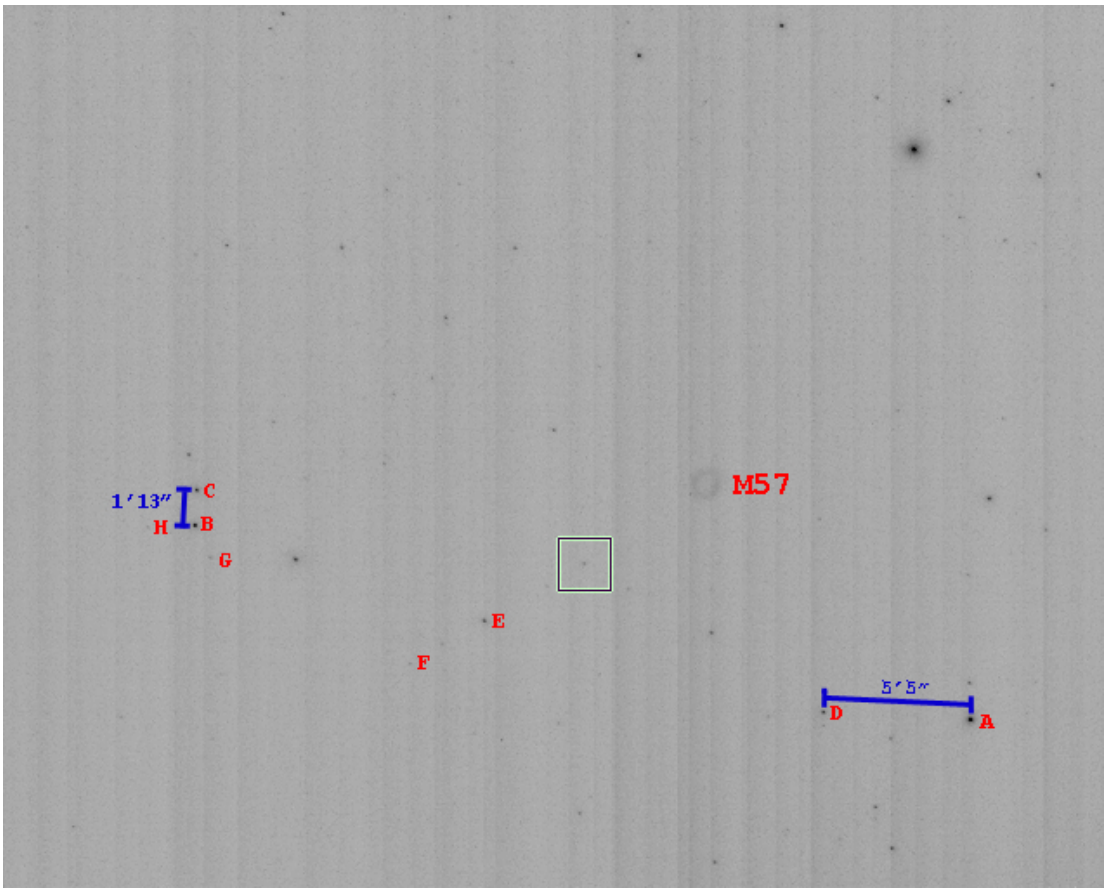

Figure 3.5: Field-of-view of the autoguider CCD through the guidescope, showing the Ring Nebula (M57). The stars are used to determine minimal observable magnitude (see Table 3.2) and platescale. The measures given on the left (vertical line) and right (horizontal) are the angular separations of the stars in the sky in arcminutes and arcseconds (of degree) as calculated in IDL, see text. The letters label stars which are immediately to their left. The box near center is the selection of a guide star in PhD Guiding, and it shows the ability of the autoguider to lock onto a star of $m_V \sim 11.5$. For this observation a 10 sec exposure was taken at 100% gain, hence the vertical line noise. The field was near zenith and there was a full Moon that night.

Table 3.2. Stars in field about M57

Name	Right Ascension	Declination	m_V	Label in Figure 3.5
TYC2642-521-1	18 53 8.7	+33 12 36.1	8.77	A*
TYC2642-1808-1	18 53 7.1	+32 45 3.9	9.53	B*
TYC2642-2502-1	18 53 12.8	+32 44 49.1	10.18	C*
TYC2642-84-1	18 53 3.7	+33 7 38.1	10.41	D*
TYC2642-1690-1	18 53 4.0	+32 55 32.7	10.54	E
TYC2642-1568-1	18 53 17.3	+32 58 21.9	11.56	boxed
TYC2642-2484-1	18 52 54.1	+32 53 27.1	12.27	F
TYC2642-1788-1	18 53 2.7	+32 45 51.9	12.40	G
TYC2642-1720-1	18 53 4.8	+32 43 30.3	12.70	H

Note. — Right ascension given in hours, minutes, seconds; declination in degrees minutes seconds; apparent magnitude in V-band (m_V) given in magnitudes. Right ascension (epoch=J2000, International Celestial Reference System (ICRS) coordinates), declination (epoch=J2000, ICRS coordinates) and m_V are from SIMBAD [http://simbad.u-strasbg.fr/], accessed 27 Apr 2012.

*Stars A & D and Stars B & C were used in determining the field-of-view and plate scale of the autoguider CCD, see Figure 3.5 and text for further detail.

3.3 Final Guiding Precision and Issues

Now to determine the quality of the autoguider, namely how precisely it guides. Ignoring the current drift, discussed later, we can use the average spread of star positions from the hour angle pixel spread measures, Figures 2.9–2.10, to determine the best possible pointing precision of this system. Doing this we find a spread of $\sim$1.5 pixels in RA and $\sim$1 pixel in Dec. This means that the autoguider should be able to keep any given star on the same pixel over the course of an observation. Using the 24" CCD platescale of $0.34''$/pixel this precision corresponds to $\sim 0.51''$ in RA and $\sim 0.34''$ in declination, or an average of about $0.43''$; for comparison average seeing at VVO is about $3''$ (Konon 2008). A qualitative measure of the autoguider's efficacy is shown in Figure 3.6. Overall, these calculations suggest that if the autoguider worked nearly-perfectly, i.e. without our observed drift, it would be able to guide to sub-seeing precision.

Even with the elimination of many possible factors, discussed at length in the previous chapter, there is still a consistent drift present in extended observations. From the hour angle pixel drift measures, Figure 2.7–2.8, and personal approximations from plots of drift, we come upon a value of about 10 pixels per hour northward and eastward (with the RA drift being a bit less than the Dec drift). On the 24" CCD 10 pixels corresponds to about 3.4″, which by chance is about the seeing at VVO. However this is not seeing as it is a net drift in the star position not its spread about a single point. Visual inspection shows no effect, as one would expect for drift nearly the same magnitude as seeing (Figure 3.6).

The exact reason for this remaining drift is not yet known though there are several possibilities:

- One possibility is that the drift is due to differential flexure. With the autoguider mounted on the 24" tube it is possible that when looking at parts of the sky the two telescopes, 24" and autoguider, come out of alignment such that the autoguider is still centered on its guide star while the 24" is pointed slightly off, or vice versa. The autoguider, thinking it is centered/off-centered does not/does adjust, respectively, and a net drift results. This could be remedied if the autoguider was using a pick-off mirror instead of a piggy-back telescope, however, as mentioned before, this would drastically reduce the field-of-view of the autoguider and it may be more difficult to always have a sufficiently bright guide star in view.

- Another issue, that has come up several times, is the 'guide' speed motors not working well for the 24" telescope. Specifically, when a guide signal was sent to them, the motors did not respond. This may in part be due to the signals being sent from the computer or warm room control box not being

sufficient for the motor to detect. Also there have been issues where the motors themselves, even when receiving the proper signal do not work in 'guide' speed, this has been most prevalent for the RA guide motor.

- One further issue is that the guide star, as seen by the autoguider and 24" CCD, never returns to its initial position after calibration. Rather it ends slightly south and west of its original location, a very possible cause or symptom of a north and east drift.

An additional property of this drift is that, though it is uniform in direction (N and E) the precise shape of the drift is different each time which in part suggest multiple causes, or just the natural variance from night-to-night. There are still many avenues to try and fix this issue.

All in all, even with the lingering drift issues, the autoguider has cut drift down by about a factor of five compared with the telescopes tracking abilities without autoguiding. Before the autoguider, transit observations were to keep their target star within a ± 10 pixel region, recentering by hand every 20-30 minutes, now with the autoguider a similar region may only need to be adjusted/recentered every hour, if even that. This precision of pointing also allows for much longer single exposures (rejoice in Figure 3.6) and a probable reduction in noise due to pixel-to-pixel sensitivity variations.

3.4 Autoguider Operating Procedure

The following is a step-by-step procedure on how to use the autoguider, followed by some possible troubleshooting points.

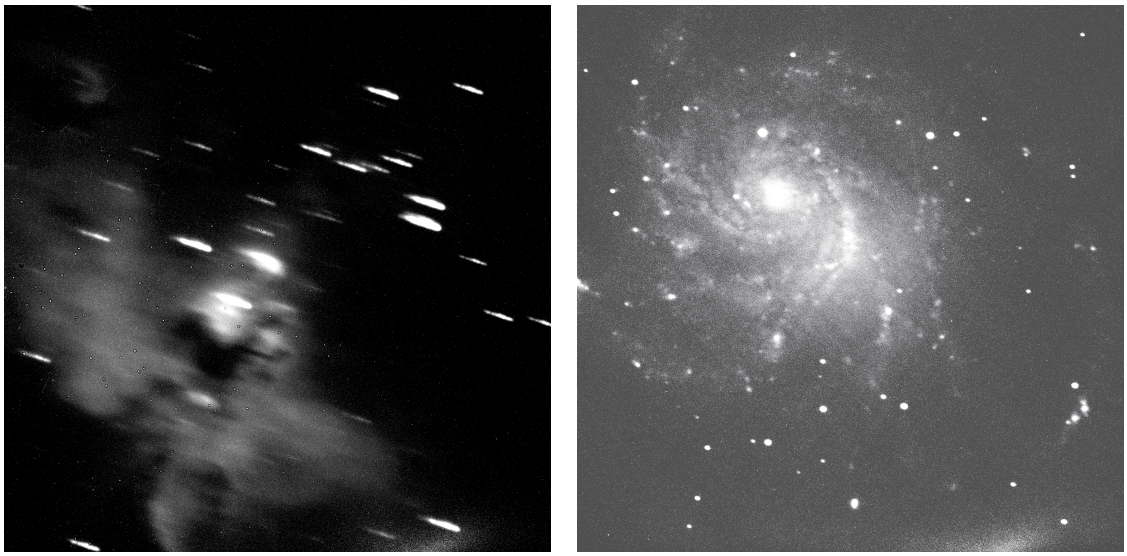

Figure 3.6: *Left*: The Eagle Nebula (M16) shown for 1 hour exposure in H-alpha, with no guiding. *Right*: The Pinwheel Galaxy (M101) shown for 1 hour exposure in B filter, with autoguiding (brightened for clarity).

3.4.1 Step-by-Step: Autoguider Operation

1. First begin by plugging in the USB cord for the autoguider, as it cannot be turned on/off except in this way if the dome computer is to be left on.

2. Open up MaxIm DL and make sure 'SS Autoguider' is selected as the secondary camera & connect to the cameras in MaxIm DL.

3. Continue with opening up the 24" as normal until you are at your target starfield and ready to being guiding.

4. Once at your target starfield, remove the 'slew/set' paddle from the telescope, so that it is no longer hanging on the telescope, and place it gently on the ground or ladder, somewhere where it will not disturb the telescope

when you use it during observations. On the side of the 24" telescope mount, flip the switch for the 'slew/set' speed to 'paddle' control and the 'set/guide' speed to 'computer' control.

5. Flip the switch on the side of the warm room control box from 'control box' to 'autoguider'.

6. Set RA and Dec speeds on the control box to 'guide'.

7. Select the 'Guide' tab in MaxIm DL then click on the 'Exposure' button to see the starfield. If a guide star is not chosen automatically you can chose it yourself by clicking on one.

8. Once you have selected a guide star, click 'Calibrate' mode, then press start. The guide star should be seen to make an L-shape as the software calibrates movements in all four cardinal directions.

9. After the calibration is complete, click 'Track' mode then press start.

10. At this point the autoguider is guiding.

11. Before beginning exposures for the night set the dome position such that the 24" points out the left most side, making sure not to obscure any of the 24" telescope aperture or the guidescope view. Doing this usually affords about an hour before the dome needs to be readjusted; shorter when looking near zenith, longer when about the celestial pole.

12. Now with the autoguider and dome ready, you can begin taking exposures as normal.

13. Adjust the dome every half-hour using the 'slew/set' paddle inside the 24" dome. Be careful not to have extraneous light sources or to bump or pull the wires on the telescope.

14. When you are finished observing for the night, disconnect the cameras in MaxIm DL, unplug the USB cord to the autoguider and proceed with closing-up as normal.

3.4.2 Troubleshooting

I'm looking at a different region of sky than when I originally calibrated.

It is good, if time permits, to recalibrate using this new starfield in case any physical adjustments of the scope affect the pointing abilities. If time is very pressured, it may be fine to eschew another calibration in favor of catching a specific observation.

The guide star does not move enough, and autoguider can't calibrate.

In this case, especially if you are observing near the celestial pole, you can put the RA speed to 'set' which should hopefully fix the problem. Putting Dec to 'set' speed usually results in lots of overshooting. If this problem occurs when you are not observing near the pole check that the guide motors are working properly in the telescope, as this may a symptomatic of a more serious recurrent issue with the telescope motors.

Wires coming from the telescope are taut/strained.

It is good practice during the course of a night to check, by eye, that none of the wires coming from the telescope are taut. If any are, gently loosen them and

note it in the observing log. This may cause a slight bump, drift or displacement in the starfield so if your observation is very close to being done you can leave the wires and loosen them when you finish. If left alone for a long time however, the tension on the wires, along with being bad for the telescope, may cause it to drift.

Chapter 4

Exoplanet Transits

The inital reason for the autoguider was to help reduce noise in observations made at Van Vleck Observatory, especially exoplanetary transits. In this chapter I shall explore transit data taken on WASP-33b and look for signs of transit timing variations.

4.1 Data Reduction & Analysis

4.1.1 Previous Work

The Wesleyan Transiting Exoplanet Program (WesTEP) had contributions by Leiner (2010) who wrote the light curve fitting programs based on quadratic limb darkening fits in Mandel & Agol (2002), allowing for both fitted and fixed limb darkening parameters. Johnson (2011) modified some of the fitting programs as well as wrote the program to create observed minus calculated ($O - C$) plots, allowing for the determination of transit timing variations (TTVs).

4.1.2 Current Work

Here I shall discuss an overview of the method used to go from raw images to an $O - C$ plot and determination of possible TTVs. The same programs as Johnson (2011) were used without modification unless noted; a more complete

step-by-step methodology is given in Appendix C.

To begin, images are first calibrated by appropriately subtracting darks, biases and flats via the 'reduceI' script in IRAF. After the images are reduced the target star and comparison stars are chosen and a two-dimensional Gaussian function is fit to each. I added a functionality to these files which automatically detects, removes and notifies the user of images where the target star has saturated (above 57,000 counts[1]), zero or negative count values. Then aperture photometry is done for the target star, its out-of-transit flux is fit and a light curve is produced. This light curve is then fit with a quadratic limb darkening fit using fixed limb darkening parameters. If the transit is partial, i.e. having only ingress or egress observed, then the radius of the star, the planet, and the inclination are also fixed which effectively fixes transit duration. The transit center is then calculated from this light curve fit and plotted on an $O-C$ diagram, which shows the observed transit center time minus the calculated transit center time for a single-planet, single-star system, in our case. Any deviation from the $O-C=0$ line is considered a TTV and periodicity in these observed TTVs is then determined by use of a periodogram.

4.2 Results: WASP-33b

4.2.1 Previous Work

Using photometry and time-series spectroscopy Collier Cameron et al. (2010) confirmed the existence of a hot-jupiter orbiting the star WASP-33 (HD15082); the planet being appropriately named WASP-33b. Properties for this system are

[1]This number was chosen because it was the last point of linearity for the 24" Perkin Telescope's CCD as per Konon (2008), Figure 4.19.

Table 4.1. Properties of the WASP-33 system

Star		Planet	
RA	02h 26m 51s	# Known Planets	1
Dec	+37° 33m 02s	$M \cdot sin(i)$	<4.59 $M_{\mathcal{Y}}$
Spec. Type	A5	Radius	$1.438\ ^{+0.062}_{-0.03}$ $R_{\mathcal{Y}}$
App. Mag. (V)	8.3	Semi-Axis Major	0.02558 ± 0.00023 AU
Distance	116 ± 16 pc	Period	1.21986967 ± 4.5×10^{-7} days
Mass	1.444 ± 0.031 $M_{\odot}$	Eccentricity	0
T_{eff}	7400 ± 200 K	Inclination	$87.67°\ ^{+1.6}_{-2.4}$

Note. — All data from Schneider et al. (2011), except planet mass, M·sin(i), which is from Smith et al. (2011)

given in Table 4.1. WASP-33b is the first known planet to orbit a δ Scuti variable, with its host star having a ∼68 minute period oscillation of semi-amplitude 1 mmag in the Johnson R band (Herrero et al. 2011). In addition, it is one of the hottest known exoplanets with a brightness temperature of $3620\ ^{+200}_{-250}$ K (Smith et al. 2011).

From Johnson (2011), six transits of WASP-33b were observed and combined with data from Herrero et al. (2011) showed suggestive evidence of nonlinear transit timing variations. However, there was only one data point above the 1σ error in $O - C = 0$ and when combined with data from the Exoplanet Transit Database[2] the trend went away.

4.2.2 Current Work

From this observing season 12 transits of WASP-33b were observed (Table 4.2), of those only 9 were usable, Figure 4.1–4.7. The three unusable transits (Nov 26, Jan 2, Jan 24) are discussed later.

[2]http://var2.astro.cz/ETD/index.php

Transits used for TTVs

Of the nine used transits, four were full transits while the remaining five were partial. I define full and partial transits as follows: a full transit has consistent data, after proper data reduction (Appendix C), during the entirety of the transit as well as some additional time before and/or after transit; partial transits only have data points about ingress, egress, or do not have consistent data points throughout transit. Of the full transits though only one observation shows a clean transit, December 11, the issues with the other observations are listed in Table 4.2.

Due to the fact that the majority of transits did not show canonical lightcurves, two different methods of fitting them were used: one where the stellar radius, planetary radius and inclination were kept constant at the literature values given in Collier Cameron et al. (2010) and the start time of transit was allowed to vary, hereafter 'fixed fit', while the other method of fitting allowed the stellar radius, planet radius and inclination to vary as well as the transit start time, hereafter 'free fit'. The fixed fit allows the transit duration to remain constant so as to be able to fit those transits where a clear ingress and egress were not visible. The free and fixed fits are shown in Figures 4.1 and 4.2, respectively.

For the free fits one can see that the transit fit varies dramatically. For the Nov 8–9 transit the depth is very much deeper than Dec 11, while the Nov 24 transit was much shorter and shallower. The Nov 8–9 transit, especially around mid-transit, may be affected by dome obscuration which was an issue during that observation. In the case of the Oct 18, Oct 22–23 and Nov 24 transits the duration is greatly shortened because of the lack of data points around ingress or egress. For these reasons and the large shape difference of the fits, it was decided to

assume a constant transit duration and simply adjust the time of transit, which is all that is needed to calculate TTVs. This was borne out in the fixed fits, Figure 4.2. Aside from transit shape, the fit of ingress and/or egress between the fixed and free parameter fits are different. A dramatic example of this is with the Nov 24 transit where the free fit puts ingress near –0.04 days from transit center, while the fixed fit puts it at about –0.06 days.

To see whether there was a noticeable difference between the TTV results for the free and fixed fits, $O - C$ diagrams were made for each (Figure 4.3–4.4). Comparing the two $O - C$ diagrams one can see that these two fitting methods calculate very different TTVs for the partials transits with very little change for the full transits. The spread in both cases is about the same, $\sim$40 minutes, where the approximate mean for the free parameter fit is about 10 min more positive than the fixed parameter fit. To determine whether these TTVs were periodic, the $O - C$ data were put into a Lomb-Scargle periodogram (Scargle 1982; Horne & Baliunas 1986) used by Johnson (2011). The periodograms for each fit method are shown in Figures 4.5–4.6. The periodogram checked periods ranging from one day up to 365 days, being roughly one year since last season's observations. Between both fitting methods there was no single dominant period, each produced a different peak period. For free fitting the most favored period was found at about 8.9734 days while the fixed fitting had a most favored period around 1.8097 days. However it is clear that for each fit the most favored period is not conclusive or significantly favored. For example the free fit periodogram has a peak period around one day which is close in power to an eight day period. For the fixed fit, a period of around 12 days is close in power to the one day period. Using these peak periods, phased versions of the $O - C$ plots shown in Figures 4.3–4.4 can be made (Figure 4.7). Along with phasing free fit data and fixed fit data with their

respective favored period, they were also phased with the opposite fit method's period (i.e. free fit data with fixed fit period and vice versa). In addition they were also fit with a period of 14.1739 days, the period found by Johnson (2011). None of the phased graphs are conclusive, however the most promising one is the fixed fit data phased to the period found by Johnson (2011).

From these data there is no clear transit timing variation observed for WASP-33b. However, due to the quality of transits observed this season, this is by no means a closed case. Overall the fixed parameter fits seem to be a better choice in theory because many of the transits observed this season were partial and free parameter fits fit the partial lightcurves as if they were the full transits, while the fixed parameter fits just used the observed ingress or egress to determine the time of transit. There is support that fixing the duration of the transit is a valid assumption because the transit duration for WASP-33b has a relative uncertainty of 0.01% (Smith et al. 2011). Additionally, though it has been suggested that WASP-33b should show an observable transit duration variation (TDV) due to its orbital geometry (Damiani & Lanza 2011), there have not yet been any TDVs observed in a confirmed planetary system (Szabó et al. 2012). The fact that full transits showed little TTV difference when fit with fixed versus free parameter fits also gives credence to the notion that transit duration variations for WASP-33b are negligible, as well as validating our method of fixed parameter fits. Though the periodograms showed no distinct period for a possible perturbing planet, there was an occurrence of a fairly strong peak around 12 days for the fixed parameter fit, in rough accordance with the 14 day period of Johnson (2011), cf. Figure 4.7. It should be noted that false alarm probabilities and issues of aliasing were not determined for these periodograms, due to constraints of time.

Table 4.2. Comments on observed WASP-33b transits for the 2011-2012 observing season

Date	Transit Amt Obsv	Comments	Autoguided
Jul 27	—	Out of transit	Yes
Aug 18	Full	Cloudy in the beginning, ice crystal by target star	No
Oct 18	Partial	Clouding at end	No
Oct 22-23	Partial	Used flats from night of 23 Oct 2011	No
Oct 24	Full	Clouding towards end	Yes
Nov 2	Partial	—	No
Nov 8-9	Partial	Major saturation; dome obscuration issues	No
Nov 24	Partial	Large dip near nominal ingress; Large saturation around egress removed	No
Nov 26	Partial	Observation began after ingress, ended before egress	No
Dec 11	Full	—	No
Dec 28-29	Full	CCD restarted between observations and calibrations	No
Jan 2	Partial	Changing exposure times; not uniform cadence until after egress	No
Jan 24	Partial	Observation ended before ingress	No
Jan 31	—	Out of transit	Yes
Feb 13	—	Out of transit	No

Note. — Dates given are the local day(s) of transit.

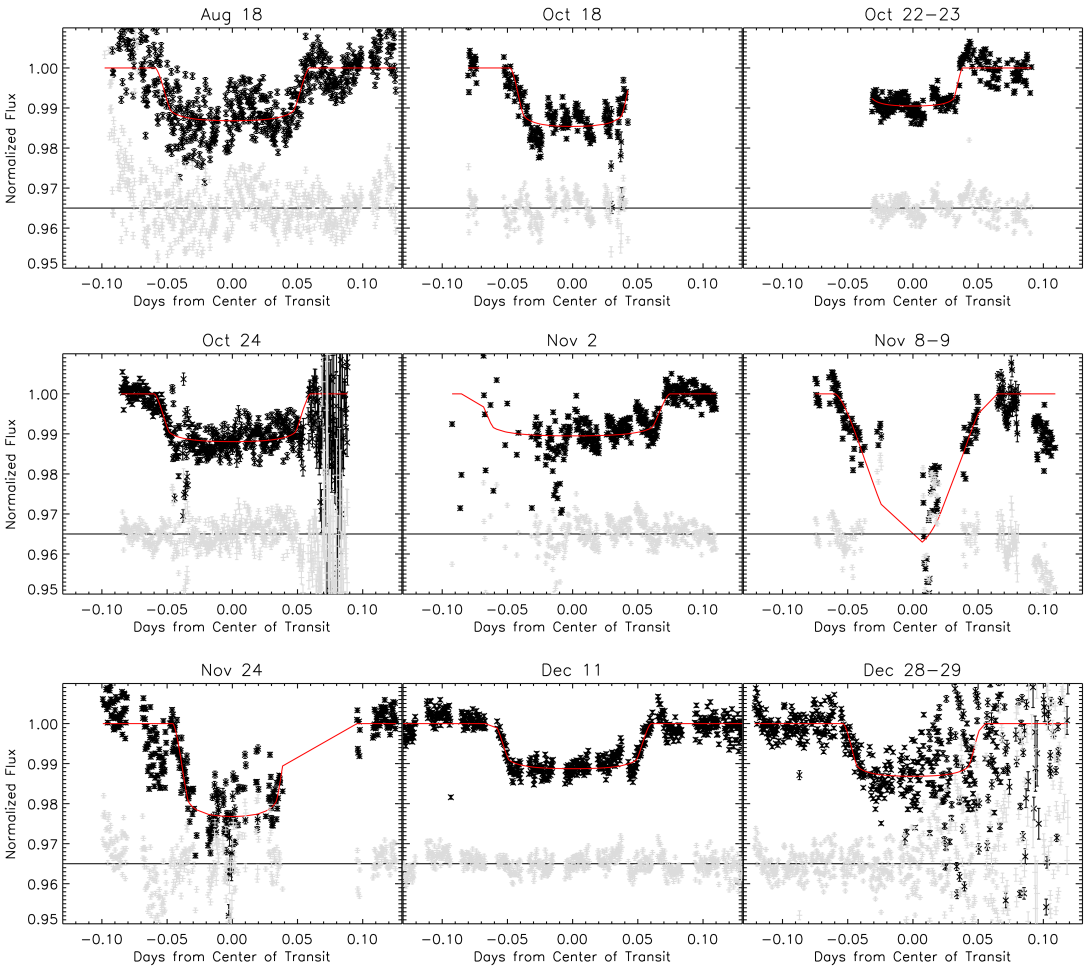

Figure 4.1: Free parameter fits for usable WASP-33b transits in the 2011-2012 season. The upper portion of each graph is the normalized light curve with best fit in red. The lower portion shows the residuals from the best fit. The dates given are the local date(s) that the transit spanned. For gaps in data, the plot of the fit simply extends a line to the next data region; this not a factor of the actual fit.

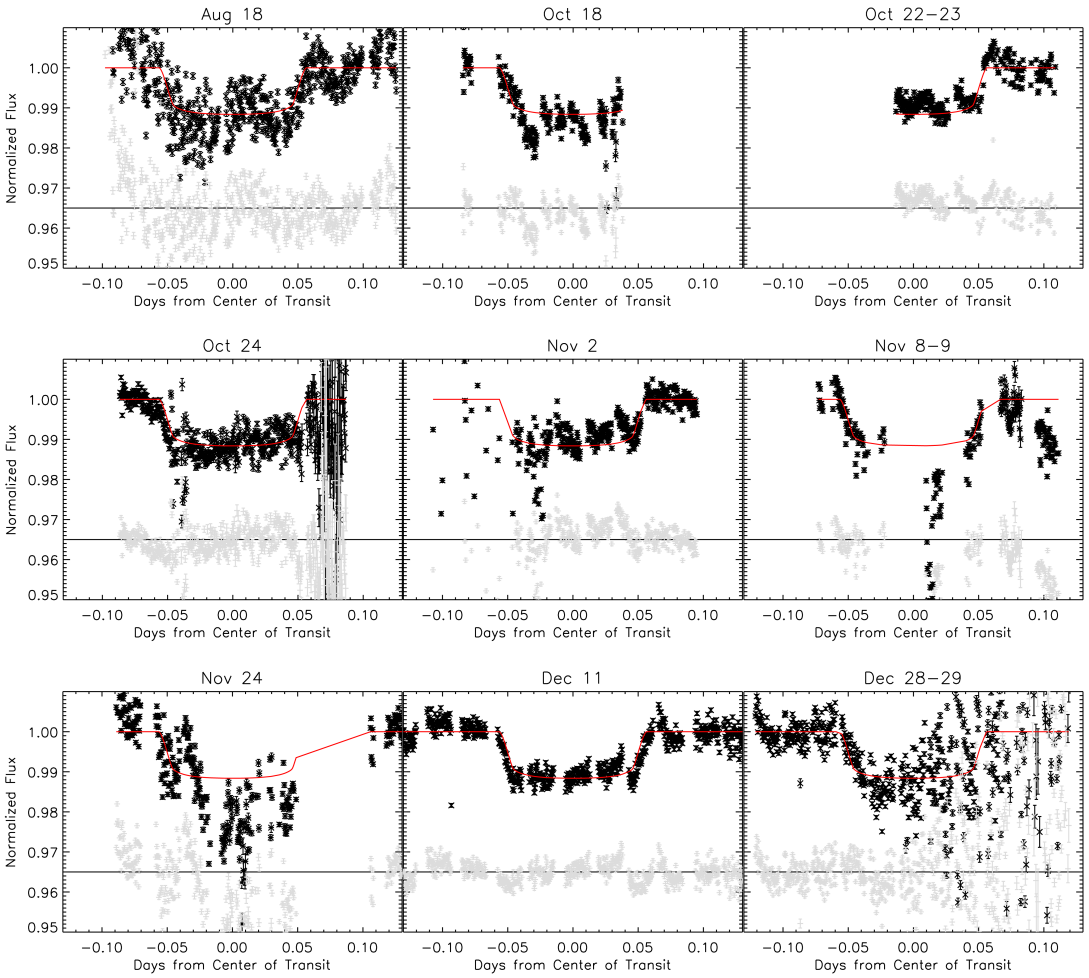

Figure 4.2: Fixed parameter fits for usable WASP-33b transits in the 2011–2012 season. The upper portion of each graph is the normalized light curve with best fit in red. The lower portion shows the residuals from the best fit. The dates given are the local date(s) that the transit spanned. For gaps in data, the plot of the fit simply extends a line to the next data region; this not a factor of the actual fit.

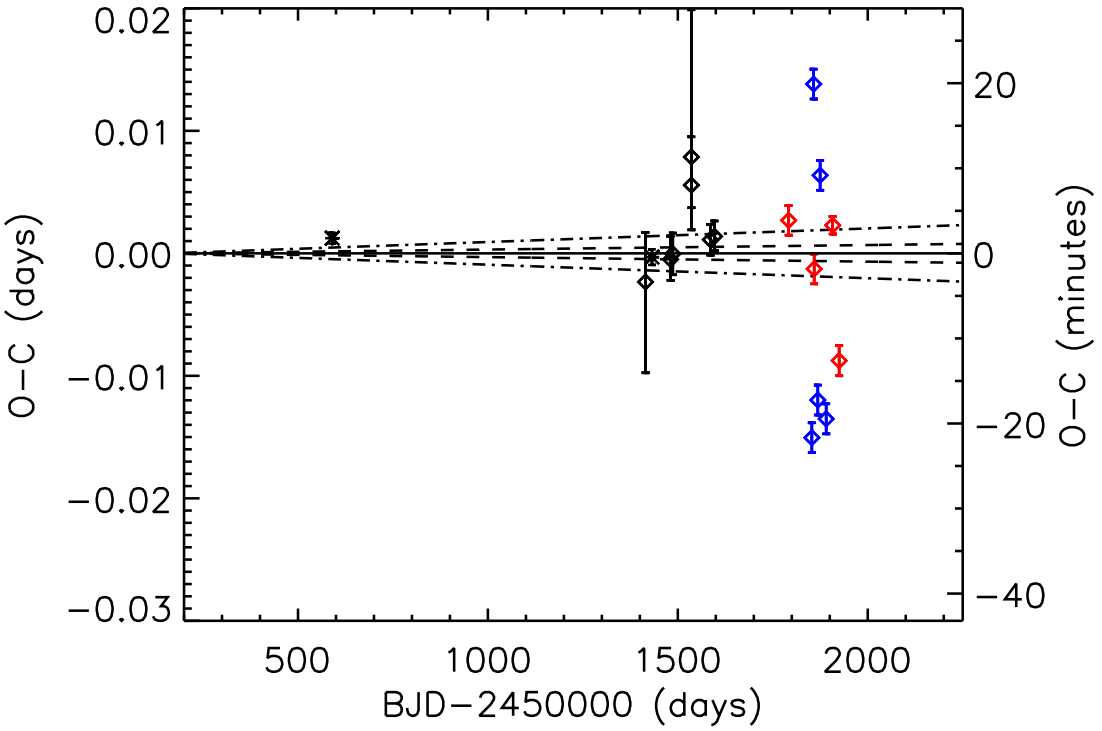

Figure 4.3: Free parameter fit WASP-33b transit timing variations. Black asterisks are literature values. Black diamonds are data collected at Van Vleck Observatory during the 2010–2011 observing season. Red and blue diamonds are data points for this observing season, 2011–2012. Red show full transits; blue partial. The errors on this season's observations are rough lower limits gotten from the approximate average of the previous year's data points; the red point with the smaller error bars denotes the 11 Dec 2011 transit. The dashed line is the 1σ error and dot-dashed the 3σ error on the predicted times.

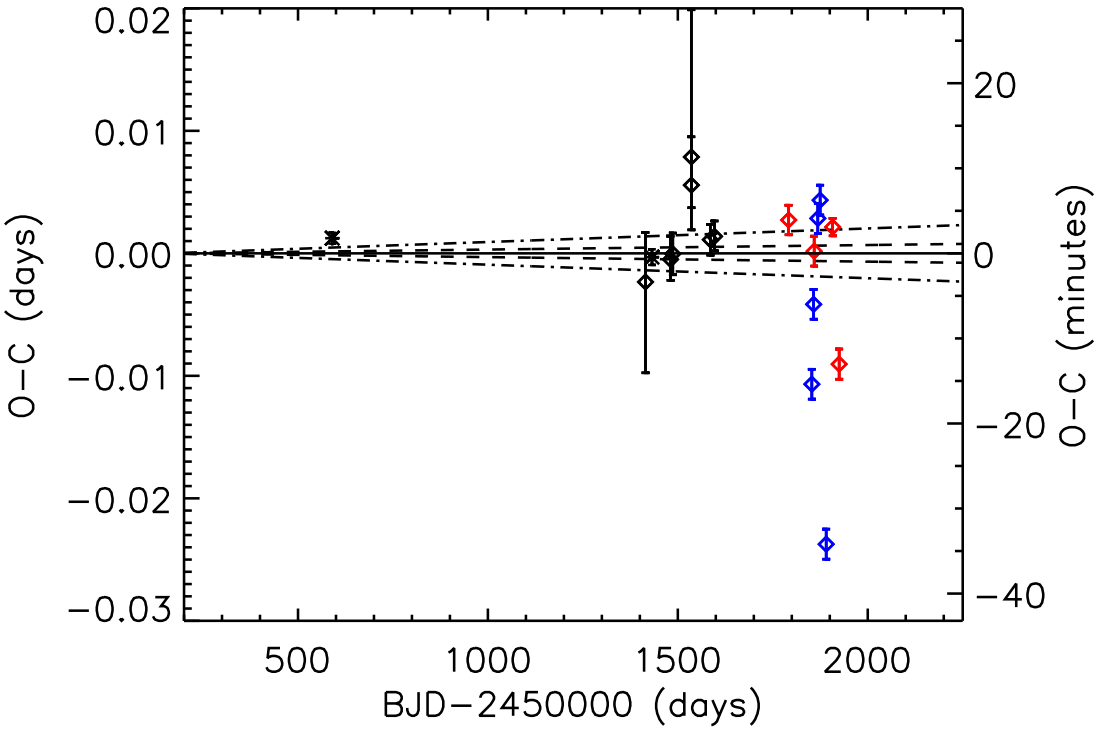

Figure 4.4: Fixed parameter fit WASP-33b transit timing variations. Black asterisks are literature values. Black diamonds are data collected at Van Vleck Observatory during the 2010–2011 observing season. Red and blue diamonds are data points for this observing season, 2011–2012. Red show full transits; blue partial. The errors on this season's observations are rough lower limits gotten from the approximate average of the previous year's data points; the red point with the smaller error bars denotes the 11 Dec 2011 transit. The dashed line is the 1σ error and dot-dashed the 3σ error on the predicted times.

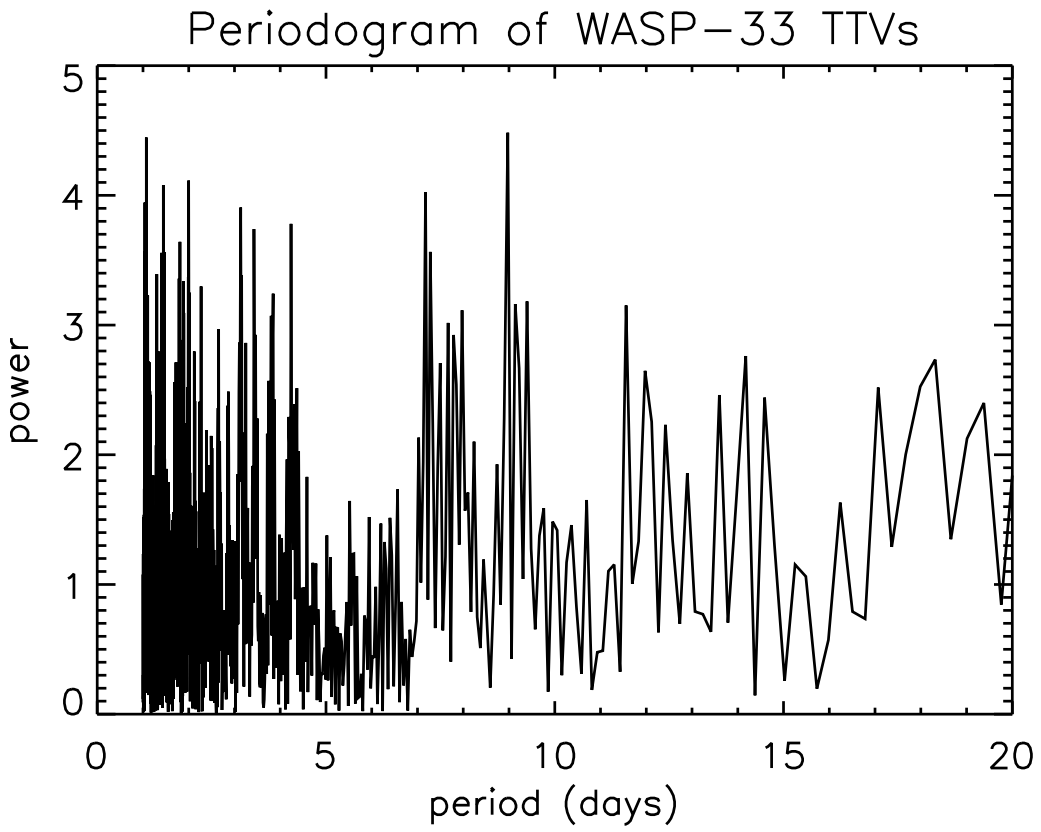

Figure 4.5: Periodogram of free parameter fit WASP-33b transit TTVs from Figure 4.3. A maximum peak is found at 8.9734 days. Periods larger than 20 days have lower peaks than those less than 20 days, and are not shown for clarity.

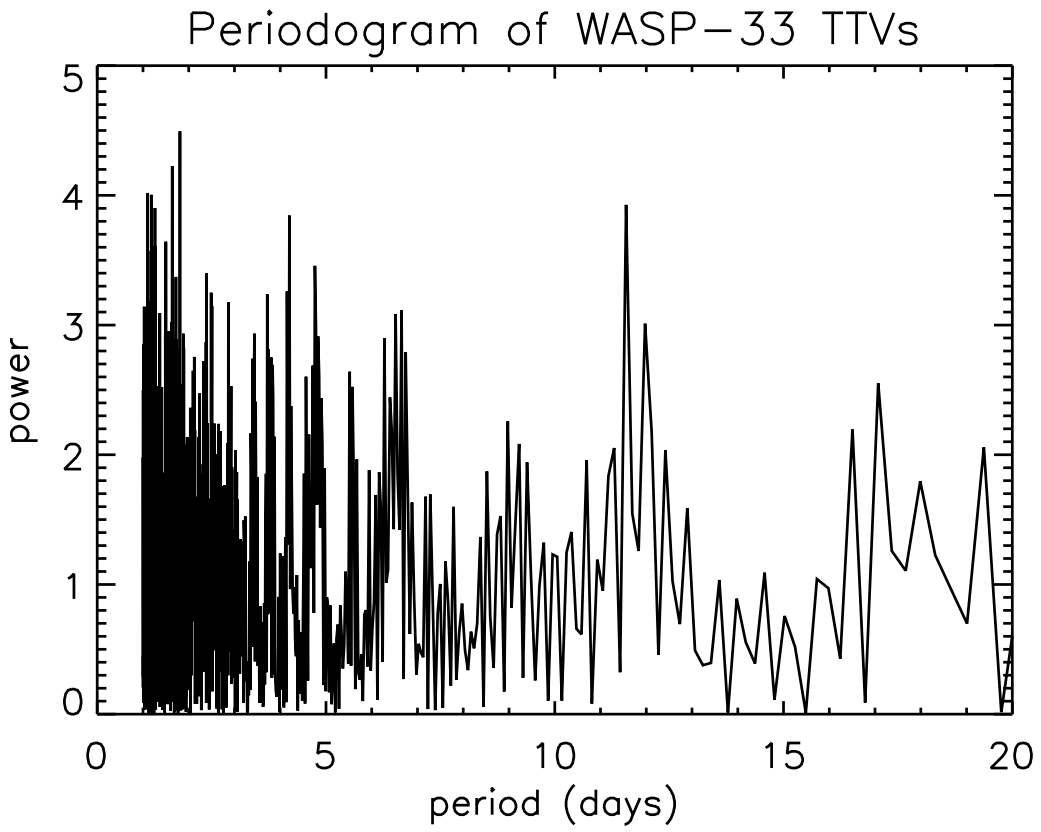

Figure 4.6: Periodogram of fixed parameter fit WASP-33b transit TTVs from Figure 4.4. A maximum peak is found at 1.8076 days. Periods larger than 20 days have lower peaks than those less than 20 days, and are not shown for clarity.

Issues with transits used for TTV data

For the transits used in the TTV data, the noise and issues seen in them came from many varied sources, Table 4.2. Some of these large noise features are due to clouds (e.g. Oct 24 and Dec 28–29), while another is likely from an ice crystal on and near the target star in the CCD field-of-view (Aug 18). Large gaps in the transits (e.g. Nov 8–9 and Nov 24) are due to the automatic removal of images where the target star saturated (greater than 57,000), zero or negative counts, as mentioned in the previous section.

An issue arose where a few transits had depths that were much shallower than the others and also shallower than would be predicted by the literature values for WASP-33b. Upon looking into this further the issue turned out to be that two stars had identical lightcurves, in both shape and intensity. The two offending stars were usually close to each other in the starfield and the search region used to look for each star in the aperture photometry overlapped. Upon removing one of the offending stars from the aperture photometry the transit regained a normal depth.

Additionally, the large noise spikes seen in the Nov 8–9 transit are likely due to partial obscuration of the telescope aperture by the dome slit, as noted in the observers log. There is a large dip near ingress for the Nov 24 observation. From the observers log there is nothing that suggests any issues with dome obscuration. Additionally a look at all the light curves of the target and comparison stars show nothing unusual that might suggest one star or another as a cause for the dip. The focus however was very tight for WASP-33b, FWHM $\sim$5–7 pixels, and around the time when this dip occurred there was a jump of about 10 pixels in the star's position. This suggests that the dip may be due to pixel-to-pixel sensitivity

variations.

There is additional cause for caution when looking at these lightcurves: stellar variability. We know that WASP-33 is a variable star of period ∼68 minutes meaning that over the course of a transit (∼2.7 hrs) variability of the star could affect photometry (Collier Cameron et al. 2010; Herrero et al. 2011; Smith et al. 2011). In addition, the variability of the comparison stars is not known. The exact way in which one models the out of transit regions is also important. Currently we use a linear fit for these regions, however due to stellar variability it may be more precise to use a higher order fit.

Unused transits

Now to discuss the reason for deeming three WASP-33b transits unusable. First and foremost the unusable observations were partial ones made on Nov 26, Jan 2 and Jan 24. The Nov 26 was unusable because the observation began after the predicted ingress and ended before egress and there was no observable transit or ingress/egress. The Jan 2 observation was not used because it not only involved many images where the exposure time varied greatly but also was very sporadic in cadence having only one image every 10–20 minutes through the duration of the transit. Finally the Jan 24 observation was unusable because the observation ended before predicted ingress and there was no observable transit in its light curve.

In addition to in-transit observations of WASP-33, out of transit observations were taken the nights of 27 July 2011, 31 Jan 2012 and 13 Feb 2012. No unexpected transits were observed.

Table 4.3. Transits of WASP-33b during the 2011-2012 observing season visible from VVO

Date	Start Time	Airmass	Date	Center Time	Airmass	Date	End Time	Airmass
July 5[a]	02:34	2.270	July 5	03:56	1.553	July 5	05:17	1.235
July 16[a]	02:04	2.121	July 16	03:52	1.492	July 16	04:47	1.192
Aug. 7	01:03	2.778	Aug. 7	02:24	1.385	Aug. 7	03:46	1.044
Aug. 18	**00:33**	**2.538**	**Aug. 18**	**01:55**	**1.336**	**Aug. 18**	**03:16**	**1.031**
Aug. 29	00:02	2.350	Aug. 29	01:23	1.289	Aug. 29	02:45	1.022
Sep. 4	02:25	1.229	Sep. 4	03:46	1.011	Sep. 4	05:08	1.072
Sep. 8	23:32	2.176	Sep. 9	00:54	1.250	Sep. 9	02:15	1.014
Sep. 15	01:55	1.194	Sep. 15	03:17	1.006	Sep. 15	04:38	1.092
Sep. 19	23:01	2.037	Sep. 20	00:22	1.212	Sep. 20	01:44	1.009
Sep. 26	01:24	1.164	Sep. 26	02:45	1.003	Sep. 26	04:07	1.112
Sep. 30	22:31	1.906	Sep. 30	23:53	1.181	Oct. 1	01:14	1.005
Oct. 7	00:54	1.136	Oct. 7	02:16	1.002	Oct. 7	03:37	1.137
Oct. 11	22:00	1.801	Oct. 11	23:21	1.151	Oct. 12	00:43	1.003
Oct. 13	03:17	1.005	Oct. 13	04:39	1.180	Oct. 13	06:00	1.910
Oct. 18	*00:23*	*1.113*	*Oct. 18*	*01:44*	*1.003*	*Oct. 18*	*03:06*	*1.163*
Oct. 22	*21:30*	*1.700*	*Oct. 22*	*22:52*	*1.126*	*Oct. 23*	*00:13*	*1.003*
Oct. 24	**02:46**	**1.008**	**Oct. 24**	**04:07**	**1.213**	**Oct. 24**	**05:29**	**2.031**
Oct. 28	23:53	1.091	Oct. 29	01:15	1.006	Oct. 29	02:36	1.195
Nov. 2	*20:59*	*1.618*	*Nov. 2*	*22:20*	*1.103*	*Nov. 2*	*23:42*	*1.004*
Nov. 4	02:16	1.014	Nov. 4	03:38	1.248	Nov. 4	04:59	2.181
Nov. 8	*22:22*	*1.073*	*Nov. 8*	*23:43*	*1.011*	*Nov. 9*	*01:05*	*1.227*
Nov. 13	19:29	1.537	Nov. 13	20:51	1.083	Nov. 13	22:11	1.008
Nov. 15	00:45	1.022	Nov. 15	02:06	1.290	Nov. 15	03:28	2.342
Nov. 19	21:52	1.056	Nov. 19	23:14	1.017	Nov. 20	00:35	1.267
Nov. 24	*18:58*	*1.475*	*Nov. 24*	*20:19*	*1.065*	*Nov. 24*	*21:41*	*1.013*
Nov. 26	*00:15*	*1.032*	*Nov. 26*	*01:37*	*1.334*	*Nov. 26*	*02:58*	*2.545*
Nov. 30	21:21	1.043	Nov. 30	22:42	1.026	Dec. 1	00:04	1.308
Dec. 5	18:28	1.411	Dec. 5	19:50	1.051	Dec. 5	21:10	1.020
Dec. 6	23:44	1.043	Dec. 7	01:05	1.386	Dec. 7	02:27	2.766
Dec. 11	**20:51**	**1.031**	**Dec. 11**	**22:13**	**1.036**	**Dec. 11**	**23:33**	**1.352**
Dec. 16	17:57	1.361	Dec. 16	19:18	1.037	Dec. 5	20:40	1.030
Dec. 17	23:14	1.058	Dec. 18	00:36	1.441	Dec. 18	01:56	3.019
Dec. 22	20:20	1.022	Dec. 22	21:41	1.050	Dec. 22	23:03	1.408
Dec. 27	17:27	1.310	Dec. 27	18:48	1.027	Dec. 27	20:09	1.041
Dec. 28	**22:43**	**1.073**	**Dec. 29**	**00:04**	**1.507**	**Dec. 29**	**01:26**	**3.369**
Jan. 2	*19:50*	*1.014*	*Jan. 2*	*21:12*	*1.064*	*Jan. 2*	*22:32*	*1.463*
Jan. 8	22:13	1.093	Jan. 8	23:35	1.575	Jan. 9	00:55	3.741
Jan. 13	19:19	1.008	Jan. 13	20:40	1.082	Jan. 13	22:02	1.534
Jan. 20[a]	21:42	1.268	Jan. 20	23:03	1.621	Jan. 20	00:25	2.444
Jan. 24	*18:49*	*1.004*	*Jan. 24*	*20:10*	*1.101*	*Jan. 24*	*21:31*	*1.604*
Feb. 4	18:18	1.003	Feb. 4	19:40	1.123	Feb. 4	21:01	1.694
Feb. 11[a]	20:41	1.344	Feb. 11	22:02	1.831	Feb. 11	23:24	2.897
Feb. 16[a]	17:47	1.031	Feb. 16	19:08	1.143	Feb. 16	20:30	1.389

Note. — Observed transits are listed in bold type; transits that were partially observed are italicized. Times are in local 24hr time (EDT/GMT-4 before Nov. 6, EST/GMT-5 after Nov. 6). Unobserved transits were missed due to poor weather unless otherwise noted.

[a]From ETD [http://var.astro.cz/ETD] where pre- or post-transit times were insufficient due to local horizon or sunrise/sunset to be calculated from our WesTEP program, though the transit itself is visible; airmass calculated from Birney, D.S., Gonzalez, G., and Oesper, D. (2006).

4.3 Other Observed Transits

Along with the observations of WASP-33b transits, 29 additional transits of various systems were observed, Table 4.4. A few of these targets, HAT-P-16 and WASP-3, were targets of interest of Johnson (2011). Additionally, the 20 Feb 2012 transit of HAT-P-24b and the 13 Apr 2012 transit of WASP-43b were observed simultaneously with Wellesley College.

Table 4.4. Observations of other transits during the 2011-2012 season

Planet Name	Date	Start Time	Airmass	Date	Center Time	Airmass	Date	End Time	Airmass	Comments
TrES-3b	*June 4*	*01:42*	*1.013*	*June 4*	*02:21*	*1.007*	*June 4*	*03:00*	*1.059*	started circa end of transit
HAT-P-5b	*June 6*	*22:47*	*1.600*	*June 7*	*00:15*	*1.080*	*June 7*	*01:42*	*1.015*	recooled CCD midtransit
HAT-P-11b	July 2	00:55	1.081	July 2	02:04	1.007	July 2	03:12	1.086	
Qatar-1b	*July 2*	*21:58*	*1.467*	*July 2*	*22:47*	*1.268*	*July 2*	*23:35*	*1.150*	clouded out
WASP-2b	July 5	00:38	1.528	July 5	01:32	1.258	July 5	02:26	1.238	
WASP-3b	July 6	00:39	1.023	July 6	01:59	1.053	July 6	03:19	1.417	
HAT-P-11b	*July 6*	*22:13*	*1.437*	*July 6*	*23:22*	*1.108*	*July 7*	*00:31*	*1.008*	clouded out mid-transit
WASP-2b[a]	*July 30*	*20:29*	*1.086*	*July 30*	*21:23*	*1.192*	*July 30*	*22:17*	*1.344*	CCD recooling at beginning of transit
WASP-3b	Aug. 24	21:24	1.022	Aug. 24	22:44	1.055	Aug. 25	00:03	1.417	
HAT-P-16b	Sep. 2	21:46	2.337	Sep. 2	23:18	1.254	Sep. 3	00:50	1.007	cloudy at beginning
WASP-48b	Sep. 9	23:32	1.055	Sep. 10	01:08	1.341	Sep. 10	02:43	2.278	no egress
Qatar-1b	*Oct 25*	*22:31*	*1.219*	*Oct 25*	*23:19*	*1.386*	*Oct 26*	*00:07*	*1.650*	clouded out near end of transit
CoRoT-Exo-7b	Nov 3	02:44	1.708	Nov 3	03:18	1.467	Nov 3	03:51	1.367	
WASP-48b	Nov. 6	19:36	1.102	Nov. 6	21:12	1.523	Nov. 6	22:48	2.874	patchy data
HAT-P-28b	Nov 7	20:00	1.209	Nov 7	21:36	1.007	Nov 7	23:13	1.218	
GJ 436b	Nov 25	04:16	1.396	Nov 25	04:47	1.209	Nov 25	05:17	1.099	
Qatar-1b	Dec 1	19:37	1.271	Dec 1	20:25	1.470	Dec 1	21:13	1.776	
HAT-P-30b	Dec 1	23:26	3.354	Dec 2	01:00	1.640	Dec 2	02:34	1.268	
HAT-P-25b	Dec 18	22:59	1.051	Dec 18	00:23	1.344	Dec 19	01:48	2.937	
HAT-P-3b	*Dec 25*	*03:13*	*1.588*	*Dec 25*	*04:15*	*1.195*	*Dec 25*	*05:16*	*1.034*	clouded out towards transit end
HAT-P-16b	*Jan. 5*	*18:49*	*1.000*	*Jan. 5*	*20:21*	*1.172*	*Jan. 5*	*21:52*	*1.979*	cloudy
CoRoT-Exo-7b	Jan 18	21:28	1.506	Jan 18	22:02	1.379	Jan 18	22:36	1.363	
HAT-P-16b	*Jan. 30*	*18:25*	*1.035*	*Jan. 30*	*19:57*	*1.407*	*Jan. 30*	*21:29*	*3.073*	clouded out
HAT-P-12b	Feb 6	22:05	4.034	Feb 6	23:15	1.860	Feb 7	00:25	1.241	
GJ 436b	Feb 9	20:24	3.880	Feb 9	20:55	2.392	Feb 9	21:26	1.746	
HAT-P-24b	Feb 20	20:00	1.360	Feb 20	21:21	1.143	Feb 20	23:39	1.924	
HAT-P-3b	Mar 26	23:11	1.324	Mar 27	00:13	1.082	Mar 27	01:15	1.007	
XO-2b	Apr 2	23:31	1.132	Apr 3	00:52	1.580	Apr 3	02:12	2.956	
WASP-43b	Apr 13	21:42	1.610	Apr 13	22:17	1.623	Apr 13	22:52	1.798	

Note. — Observed transits are listed in normal type; transits that were partially observed are italicized. Times are in local 24hr time (EDT/GMT-4 before 02:00EDT Nov. 6, 2011 and after 02:00EST Mar. 11, 2012; EST/GMT-5 between 02:00EDT Nov. 6, 2011 and 02:00EST Mar. 11, 2012).

[a]From ETD [http://var.astro.cz/ETD] where pre- or post-transit times were insufficient due to local horizon or sunrise/sunset to be calculated from our WesTEP program, though the transit itself is visible; airmass calculated from Birney, D.S., Gonzalez, G., and Oesper, D. (2006).

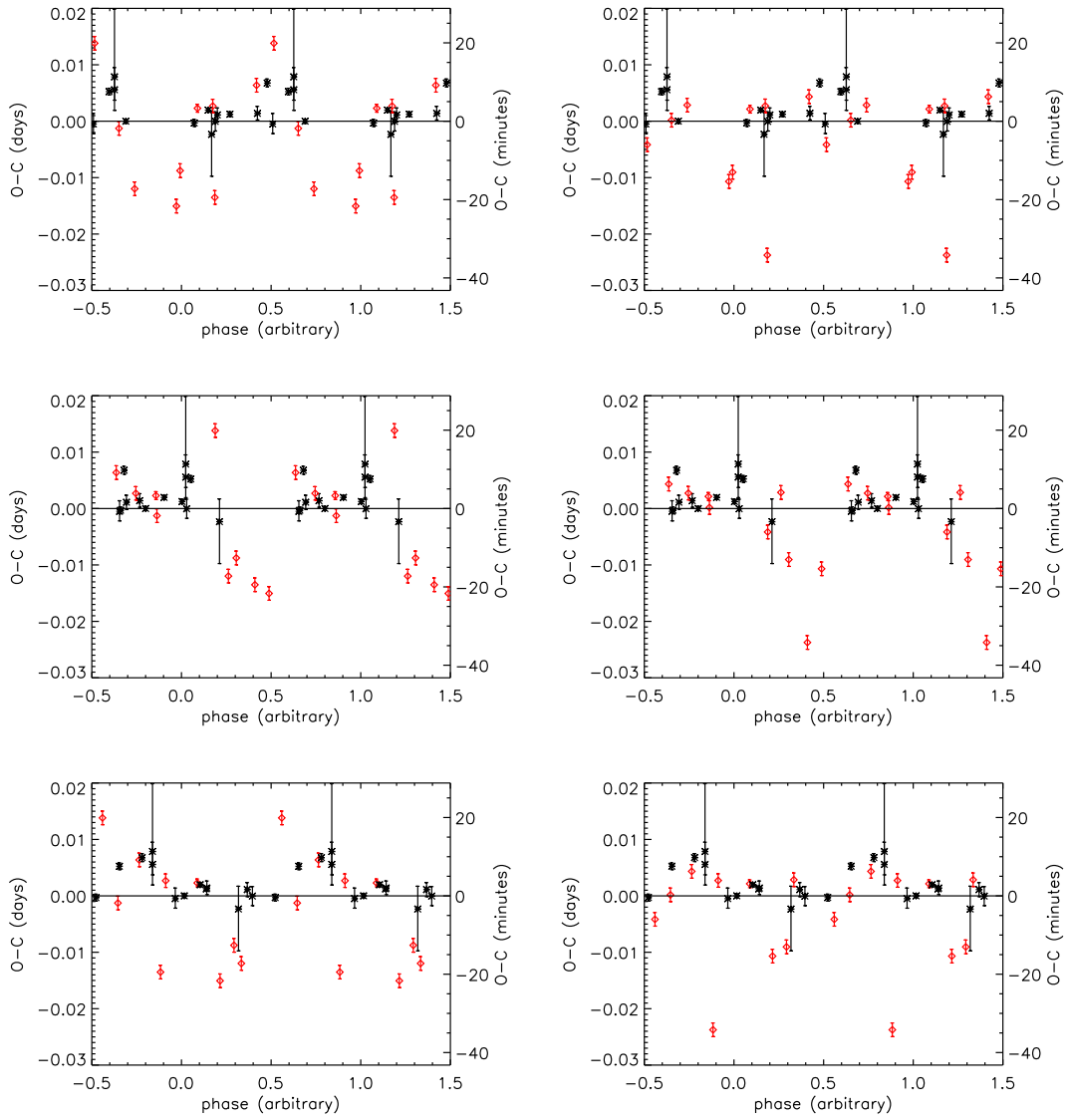

Figure 4.7: Here are $O - C$ points phased to a given period. The left column is $O - C$ points from free parameter fits; the right, from fixed parameter fits. *LEFT:: Top:* Free parameter fit phased to the period determined from its periodogram: 8.9734 days. *Middle:* Free parameter fit phased to period determined by periodogram of fixed parameter fit: 1.8076 days. *Bottom:* Free parameter fit phased to period determined by Johnson (2011): 14.1739 days. *RIGHT:: Top:* Fixed parameter fit phased to period determined from periodogram of free parameter fit: 8.9734 days. *Middle:* Fixed parameter fit phased to period determined from its periodogram: 1.8076 days. *Bottom:* Fixed parameter fit phased to period from Johnson (2011): 14.1739 days.

Chapter 5

Conclusions and Future Work

5.1 Conclusions

Overall the autoguider has helped to increase the pointing precision of the 24" telescope. Even with slight drifts still present the pointing precision has increased 5-fold over the telescope unguided. This increased precision should decrease noise in transits due to pixel-to-pixel sensitivity variations which ideally will bring our photometric precision to sub-centimagnitude levels (Konon 2008). The enhanced pointing precision, at its current state, allows for single exposures of $\sim$6 minutes or less to have a drift of $\lesssim$1 pixel ($\lesssim 0.34''$).

Direct photometric comparisons were not made between autoguided transits and those where the target star was manually recentered. Ideally the reduced drift should result in reduced photometric noise, however in real observations there are many other factors which may contribute to noise, e.g. clouds and seeing. Additionally, direct comparisons between autoguided and manually recentered transits may be difficult to compare as it would require observations of the same target both autoguided and manually recentered. To do this during a single transit would compromise the usefulness of the transit. Observing the same target on different nights, for proper comparisons, would require identical conditions both of weather and also the temperature of the 24" CCD. For these reasons the

pointing precision of autoguider was used as the measure of its efficacy instead of photometric noise levels.

The autoguider now also allows for higher cadence observations of transits, as observations do not need to be stopped to recenter the telescope. However, the telescope may need to be stopped periodically to adjust and hold a given focus; a proposed solution is discussed in the next section. These higher cadence observations may allow us to time transits more precisely and get down to the limiting timing precision of about 12 sec, this being the readout time of the 24" CCD assuming an exposure of <1 sec. This increase of timing precision can allow us to try and detect smaller transit timing variations, which in turn can mean the detection of smaller planets.

On the subject of transit timing variations, there were no conclusive timing variations found for WASP-33b. It is interesting to note that a TTV period of roughly 12–14 days has appeared as a possibility. However, the majority of light curves used here were only partial transits, therefore more full transit observations will be needed to distinctly show whether or not these TTVs are truly there or merely results of noise and hope.

So with all this said, now it is time to look to the future and what the observing program at VVO can become.

5.2 Future Work

First on the list is figuring out what is causing the remaining drift seen with the autoguider, likely something mechanical with the 24" telescope, and fix it. Ideally getting the autoguider to guide to sub-pixel accuracy would be great. This may then allow for single exposures up to the camera's limit of 3 hours 3 minutes (24"

CCD Manual: Apogee Alta U42) and full night observations, ∼8 hours, that do not show noticeable drift.

The next step in instrumentation for the 24" should be an autofocuser. This autofocuser would allow for even higher cadence observations than with just the autoguider, as it would obviate the need to stop an observation to regain or keep proper focus of the target. It could be a 'simple' plan using the current focusing system, which adjusts the position of the secondary mirror of the 24" telescope. Have MaxIm DL read out the FWHM on a given 'focus star' then send output, via a custom written pipeline, to the focus controllers to adjust the focus in order to keep a constant FWHM, within tolerance. This, however, will require the focuser to be on much finer controls than it currently is. The hand controls are much too aggressive and the nature of fine focusing right now with the telescope is generally overshooting one way or another until desired focus is reached.

The search for transit timing variations should continue at VVO. If we take the *Kepler* estimates (Ford et al. 2011) to be representative of the whole population of transiting exoplanets, then about 1 in 10 systems should show TTVs, a few of which should be detectable from VVO (Maciejewski et al. 2010, 2011).

Between Leiner (2010) (1), Johnson (2011) (20) and this thesis (38) there have been 59 transits observed from VVO. Therefore now, and especially in a few observing seasons, archival research can be done with data collected solely at VVO. Not only could these data be used to look for TTVs in other transiting systems, but they could also be used to look at the long term variability of stars. For WASP-33 this would be particularly beneficial as it is a known variable (Collier Cameron et al. 2010; Herrero et al. 2011). In addition to observations made solely with the 24" telescope, there have also been collaborations with Wellesley College and Swarthmore College, on planetary transits. Such collaborations, and espe-

cially simultaneous observations, are useful in removing systematic errors due to observing location and equipment, allowing for better measurements of transits. Simultaneous observations with separate telescopes may soon be done at VVO as well. The 16" telescope will shortly have an operating CCD, as well as spectrometer, which can be used for transit and other observations (Roy Kilgard, personal communication 2012).

As a whole, the field of astronomy, maybe more than others, is greatly reliant on the advances in technology and instrumentation to collect new and higher quality data. I believe that a strong focus on maintaining and advancing the instruments here at VVO will help to advance the precision and breadth of data collected, and in turn expand the types of research that we are able to do here at our humble, hilltop home.

Appendix A

Autoguider Manual

INSTRUCTION MANUAL

Orion® StarShoot™ AutoGuider
#52064

ORION®
TELESCOPES & BINOCULARS
Providing Exceptional Consumer Optical Products Since 1975

Customer Support (800) 676-1343
E-mail: support@telescope.com
Corporate Offices (831) 763-7000
89 Hangar Way, Watsonville, CA 95076

IN 324 Rev. C 02/09

Welcome to a world of astro-imaging with trouble-free automatic guiding! Your StarShoot AutoGuider (SSAG) automatically fixes on a star and sends tracking corrections to your mount to enable perfectly round stars in your astro-images. Autoguiding is an immense help for your astro-imaging productivity. The SSAG enables your telescope to precisely track the apparent movement of the night sky without the need for you to monitor your telescope setup every second. The tracking corrections made by the SSAG will compensate for mechanical imperfections inherent in all telescope mounts. This essential astro-imaging tool allows you to relax under the stars while your telescope tracks and takes images.

Parts List

- StarShoot AutoGuider
- 10' USB Cable
- 6' autoguide interface cable
- CD-ROM

System Requirements

[Quick setup diagram (Figure 1a & 1b)]

Primary Telescope/Main Imaging Scope

Your main imaging scope will be used with your main astro-imaging camera. The main imaging scope can be virtually any scope suitable for your CCD or DSLR camera.

Guide Scope

You will need an additional telescope for guiding, referred to as a guide scope. The guide scope is mounted on top of, or beside the main imaging scope. Adjustable guide scope tube rings (available from Orion) are recommended and allow you to move the guide scope around without moving the main imaging scope (Figure 2). The guide scope is adjusted in the same fashion as a finder scope.

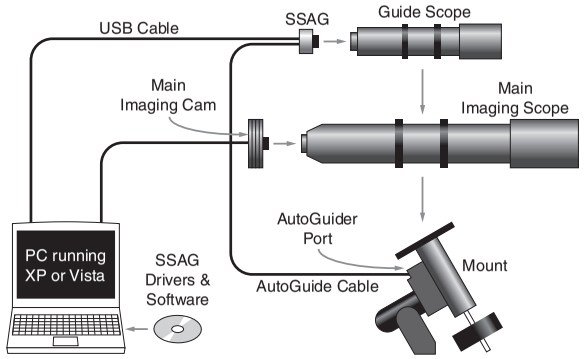

Figure 1a. A traditional imaging setup contains a main imaging scope and separate guide scope. The SSAG interfaces with your computer via the USB cable, and connects to your mount's autoguide port via the autoguide cable.

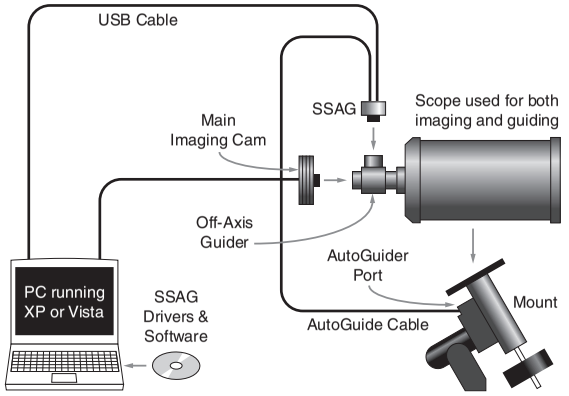

Figure 1b. Cassegrain style telescopes can be used with an off-axis guider. This allows both the main imaging camera and autoguider to use the same telescope.

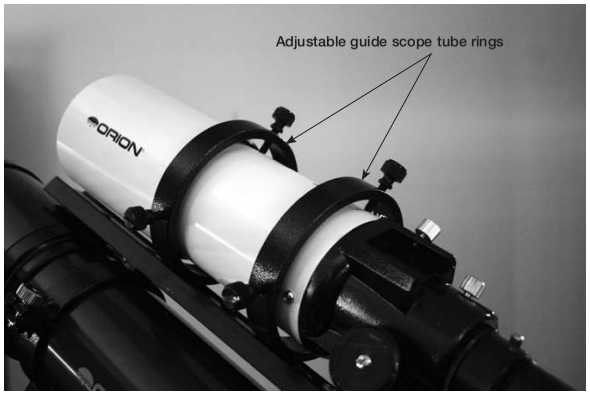

Figure 2. Adjustable guide scope tube rings allow you to adjust the position of the guide scope without moving the main imaging scope.

Because of the high resolution and accuracy of the SSAG, you do not need a large guide scope; any small refractor will serve well for this purpose. Separate refractor optical tube assemblies, such as the Orion Short Tube 80, make excellent guide scopes.

The only exception to using a guide scope is to is use an off-axis guider, which is typically made for Schmidt-Cassegrain telescopes (Figure 1b). The off-axis guider uses a prism to intercept a small portion of the light path in front of the camera, thus allowing the camera and guider to use the same telescope. Off-axis guiders require a large amount of inward focus travel which is why they are generallly only suitable for Schmidt-Cassegrain telescopes.

Mount

An equatorial mount with dual axis motors and a RJ-12 autoguide port is required. Just about any equatorial mount equipped with an autoguide port will work with the SSAG (Figure 3a). The SSAG is "ST-4" compatible which uses the same pin out configuration as the first generation CCD autoguiders (Figure 3b). Most computerized goto mounts also have this autoguide port. For short exposure deep space photography (typically 45 seconds or less) the SSAG can successfully guide with a computerized altitude-azimuth or fork mounted telescope, popular among computerized Schmidt-Cassegrain telescopes. However, guided exposures longer than one minute in an altitude-azimuth mount will cause field rotation to occur in the image (Figure 4). An equatorial mount will yield the best overall performance for guided deep space astrophotography.

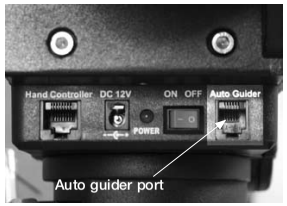

Figure 3a. The SSAG works with any mount equipped with an ST-4 compatible autoguide port, shown here on the Sirius EQ-G mount.

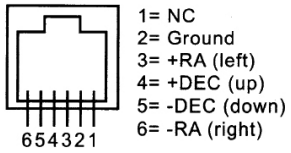

Figure 3b. This is the pin diagram for the SSAG and ST-4 compatible mounts.

Figure 4. Field Rotation occurs in long exposure images taken with an altitude-azimuth mount or poorly polar aligned equatorial mount.

Computer

The SSAG requires a PC running Windows XP or Vista. For astro-imaging in the field at night, a laptop computer is highly recommended.

The computer hardware should have at least the following:

- Pentium™ Processor
- 128MB RAM
- Disk Space – 50MB, 100MB or more is recommended
- Video Display – 800 X 600, 16-bit color or higher, 1024 x 768 or higher is recommended
- Mouse
- USB High Speed 2.0 port

Software and Driver Installation

Before the camera can be used, software and camera drivers must be installed onto your computer. Turn on your computer and allow the Windows operating system to load as normal. Insert the included CD-ROM into your computer's CD-ROM drive, and the Launcher will appear (Figure 5). This allows you to install the PHD Guiding software. Do not connect the camera to your computer before you have installed the software.

Figure 5. The launcher offers and easy way to start installing the camera and software.

Software Installation

1. Insert the CD-ROM and wait for the **Launcher** window to appear. If you are using Windows Vista, the **AutoPlay** window will appear first, then select **Run Opener.exe**.
2. When the launcher appears, select **Install PHD Guide**.
3. Read the license agreement and select **I accept the agreement** if you agree with the terms. Follow the prompts to complete the software installation.

Installing the camera using a Windows XP computer:

1. Insert the CD-ROM and wait for the launcher window to appear.
2. When the launcher appears, select **Install Drivers**. Do not plug the camera in before loading the drivers.

3. Once the drivers have been installed, connect the SSAG to your computer's USB port.
4. In Windows XP a **Found New Hardware Wizard** appears (Figure 6).

Figure 6. In Windows XP the Found New Hardware Wizard appears when you first plug the SSAG into your USB port.

5. Windows will ask if you want to search for drivers and updates online. Select **No, not this time** and click **Next**.
6. Next, choose **Install the software automatically**.
7. Windows will note that the driver has not passed Windows Logo testing. This is normal. Click the **Continue Anyway** button. When the Wizard has completed, click the **Finish** button.
8. You will immediately be prompted with a **Found New Hardware Wizard** again. This time the camera firmware will be installed. Make the same selections again in the Wizard, **No, not this** time, click **Next**, and choose **Install the software automatically**. The camera is now installed on your computer and the red LED on the camera should be on.

Installing the camera using a Windows Vista computer:

1. Insert the CD-ROM and wait for the **AutoPlay** window to appear. Load **Run Opener.exe.** (Figure 7)

Figure 7. In Windows Vista the **AutoPlay** screen appears when you insert the CD-ROM into your computer. Select **Run Opener.exe** when prompted with this screen.

2. Select **Install Drivers.** Follow the prompts in the install screen to complete the driver installation.
3. Windows will note that the driver has not passed Windows Logo testing. This is normal. Click the **Continue Anyway** button. When the Wizard has completed, click the Finish button.
4. Once the drivers have been installed, connect the SSAG to your computer's USB port.
5. Windows Vista will automatically detect the camera and install the device for you. Wait for the dialog box in the taskbar to say **Device Installed Successfully**. The camera is now installed on your computer and the red LED on the camera should be on.

Getting Started During the Day

We recommend using the SSAG for the first time during the day. This way, you can become familiar with the basic camera functions without having to stumble around in the dark. Setup your telescope and mount so the optical tube is pointing at an object that is at least a couple of hundred feet away. Insert an eyepiece and focus as you normally would.

Note: Under normal use the SSAG is coupled to a separate guide scope which is mounted or piggy-backed onto the imaging scope. For initial setup during the day, you do not need to have both telescopes setup, but you should use the same guide scope you intend to use later at night.

First let's explore the interface of PHD Guiding. PHD Guiding makes the task of autoguiding very easy and the setup can be accomplished in minutes.

PHD Guiding Screen Layout

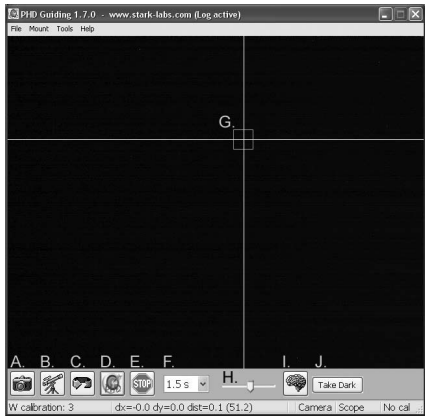

A. Connect to Camera: Selects and connects to the autoguider camera. Choose the StarShoot AutoGuider or the older StarShoot DSCI camera

B. Connect to Telescope: This command connects the SSAG to your mount. To connect the SSAG to your mount, go to the **Mount** menu and select **On-camera**, then click this icon.

C. Looping Exposures: Takes continuous exposures for acquiring and focusing the guide star.

D. PHD Guide: Automatically calibrates and guides. Once your guide star is found and focused, simply click on the star and click PHD Guide. The rest is automatic!

E. Stop: Stops either calibrating, guiding, or looping exposures.

F. Exposure Selection: Choose from 14 different exposure times for the camera.

G. Guide Star Box: When a guide star is selected, a green box appears around it. PHD Guiding will display the pixel coordinates of the star in the lower left screen. When the calibration routine starts, yellow crosshairs are displayed around the box. When the autoguiding begins, the crosshairs turn green. This box does not appear until a guide star has been selected. (See "Start Autoguiding")

H. Gamma Adjustment: Adjust the apparent screen brightness level in the image by moving the slider bar left (brighter) or right (fainter).

I. Advanced Parameters: Control the camera and guiding routine settings. You do not typically have to adjust the advanced parameters. For very bright guide stars, or for daytime testing, the camera gain can be adjusted in this menu. (See "Advanced Autoguider Settings" for more detail about this menu.)

J. Take Dark Frame: Captures and internally saves a dark frame that is automatically subtracted from future exposures. Taking a dark frame is optional and not required for normal use. See "Dark Frames and Noise Reduction" for more information.

Since the SSAG camera is so sensitive to light, you will need to reduce the gain of the camera to effectively use it during the day.

1. Plug the SSAG into your computer's USB port.
2. Insert the SSAG into the 1.25" eyepiece holder on your guide scope.
3. Open PHD Guiding and select the **Connect to Camera** icon.
4. Click on **Advanced Parameters** (the brain icon) and locate the Camera gain (%) field.
5. Adjust the **Camera gain** (%) to **5%** and click **Done.**

Note: The default camera gain is 95%. After you are done using the camera during the day, change the gain back to 95% to retain the high sensitivity of the camera.

6. In the **Exposure Selection** pull down menu, select **0.05 s.**
7. Click the **Looping Exposures** icon to begin taking continuous pictures.
8. Gradually move the telescope focus inward until you get a sharp image on your computer screen (Figure 8). The SSAG focuses approximately 15mm inward from a standard 1.25" eyepiece. On most refractors, a 1.25" extension tube (available from Orion) is usually needed to reach focus. Alternatively, you can use a star diagonal. Note the approximate position of your focuser where the SSAG reached focus on your guidescope to make the same task at night much easier.
9. Experiment with the **Gamma Adjustment** as needed to see a high contrast image. The **Gamma Adjustment** during the day will likely need to be different at night, but you should become familiar with this adjustment before you setup at night.

Figure 8. Gradually move the focuser inward until you have a clear daytime image on your computer screen.

Start Autoguiding

The SSAG with the use of PHD Guiding software makes the task of autoguiding simple and easy to setup. The calibration and guiding is automatic once you initially find and focus a guide star. Your telescope must first be prepared for astroimaging. Make sure your mount is polar aligned well. Your guide scope should be securely attached to your main imaging scope; or if you are using a Schmidt-Cassegrain, the off-axis guider and main camera should already be attached to the telescope.

Note: Autoguiding can correct for a mount that is poorly polar aligned. However the image will be harder to initially locate and center since it will still drift away from the camera's field of view. Additionally, guiding with a poor polar alignment will eventually cause field rotation in a long exposure image.

1. Locate, center and focus the celestial object you wish to image with your CCD or DSLR camera in your main imaging scope. Once you have centered the desired object, it is important to make sure the tracking on your mount is engaged so you don't loose the object before the guiding starts.
2. Using a low power 1.25" eyepiece, locate and center a fairly bright star in your guide scope. Do not move the main imaging scope or your object will be lost! As stated in "System Requirements", we recommend using adjustable guide scope tube rings to allow independent movement of the guide scope.
3. Remove the eyepiece and insert the SSAG into your guide scope.
4. Plug the SSAG into your computer's USB port and connect the autoguider cable from the SSAG to your mount's autoguide port. Load PHD Guiding on your computer.
5. Click the **Connect to Camera** icon and select the **StarShoot AutoGuider.**
6. In the **Exposure Selection** pull down menu, select **2.0 s** (Figure 9).

7. Click on the **Looping Exposures** icon to begin continuously taking pictures.
8. Gradually move the focus inward on your guide scope until you see the star come into focus. As you get close to focused, the camera may start detecting several faint background stars.
9. Once you have reached focus and you can see at least one clearly defined star, click the **Stop** icon.
10. Click on the star you want to guide on. A green guide star box should appear around the star you selected. In the lower left screen, the pixel coordinates of the star is displayed. If the guide star box is yellow, a message appears at the bottom of the screen **LOW SNR**. If you see this message, you need to select a brighter star. Increase the exposure time if necessary.

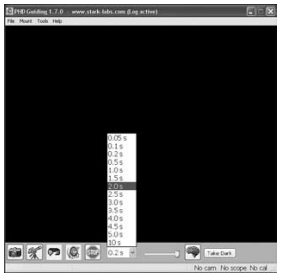

Figure 9. Select **2.0 s** in PHD Guiding to set the exposure time to 2 seconds.

Figure 10. Yellow crosshairs appear once the calibration begins. The process is automatic. The crosshairs turn green when guiding begins.

11. Go to the **Mount** menu and make sure **On-camera** is selected. Click on the **Connect to Telescope** icon.
12. Click the **PHD Guide** icon and the calibration will begin (Figure 10). The rest is automatic! Yellow crosshairs are displayed around the guide star box when the calibration starts. The calibration is automatic and takes a few minutes. When the calibration is complete, the autoguiding begins automatically and the crosshairs turn green. You are now ready to take astro-images with precise tracking!

Note: Be patient while PHD Guiding completes the calibration. The telescope cannot be disturbed during the calibration process. It is just as critical not to touch the telescope during calibration as it is when exposing an astro-image. The calibration ensures that the AutoGuider knows the movements and tracking behaviors of your mount.

Dark Frames and Noise Reduction

All CCD and CMOS cameras have inherent noise which becomes more apparent with longer exposure images. If you require taking longer exposures (typically longer than 3 seconds) you may start to see vertical lines and bright dots (hot pixels). There are several ways to reduce the amount of noise seen in your guiding images. You will get the best guiding performance when your image background looks smooth and black. The **Gamma Adjustment** will help clip the low level background noise by adjusting the slider bar left or right as needed. You can also reduce the camera **Gain** or enable **Noise Reduction** (see "Advanced Autoguider Settings"). **Take Dark** saves a dark frame which is subtracted from your guiding images to remove most of the noise. Dark frames are images taken with the camera capped from incoming light, revealing only the camera noise in the image. This noise is subtracted from a "light frame" which is the image you want to see from the camera.

To take the dark frame:

1. Cap the objective of your guide scope.
2. Keep the **Exposure Selection** set to the same time you wish to use for guiding. For example, if you choose **2.0 s**, then you must keep this exposure time while guiding for the dark frame to be effective.
3. Click **Take Dark.**
4. Remove the cap from your guide scope and resume taking pictures or guiding. PHD Guide will automatically subtract the dark frames from all of your exposures. To remove the dark frame, go to **Tools** and select **Erase Dark Frame.**

Advanced Autoguider Settings

The **Advanced Parameters** (the brain icon) in PHD Guide allows you to change several settings to better customize the guiding performance of your SSAG. Under normal use, you should not have to make any major adjustments to the **Advanced Parameters**. All of the calibration and autoguiding is done automatically simply by pressing the **PHD Guide** icon. However the following settings can be adjusted to cater to your specific guiding setup:

Advanced Parameters

R.A. Aggressiveness: Adjusts the percentage of R.A. correction per step. The default value is 100, meaning that the guider will move the full distance of the correction. If the seeing conditions are not steady, the aggressiveness can be turned down to smooth out the quick movements and reduce the correctional movement.

R.A. Hysteresis: Implements a percentage of the previous averaged tracking corrections to the current tracking corrections. This setting can be useful if you are experiencing some wind or severe periodic error, since the guider will partially

ignore some of the radical movements and repeat a percentage of the previous tracking corrections.

Dec Guide Mode: This setting should not be changed under normal use. You can optionally disable dec guiding, or limit which direction the guider will allow dec to be corrected on (north or south). The default setting automatically finds which side dec is drifting (north or south).

Dec Algorithm: Ideally corrections made in declination should only be one consistent direction, usually based on how well the mount is polar aligned. The **Dec Algorithm** takes this into account and attempts to keep the declination tracking consistent. Choose **Resist switching** or **Lowpass filter** which are algorithms that try to keep dec on one side of drift, or average the corrections made in dec.

Calibration Step: Adjusts how long each guide pulse is during calibration. The default is 500 milliseconds. The calibration step can be increased to provide a better sample of movement. However, if the calibration step is increased too much, the guide star will move out of the camera's field of view during calibration.

Min. Motion: Number of pixels the star must move before PHD will make a guiding correction. The default is 0.25 pixels.

Search Region: The area in pixels that the guide star is searched for and looked at. The default is 15x15 pixels. Under normal use, this setting should not be changed.

Noise Reduction: Choose from 2x2 mean or 3x3 median to smooth out noise and blur out hot pixels.

Time Lapse: This setting optionally sets a delay between each guiding correction. For mounts that track exceptionally well, you can add a delay between each correction.

Gain: The gain adjusts the camera's internal brightness level and sensitivity. The default is 95%. If you are experiencing excessive noise or hot pixels, you can reduce the gain. The camera remains very sensitive as low as 50% gain. If you are guiding on a very bright guide star, you can afford to turn down the gain and further decrease the noise in your image.

Force Calibration: Enabling this setting makes PHD Guide calibrate every time a new star is chosen. If you move your telescope to another object in the sky, you will need to recalibrate the autoguider. The default has this setting enabled.

Log Info: You can log all actions into a text file saved in the PHD directory.

Disable Guide Output: This setting deliberately shuts off the autoguider output for potential troubleshooting measures.

Tips & Tricks

If all conditions are ideal, and your tracking is superb, you typically do not have to alter any of the camera's default settings. However, if your setup is tracking much worse than usual (such as a night with high wind or poor seeing), you may need to customize your settings to better adapt to the current conditions in the field.

Reduce the R.A. **Aggressiveness** in the **Advanced Parameters** menu to better stabilize the guiding during bad seeing or wind gusts. You may also want to decrease the **R.A. Aggressiveness** if your guiding exposures/corrections are set very quickly (less than 1 second). If the guider sends several corrections per second to the mount, the mount's movement may osculate due to the response time of your mount. Additionally the varying seeing conditions makes the star appear to jump around rapidly and cause the guider to make unnecessary corrections, sometimes referred to as "chasing the seeing". If seeing is poor, keep the guiding correction intervals/exposures to 1 second or more. For most guide scopes, we recommend setting the autoguide exposures between 1-4 seconds for best results.

Polar Alignment

A good polar alignment of your EQ mount is of critical importance for long-exposure imaging. Inaccurate polar alignment leads to field rotation, even with the autoguider tracking. If your equatorial mount uses a polar axis finder scope, we highly recommend utilizing it for polar alignment. If not, a technique known as the "drift method" of polar alignment has been used for many years, and can achieve an extremely accurate polar alignment. Unfortunately it is very time consuming, since the drift of a star over time must be observed. The basic idea is to let the telescope mount track while watching a star to see which way the star drifts. Note the direction of the drift, and correct by moving the mount in the appropriate direction.

To perform the drift method of polar alignment:

1. Roughly polar align your mount by pointing the R.A. axis of the mount at Polaris (the NorthStar).
2. Find a bright star near the meridian (the imaginary line running north-to-south through zenith) and near the celestial equator (zero degrees declination). Point the telescope at this star, and center it in an illuminated reticle eyepiece (available from Orion). If you don't have an illuminated reticle eyepiece, use your highest- magnification eyepiece.
3. Determine which way is north and south in the eyepiece by moving the telescope tube slightly north and south.
4. Now, let the mount's motor drive run for about five minutes. The star will begin to drift north or south. Ignore any east-to-west movement.
5. If the star drifts north, the telescope mount is pointing too far west. If the star drifts south, the telescope mount is pointing too far east. Determine which way the star drifted and make the appropriate correction to the azimuth position of the mount. Rotate the entire mount (and tripod) slightly east or west as needed or use the azimuth adjustment knobs (if your mount has them) to make fine adjustments to the mount's position.
6. Next, point the telescope at a bright star near the eastern horizon and near the celestial equator (Dec. = 0).

7. Let the telescope track for at least five minutes, and the star should begin to drift north or south.
8. If the star drifts south, the telescope mount is pointed too low. If the star drifts north the telescope mount is pointed too high. Observe the drift and make the appropriate correction to the mount's altitude (or latitude); most mounts have some sort of fine adjustment for this.

Repeat the entire procedure until the star does not drift significantly north or south in the eyepiece after a few minutes. When this is accomplished, you are very accurately polar aligned. Autoguiding on a well polar aligned mount will yield the best results for your images. The fewer tracking corrections that have to be made, the better your images will be.

Differential Tube Flexure

A common obstacle in guiding with a separate guide scope and imaging scope is differential tube flexure, the unwanted movement of a guide scope in relation to the main imaging scope. If any part between the autoguider and imager moves or flexes during the exposure, then the resulting image will have oblong stars which gives the appearance of poor tracking. There are a few basic measures to ensure your guide scope is securely in place:

1. If your guide scope has a focus lock, firmly tighten the focus lock thumb screw after you have focused on your guide star.
2. If you are using adjustable guide scope tube rings, make sure all thumb screws are firmly tightened against the guide scope tube.
3. The guide scope tube rings and mounting plate should be tightened very securely against the main imaging scope. Check for any visual flexure or movement by gently pressing against the guide scope.
4. The focuser and tube rings on the main imaging scope should also be firmly in place. It is not uncommon for screws and bolts to come loose after a few usages; so they should be checked before each imaging session.

Cabling

The SSAG uses only two light-weight cables; a USB cable and the autoguide cable. Keep an eye on the cables as you move the scope around. If there is any stress on the cables, your tracking may be affected.

Some imaging cameras use heavy-duty cables with significant weight. These cables can contribute to differential tube flexure. If you are getting images with oblong stars and your tracking appears to be good otherwise, try tying any heavy cables to a secure location on your mount. It does not take much resistance against the autoguider or imager to create poor tracking.

USB Extension Cable

In many instances, it is likely a longer cable for the SSAG will be needed in order to comfortably setup the telescope, camera, and computer. We recommend purchasing a 10' USB extension cable if you need more cord length (available from Orion).

Using the SSAG with MaxIm DL Essentials

For StarShoot Deep Space Imaging Camera users MaxIm DL Essentials version 1.08 and later supports the use of the SSAG. You can simultaneously operate the StarShoot AutoGuider and StarShoot Deep Space Imager at the same time.

1. Plug the SSAG and the SSDSCI/SSDSMI (II) into the USB ports on your computer.
2. Load MaxIm DL Essentials. The **Camera Control** window should have an option to select **Cam 1** or **Cam 2** (Figure 11). You will also notice the **Imaginova StarShoot AutoGuider** window appear in the center of the screen (Figure 12). This window allows you to adjust the camera gain and optionally enable noise reduction.

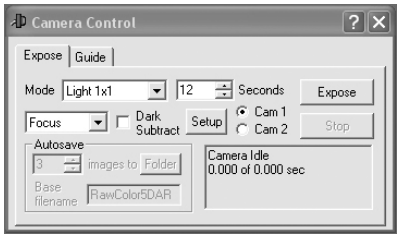

Figure 11. **Cam 1 / Cam 2** camera control window in MaxIm DLE

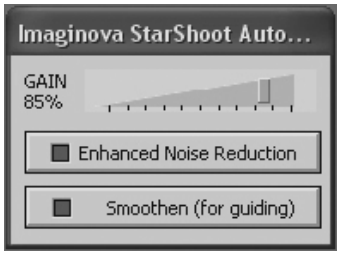

Figure 12. MaxIm DLE AutoGuider window allows you to adjust the camera gain and optionally enable noise reduction to smooth out the background noise.

3. Determine which camera the SSAG is, **Cam 1** or **Cam 2**. This is done by taking a 1 second exposure in each camera. The camera that has the larger 1280x1024 image is the SSAG.
4. Click the **Autoguide** tab in the camera control window. Select the camera that corresponds to the SSAG.
5. Click the **Settings** button.
6. Maxim DL Essentials needs to know how fast the telescope moves in right ascension (R.A.) and declination (Dec.) when the autoguider commands are issued. To do this, the software will Calibrate the mount by moving it back and forth on each axis. The **Calibration Time** determines how long it activates the motors each time. The default value is 10 seconds. Make sure all of the **Guider Enables** boxes are checked (Figure 13).

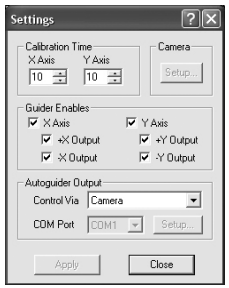

Figure 13. The autoguide **Settings** window controls the **Calibration Time** in each axis, movement in both axis, and the **Autoguider Output** connection to your mount.

7. For **Autoguider Output**, set **Control Via** to **Camera**.
8. Click **Apply**. You can leave this dialog box open, or **Close** it if you wish. On the **Guide** tab, set to **Expose**, and click the **Start** button. A single image will be taken. Ensure that a well-focused bright star (near the actual object to be imaged) appears in the image. If not, adjust the guide scope and try again. Make sure the star is not close to the edge of the camera's field of view or it may drift out during calibration.

Note: The algorithm can be confused if another star appears in the frame; to minimize this risk, calibrate on an isolated bright star.

9. Now, set to **Calibrate**, and click the **Start** button. A series of five exposures will be taken; each time the telescope will be moved slightly. If the telescope does not move, check the Settings.
10. The star should move in an "L" shape. If it does not move enough, a warning message will appear. The recorded positions will be displayed in the scrolling log, along with any error messages.

*Note: If the star does not move far enough, or moves too far (i.e. the star leaves the field), the duration of the calibration move commands can be adjusted by clicking the **Settings** command and changing the **Calibration Time** fields (measured in seconds). A longer calibration time will increase the motion of the star; a shorter time will decrease the motion. Typical values range from five to ten seconds, depending on the correction speed, focal length, and pixel size.*

11. Once you have successfully calibrated, switch to the **Track** mode. Click **Start**, and watch the star. It should move to the center of the small track box, and whenever it drifts off it should be pulled back again. Also the tracking errors will be displayed in the scrolling log (Figure 14).

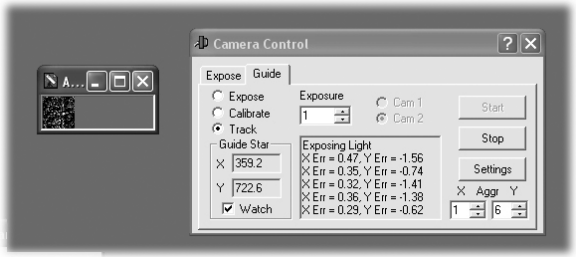

Figure 14. Autoguiding in MaxIm DL displays the guide star in a small window with the **Watch** box enabled. The tracking corrections are also displayed in the **Camera Control** window.

12. If the star bounces back and forth, reduce the aggressiveness for that axis. If it corrects too slowly, increase the aggressiveness. Changes to the aggressiveness settings take effect immediately.

Care and Maintenance

When the SSAG is not in use, the cover cap should be replaced on the end of the nosepiece. This prevents dust from accumulating on the SSAG's optical window. The optical window should only be cleaned if significant dust builds up for if the window is touched. Any quality optical lens cleaning tissue and optical lens cleaning fluid specifically designed for multi-coated optics can be used to clean the glass surface of the SSAG's optical window. Never use regular glass cleaner or cleaning fluid designed for eyeglasses. Before cleaning with fluid and tissue, blow any loose particle off the surface with a blower bulb or compressed air. Then apply some cleaning fluid to a tissue, never directly on the optics. Wipe the optical surface gently in a circular motion, then remove any excess fluid with a fresh lens tissue. Use caution, rubbing too hard may cause scratches.

Specifications

Camera Sensor:	Monochrome CMOS Micron MT9M001
Sensor format:	1/2"
Pixel array:	1280 x 1024 (1.3Mp)
Pixel Size:	5.2µ x 5.2µ
Exposure Range:	0.05 seconds to 10 seconds
A/D Conversion:	8 bit
Thermoelectric cooling:	No
IR-cut filter:	No
Mounting:	1.25" nose piece or t-thread
Weight (oz.):	4.4
Dimensions:	2.5" wide x 2.35" long
Mount connection:	Via RJ-12 modular jack (6-pin)
Autoguide commands:	"ST-4" output

This device complies with Part 15 of the FCC Rules. Operation is subject to the following two conditions: (1) this device nay not cause harmful interference, and (2) this device must accept any interference received, including interference that may cause undesired operation.

Changes of modifications not expressly approved by the party responsible for compliance could void the user's authority to operate the equipment.

Note: This equipment has been tested and found to comply with the limits for Class B digital device, pursuant to Part 15 of the FCC Rules. These limits are designed to provide reasonable protection against harmful interference in a residential installation. This equipment generates, uses and can radiate radio frequency energy and, if not installed and used in accordance with the instructions, may cause harmful interference to radio communications. However, there is no guarantee that interference will no occur in a particular installation. If this equipment does cause harmful interference to radio or television reception, which can be determined by turning the equipment off and on, the user is encouraged to try to correct the interference by one or more of the following measures:

Reorient or relocate the receiving antenna.

Increase the separation between the equipment and receiver.

Connect the equipment into an output on a circuit different from that to which the receiver in connected.

Consult the dealer or an experienced radio/TV technician for help.

A shielded cable must be used when connecting a peripheral to the serial ports.

20

21

NOTE: Pages 22–23 as labeled in the autoguider manual are not shown here because they are simply lined pages for notes and contain no information.

One-Year Limited Warranty

This Orion StarShoot AutoGuider is warranted against defects in materials or workmanship for a period of one year from the date of purchase. This warranty is for the benefit of the original retail purchaser only. During this warranty period Orion Telescopes & Binoculars will repair or replace, at Orion's option, any warranted instrument that proves to be defective, provided it is returned postage paid to: Orion Warranty Repair, 89 Hangar Way, Watsonville, CA 95076. If the product is not registered, proof of purchase (such as a copy of the original invoice) is required. This warranty does not apply if, in Orion's judgment, the instrument has been abused, mishandled, or modified, nor does it apply to normal wear and tear. This warranty gives you specific legal rights, and you may also have other rights, which vary from state to state. For further warranty service information, contact: Customer Service Department, Orion Telescopes & Binoculars, 89 Hangar Way, Watsonville, CA 95076; (800) 676-1343.

Orion Telescopes & Binoculars

89 Hangar Way, Watsonville, CA 95076

Customer Support Help Line (800) 676-1343 • Day or Evening

Appendix B

Guidescope Manual

INSTRUCTION MANUAL

Orion® Deluxe 100mm f/6 Refractor

#7338

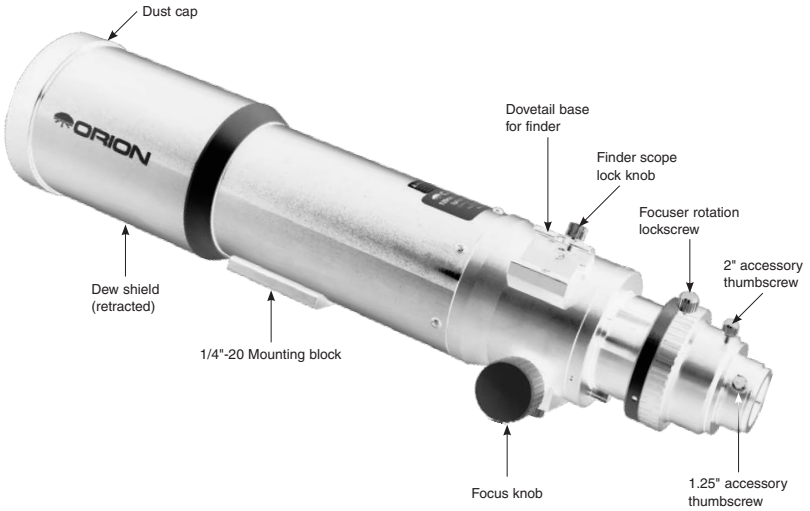

Figure 1: The Deluxe 100mm f/6 refractor optical tube.

ORION®

Providing Exceptional Consumer Optical Products Since 1975

OrionTelescopes.com

Customer Support (800) 676-1343 • E-mail: support@telescope.com

Corporate Offices (831) 763-7000 • 89 Hangar Way, Watsonville, CA 95076

© 2008-2010 Orion Telescopes & Binoculars

IN 392 Rev. A 05/10

Congratulations on your purchase of an Orion Deluxe 100mm f/6 optical tube. Your telescope has been designed with high quality precision optics and excellent mechanical construction. The linear bearing dual-speed (10:1) Crayford focuser will make getting sharp images a breeze and reduce image shift to almost zero. The intermediate f/6 focal ratio will show only moderate color fringing. Your new telescope is versatile enough to also be used as a guidescope. These instructions will help you set up and use your optical tube.

Getting Started

The Deluxe 100mm f/6 comes fully assembled from the factory. The telescope's optics have been assembled and collimated at the factory, so you should not have to make any adjustments to them.

Please keep the original shipping box. In the unlikely event you need to ship the telescope back to Orion for warranty repair service, you should use the original packaging. The box also makes a very good container for storing the telescope when it is not in use.

Optical Use

The fine optics and precision machining make the Deluxe 100mm f/6 an excellent choice for astronomical and terrestrial observation. You will need to add an optional diagonal and eyepiece to the back end of the telescope. The telescope will accept 2" or 1.25" accessories. Simply slide your diagonal into the open end of the telescope and insert the eyepiece into the diagonal and it is ready to show you the visual beauty of the night sky.

For terrestrial observation a correct image diagonal is recommended. These are typically available as 1.25" accessories only.

Use of Optional Eyepieces, Diagonal, and Finder Scope

The Deluxe 100mm f/6 does not come with a finder scope, diagonal or eyepieces in order to grant the user the greatest versatility in customizing the instrument to suit their needs. However, certain rules for using accessories still apply.

Any Orion finder scope with a dovetail bracket can be used with the Deluxe 100mm f/6. Simply unthread the thumbscrew on the dovetail mount and insert the assembled finder scope and dovetail bracket. Retighten the thumbscrew (Figure 1). Finder scopes that do not use a dovetail bracket will need to be attached by other means.

The Deluxe 100mm f/6 can use 1.25" accessories. Please note that the telescope will not come to focus without the use of a diagonal or extension tube. To install a diagonal, unthread the thumbscrew on the 1.25" adapter until it is flush with the interior of the adapter (Figure 1). Insert the diagonal or extension tube and secure it with the thumbscrew. Then insert the eyepiece into the diagonal or extension tube and secure it with the thumbscrew(s).

Use of 2" Eyepieces and Diagonals

A feature of the Deluxe 100mm f/6 is its ability to also use 2" barrel-diameter eyepieces and diagonals. At low magnifications, 2" eyepieces can give a wider field of view than standard 1.25" eyepieces. This is especially desirable for observing deep-sky objects, as many of them appear quite large, but faint.

To use 2" eyepieces, simply loosen the large thumbscrew on the 2" adapter (Figure 1). Once this thumbscrew is loosened, the entire back end of the focuser, including any 1.25" diagonal and eyepiece that may be attached, comes off, exposing the 2" adapter. Now, insert your 2" diagonal into the drawtube and secure with the thumbscrew loosened previously. Insert a 2" eyepiece into the diagonal, secure it in place with the thumbscrew on the diagonal, and you're ready to observe.

About the 2" Linear Bearing Dual-Speed Crayford Focuser

The Deluxe 100mm f/6 comes equipped with a 2" linear bearing dual-speed Crayford focuser. The linear bearing Crayford design allows for smooth, precise focusing without the image shift that rack-and-pinion and typical Crayford designs experience. The linear bearing is a "track" that guides the drawtube in and out on a precise path to further reduce any wobble in the drawtube which could cause image shift.

There is also a fine adjustment capability on this focuser. Ten turns of the small knob protruding from the right focus knob equals one turn of the coarse adjustment knob. Once you have achieved the best possible focus on an object using the coarse adjustment knob; you can fine-tune your focus using this slow motion knob to make micro-adjustments. This will allow delicate adjustments to be made to get the sharpest images possible.

If you find that the focus adjustment is too hard to turn or does not hold in place properly once you've achieved focus, you can make adjustments to the focuser tension by using the focus tension thumbscrew located on the bottom of the optical tube, between the focus knobs. Make adjustments to this thumbscrew until the focuser motion feels smooth to turn and holds in place when you have obtained focus. It may be necessary to make adjustments when the weight of your accessories change significantly.

Using as a Guidescope

The purpose of the guidescope is to monitor a guide star during long-exposure astrophotography in order to make corrections to the mount's tracking rate. This is done by centering a star on the reticle of the illuminated reticle eyepiece used with the guidescope. By keeping that star centered you assure that the view through the telescope (and imager) remains constant. Without use of a guidescope, the telescope will not

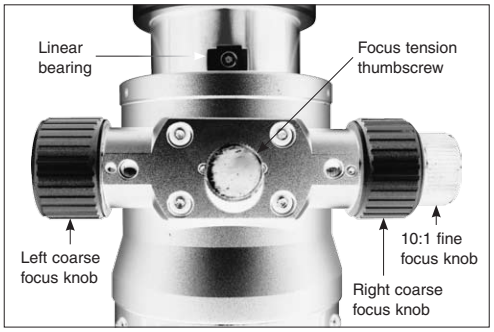

Figure 2: Focuser detail

track the motion of the night sky accurately enough and long-exposure photography will be difficult, if not impossible.

The Deluxe 100mm f/6 comes without accessories. To set up and use the guidescope for use as a guidescope you will need the following:

2 Guide scope tube rings

1 Guide scope tube ring mounting plate

1 Illuminated reticle eyepiece or Autoguider

1 Diagonal (optional)

First, adjust the guidescope in the guidescope tube rings so that it is as parallel with the main optical tube. This may involve some large adjustments to the guidescope alignment thumbscrews. Loosen and tighten the alignment thumbscrews as needed to adjust the direction of the guidescope.

Once you have centered the object you wish to photograph, you will need to center the guidescope on a bright star near the object being photographed. Look in the illuminated reticle eyepiece (with the reticle turned on) and select a star that is in the field of view. To center the star, loosen one guidescope alignment thumbscrew and tighten another until the star is centered in the reticle. Check again to make certain that the object you wish to photograph is still centered in its field of view. If it is not, you will have to start the process over again.

Once you begin exposure you will make any adjustments necessary so that the guide star remains centered in the reticle of the illuminated eyepiece.

Photography with the Deluxe 100mm f/6

The Deluxe 100mm f/6 refractor makes a very capable astrograph for your CCD or DSLR camera. With an optional camera adapter, the Deluxe 100mm f/6 becomes a 600mm f/6 telephoto lens for a single-lens reflex camera. For long-distance terrestrial or astronomical photography, you need a T-ring for your particular camera model and a camera adapter. A 2" prime focus camera adapter is suggested to obtain the best focal distance for this optical tube. Simply attach the T-ring to the camera body and thread the 2" prime focus camera adapter into the T-ring. Insert the barrel of the camera adapter into the 2" eyepiece holder on the focuser. Use the camera's viewfinder to frame the picture. Use the telescope's focuser to focus the image. Tighten the focus tension thumbscrew to make sure the camera does not slip out of focus.

Most CCD cameras will have a 1.25" or 2" barrel ready to attach directly to your telescope like an eyepiece or diagonal. No adapter is required, simply insert the barrel of the CCD camera into the 1.25" or 2" eyepiece holder and secure the camera with the silver thumbscrew lock.

The Deluxe 100mm f/6 Refractors were designed to reach focus with both DSLR and CCD cameras. However, every camera focus point is a little different. Depending on your camera, you may need to use an extension tube for your particular imaging setup. Any imaging accessory, such as a color filter wheel increases the amount of inward focus travel required. Before attaching any extra imaging accessory, try reaching focus first with the camera directly attached to the focuser, then see if you have enough focus travel left for extra accessories.

Imaging equipment is sometimes heavier than a diagonal and eyepiece. The dual-speed Crayford focuser is capable of handling the weight of your CCD or DSLR camera. Adding tension to the focuser drawtube will increase the amount of weight the focuser can handle. Install your camera onto the 2" or 1.25" adapter on the focuser during the day. Check the focuser for any slippage. If the focuser drawtube slides under the weight of the camera, you will need to add more tension to the focuser.

You may want to consider using a remote shutter release instead of the shutter release on the camera. Touching the camera can vibrate the system and blur the resulting photographic image. Also, be sure to use a solid tripod.

Attaching the Deluxe 100mm f/6 to a Tripod or Mount

The Deluxe 100mm f/6 can be attached to a tripod or mount by the use of the pre-installed 1/4"-20 mounting block. The 1/4"-20 shaft of a sturdy camera tripod will thread into the hole on the mounting block on the underside of the optical tube (Figure 1).

Optional tube rings can also be used to mount the 100mm f/6 to attach it to an equatorial mount. Tube rings with an inner diameter of 100mm (3.9"), such as Orion item #7371, are needed. If you are using tube rings, you should first attach them to your telescope mount or dovetail bar and then lay the optical tube in the tube rings. You will need to extend the dew shield in order to accommodate tube rings on each side of the ¼"-20 mounting block.

Calculating Magnification (Power)

It is desirable to have a range of eyepieces of different focal lengths, to allow viewing over a range of magnifications. To calculate the magnification, or power, of a telescope, simply

divide the focal length of the telescope by the focal length of the eyepiece:

$$\frac{\textbf{Telescope Focal Length (mm)}}{\textbf{Eyepiece Focal Length (mm)}} = \textbf{Magnification}$$

For example, the 100mm, which has a focal length of 600mm, used in combination with a 25mm eyepiece, yields a power of:

$$\frac{\textbf{600mm}}{\textbf{25mm}} = \textbf{24x}$$

Every telescope has a useful limit of power of about 50x per inch of aperture. Claims of higher power by some telescope manufacturers are a misleading advertising gimmick and should be dismissed. Keep in mind that at higher powers, an image will always be dimmer and less sharp (this is a fundamental law of optics). The steadiness of the air (the "seeing") will limit how much magnification an image can tolerate.

Always start viewing with your lowest-power (longest focal length) eyepiece in the telescope. After you have located and looked at the object with it, you can try switching to a higher-power eyepiece to ferret out more detail, if atmospheric conditions permit. If the image you see is not crisp and steady, reduce the magnification by switching to a longer-focal-length eyepiece. As a general rule, a small but well-resolved image will show more detail and provide a more enjoyable view than a dim and fuzzy, overmagnified image.

Care & Maintenance

Give your telescope reasonable care and it will last a lifetime. When not in use, keep its dust cover on as well as the dust cap on the eyepiece opening. Store it indoors or in a dry garage. Do not leave the telescope outside except when using it. The optical tube is aluminum and has a smooth painted surface that should resist scratches and smudges. If a scratch does appear on the tube, it will not harm the telescope. Smudges on the tube can be wiped off with standard household cleaners such as Windex or Formula 409.

Any quality optical lens tissue and cleaning fluid specifically designed for multi-coated optics can be used to clean the telescope's objective lens as well as the lenses of the eyepieces and finder scope. Never use regular glass cleaner or cleaning fluid designed for eyeglasses. Before cleaning with fluid and tissue, however, blow any loose particles off the lens with a blower bulb or compressed air, or lightly brush the lens with a soft camel hair brush. Apply some cleaning fluid to a tissue, never directly on the optics. Wipe the lens gently in a circular motion, then remove any excess fluid with a fresh lens tissue. Oily fingerprints and smudges may be removed using this method. Use caution; rubbing too hard may scratch the lens! Clean only a small area at a time, using a fresh lens tissue on each area. Never reuse tissues.

Specifications

Objective lens:	Achromatic doublet, air-spaced
Objective lens diameter:	100mm
Objective lens coatings:	All air-to-glass surfaces coated, with at least one surface multi-coated
Focal length:	600mm
Focal ratio:	f/6
Baffling:	Two in optical tube, two in focuser drawtube
Focuser:	2" dual-speed linear bearing Crayford (with 1.25" adapter)
Tube diameter (not including dew shield):	100mm
Tube length (with dew shield):	20.6"
Weight:	7.1 lbs.

One-Year Limited Warranty

The Orion Deluxe 100mm f/6 Refractoris warranted against defects in materials or workmanship for a period of one year from the date of purchase. This warranty is for the benefit of the original retail purchaser only. During this warranty period Orion Telescopes & Binoculars will repair or replace, at Orion's option, any warranted instrument that proves to be defective, provided it is returned postage paid to: Orion Warranty Repair, 89 Hangar Way, Watsonville, CA 95076. Proof of purchase (such as a copy of the original receipt) is required.

This warranty does not apply if, in Orion's judgment, the instrument has been abused, mishandled, or modified, nor does it apply to normal wear and tear. This warranty gives you specific legal rights, and you may also have other rights, which vary from state to state. For further warranty service information, contact: Orion Customer Service (800) 676-1343; support@telescope.com.

Orion Telescopes & Binoculars
OrionTelescopes.com
89 Hangar Way, Watsonville CA 95076
Customer Support Help Line (800) 676-1343 • Day or Evening

© 2008-2010 Orion Telescopes & Binoculars

Appendix C

WesTEP Data Reduction & Analysis

Here I present the current step-by-step procedure to reduce and analyze VVO data for WesTEP. The original procedure for use with WesTEP data was written by Marshall Johnson in 2011 which itself was based in part on a more general procedure by Sam Lawler in 2008. This is a second edition of the original WesTEP procedure. Aside from fixing a few typos and directory paths, the following major material has been added: in Section 3 the examples of what an 'ok' image is; in Section 4 the addition of the Digitized Sky Survey & Exoplanet Transit Database URLs for help with the target star starfield; in Section 4 the ability to automatically exclude images where the target star has saturated, zero or negative scale values using centfwhm.pro and doaper.pro; in Section 5 the addition of limb-darkening parameters for WASP-48 in Table 1; in Section 6 the list of .pro files, sans ominusc.pro, that need to be copied to your data directory; in Section 7 the option to list the name of all images to a file and then scroll through them in ds9 using `imexamine @file`.

How to Reduce and Analyze VVO Data for WesTEP: 2nd Edition

Jakob Schaeffer - May 10, 2012

First Edition by: Marshall C. Johnson - May 1, 2011

Based in part upon "How to reduce VVO data," by Sam Lawler, June 2008

C.1 Introduction

This document is a step-by-step guide for how to reduce and analyze photometric transit observations from the 24-in Perkin Telescope at Van Vleck Observatory. Details on the science can be found in the senior honors theses of Emily Leiner (2010) and Marshall Johnson (2011) as well as the masters thesis of Jakob Schaeffer (2012).

Throughout this document commands that should be issued on the command line are denoted in `typewriter font` . X11 command lines are denoted thus:

```
>command
```

IRAF commands thus:

```
ecl> command
```

Note that for the IRAF command line, the ecl will be replaced with the name of whatever package you have loaded. Finally, the IDL commands are denoted thus:

```
IDL> command
```

C.2 Downloading the Data

1. First you need to create a file to hold your data for the reduction and analysis process. My naming protocol is the name of the planet followed by the month and day of the transit, e.g., hatp14-0701 for the HAT-P-14b

transit of July 1 (2010), but you can use whatever naming convention you want (though it's good to be consistent).

```
>mkdir hatp14-0701
```

2. Change directories to the directory where the data is stored:

   ```
   >cd /Volumes/star/24InchData/iraf
   ```

   List the files in this folder

   ```
   >ls
   ```

   And located the folder with your data. Each night of observations is in its own folder, in the format nYYMMDD, where YY is the last two digits of the year, MM is the month, and DD is the day. For instance, data taken on January 1, 2011 would be in the folder n110101.

3. Now you need to download the data. `ls` again to display the files in the folder. The images of the target should have names like objtarget-001I.fit, where target is the name of the target, e.g., objhatp14-001I.fit. Download these with a command like

   ```
   >cp obj* ~/astro/transits/hatp14-0701/
   ```

   where the path is to whatever folder you created to hold the data. Now you need to download the flats and bias to the same folder:

   ```
   >cp flatI* ~/astro/transits/hatp14-0701/

   >cp *Dark* ~/astro/transits/hatp14-0701/

   >cp *Bias* ~/astro/transits/hatp14-0701/
   ```

   Never modify the files in the raw data directory, or use the move (mv) command!

Note: if the observers weren't paying attention it's possible that the target data do not have the proper obj* name format. If this is the case the files will have to be renamed in order for the reduction script to run. See the last section of this document for instructions on how to do this.

C.3 Reducing the Data

1. Open an xgterm window:

   ```
   >xgterm -sb &
   ```

   In the xgterm, `cd` to your IRAF directory. For me this would be

   ```
   >cd ~/iraf/
   ```

   If you don't know where your IRAF directory is, you may not have it set up. See Roy.

2. Start IRAF

   ```
   >cl
   ```

   This will cause IRAF to run in the xgterm.

3. Open the IRAF packages you will need

   ```
   ecl> noao
   ecl> imred
   ecl> ccdred
   ```

4. `cd` in the xgterm to the folder with your data. For me this would look like

   ```
   ecl> ../astro/transits/hatp14-0701/
   ```

5. Reduce the data. To run the reduction script type

   ```
   ecl> reduceI
   ```

   In order for this to run correctly the reduceI script needs to be referenced in your IRAF login.cl file. See the end of this document for instructions on how to do this.

   reduceI can take a while to run. Sit back and/or do something else for a while.

6. When reduceI has completed, you should inspect some of the images by hand to make sure that they look OK. First, open ds9 to view the images.

   ```
   ecl> !ds9&
   ```

   Now display one of the images.

   ```
   ecl> disp objhatp14-001I 1
   ```

   Do this for a selection of the images. (An alternative method of viewing images in ds9 is discussed in Section 7). If everything looks OK (e.g. no structure or noise in background, no streaks, no clouds), it's time to analyze the data in IDL. If for some reason you need to run the reduction process again, you will need to delete all of the .fits files and download the files again from scratch, as reduceI will refuse to overwrite the combined dark, flat, and bias frames. Alternately, you could rewrite reduceI so this isn't a problem.

C.4 Creating a Normalized Lightcurve

1. You will first seed to download a number of photometry routines. In an X11 terminal (not the xgterm),

```
>cd /Volumes/Groups/westep/transit_programs/reduction_programs
```

Copy apertest.pro, centdiag.pro, centfwhm.pro, and doaper.pro to the folder with your data, e.g.,

```
>cp apertest.pro ~/astro/transits/hatp14-0701/
```

2. `cd` back to the folder with your data and start IDL.

   ```
   >idl
   ```

3. Open another X11 window and `cd` to the folder with your data.

4. In ds9, display the first image of the target.

   ```
   ecl> disp objhatp14-001I 1
   ```

   You will need to find the coordinates of the target star for input into the IDL routines. Type

   ```
   ecl> imexam
   ```

   Hit enter twice. A blinking cursor will appear over the ds9 window. Click on the window, position the cursor over the target star (check a finder chart if you're not sure which one is the target. Some nice online options are the Exoplanet Transit Database (ETD): `http://var2.astro.cz/ETD/` and the Digitized Sky Survey (DSS): `http://archive.stsci.edu/cgi-bin/dss_form/`), and hit the 'r' key. This will open a window showing the radial profile of the star. Now hit the 'q' key. The coordinates of the star are listed at the top of the plot window: "Radial profile at (x position) (y position)".

5. Enter the coordinates of the corners of the search box around the target star in centfwhm.pro. Open this file.

```
>emacs centfwhm.pro &
```

You will see a number of sets of lines of the following format:

```
startx=number
endx=number
starty=number
endy=number
savefile='string.var'
```

Make sure that all of these sets of lines are commented out (with a ; [semicolon] at the start of each line) except for the one that ends in `'target'var'` ; these lines should be uncommented. Look at the position of the target star found by ds9. For startx and endx, enter the x position ± 50, and similarly for the y position.

6. Near the start of centfwhm.pro, you will see two lines labeled ra and dec. Enter the coordinates of your target star, the RA in h, m, s, the Dec in deg, m, s. This is important; if this position is incorrect your transit times will be incorrect!

7. Now to allow for centfwhm.pro to tag images to later be excluded where the target star has saturated (>57,000[1]), zero or negative scale values, scroll down near the bottom of centfwhm.pro. For the target star uncomment the following line:

   ```
   good=WHERE(scale gt 0.  and scale lt 57000.)
   ```

   in addition, a few lines below that, uncomment "good" in the line

   ```
   save,file=savename, index, fwhmx, [...]  , dec,nfiles,good
   ```

[1]This number was chosen because it was the last point of linearity for the 24" Perkin Telescope's CCD as per Konon (2008), Figure 4.19.

For comparison stars leave these commented out. This will tag only those images where the target star has a saturated, zero or negative scale value. The actual exclusion is done near the end of the doaper.pro code.

8. For both the target star and comparison stars, if saturated, zero or negative scale value images are detected a warning will be printed in your IDL terminal after centfwhm.pro has finished running specifying whether saturated images or zero/negative images were found. Regardless of whether saturated, zero or negative scale values were detected a simple statement that the centfwhm has checked for them will be printed in your IDL terminal after centfwhm.pro has finished running.

9. Save centfwhm.pro.

10. In your IDL window, run centfwhm.pro.

```
IDL> .r centfwhm

IDL> centfwhm
```

The program will prompt you for the number of images and the name of the target star. Print the name of the target star with capitalization exactly as it appears in the filename. This again requires that the filenames be in the format obj*.fit. If for some reason there is a gap in the numbering of images, you will need to either rename the images to eliminate this gap or modify the program to ignore the missing numbers(s).

What centfwhm does is to fit a two-dimensional Gaussian function to the image in the search box that you defined. This finds the centroid of the target's point spread function (PSF), which is necessary for the aperture photometry process.

11. Open centdiag.pro:

    ```
    >emacs centdiag.pro &
    ```

    Change the name of the target and the date of the transit in the third line of the program to match your transit (this is not strictly necessary). If you wish you can also change the HJD offsets for a number of the plots that this program will create, by changing the number in the lines that look like: `'!6HJD - 2454747'`. Again, this is not strictly necessary.

12. Run centidag.pro:

    ```
    IDL> .r centdiag

    IDL> centdiag
    ```

    This can take a while to run.

13. centdiag.pro creates a number of diagnostic plots. Open the postscript file that this program creates (centdiag.ps). The most important plots for the moment are the first two. These show the position of the target star centroid for each image. If it looks like the star might be straying outside your ±50 pixel search box, re-run centfwhm.pro with a larger search box.

14. Now you need to run centfwhm.pro again for each comparison star. In ds9, `imexam` another bright star in the image. In centfwhm.pro, comment out the lines for target.var and uncomment the lines for comp1.var. Enter the coordinates of a search box around this star, and run centfwhm.pro. Repeat until you reach five (or more) comparison stars, or run out of sufficiently bright stars.

15. Set up the code to do the aperture photometry. Open the code:

```
>emacs doaper.pro &
```

On the second and third line, enter the number of files and the total number of stars. If you have N comparison stars, enter the number $N + 1$ here. A few lines down enter a filename for the output file, e.g., doaperhatp14.var. You will see a number of sets of lines of the format:

```
restore,'string.var'
centerx[number,*]=cntrx+startx
centery[number,*]=cntry+starty
```

Uncomment the sets of lines corresponding to the comparison stars that you have. For instance, if you have three comparison stars, you would uncomment the comp1.var, comp2.var, and comp3.var sets, and leave the comp4.var and comp5.var sets commented out.

16. Determine if there are any images that should be excluded from the dataset for any reason, e.g., clouds, movement during the exposure, etc. Scroll down. You will see a line that looks like

    ```
    if (i le 702 or i eq 706) then begin
    ```

    Change the if statement to exclude the images that should be excluded. For instance, the statement above excludes images with numbers greater than 703, except for image 707. Remember that the array indices start from zero, so subtract one from the image number to obtain its number in the array.

    Just below this enter the name of your target in the three lines with filenames.

    Scroll down farther; you will see an identical if statement, except using j

instead of i. Change this to match the if statement above.

17. Save the file, and run doaper.pro:

    ```
    IDL> .r doaper

    IDL> doaper
    ```

    This too can take a while to run.

18. Set up the program to create a normalized lightcurve, apertest.pro. Open this file.

    ```
    >emacs apertest.pro &
    ```

    On the second line enter the name of the file that you told doaper.pro to write its output to, e.g., doaperhatp14.var. Scroll down to the lines that read:

    ```
    c1=number

    c4=number

    tc=number
    ```

    Here enter the heliocentric Julian date (HJD) for the start, end, and center of the transit, respectively, as determined by the transit prediction routine. To find these numbers, `cd` to the folder where you have the transit prediction routine. Open up the file named transittimes_name.txt, where name is the name of your target, e.g., transittimes_HAT-P14.txt. You will see three sets of columns, listing the HJD, year, month, day, hour, and minute for the start, center, and end of the transit, respectively. Scroll down and locate your transit. In apertest.pro, enter the HJD for c1, c4, and tc, leaving off the first two digits, e.g., 55596.51.

Now scroll down to the plot statement partway through the program, and where it says `xtitle='!6HJD - 2455535'`, change the number to the integer of the transit date, e.g., 2455596. Also change the same number in the next two lines.

At the very bottom, also change the integer in the printf statement to this, e.g., `hjd[i]-55596` . Again, this is not strictly necessary. A few lines above this, change the output file name to reflect the name of the system, e.g., hatp14.ascii.

If you wish to produce a lightcurve for use with the Transit Analysis Package or Exoplanet Transit Database routines, see the end of this document.

19. Run apertest.

```
IDL> .r apertest

IDL> apertest
```

20. Look at the resulting lightcurve (apertest.ps). If it looks good, proceed to the next section. If not, there are a few things you can try:

    - Try removing one or more of the comparison stars.
    - Try seeing if there are bad images and removing these.

C.5 Analyzing the Lightcurve

1. Download the reduction programs:

```
>cd /Volumes/Groups/westep/transit_programs/fitting-programs
```

Table C.1. Limb-darkening parameters for observed systems

Target	u1	u2
CoRoT-Exo-2	0.366	0.244
HAT-P-11	0.455	0.171
HAT-P-14	0.1089	0.2439
HAT-P-16	0.233	0.292
HAT-P-23	0.2524	0.3426
HD 189733	0.29	0.3
Kepler-5	0.224	0.299
WASP-2	0.29	0.32
WASP-3	0.198	0.309
WASP-33	0.140	0.320
WASP-48	0.254	0.287

Copy ellipticintegrals.pro, error_fixed_limb.pro, and fixed_limb.pro to your data folder.

2. Open fixed_limb.pro:

```
>emacs fixed_limb.pro &
```

3. Scroll down to where values can be entered for the limb-darkening parameters `u1` and `u2` (about 60 lines in to the file). If you have not observed the system before, go to the CDS website for the limb-darkening parameters from Claret, Diaz-Cordoves & Gimenez 1995, A&AS, 114, 247 (http://vizier.cfa.harvard.edu/viz-bin/VizieR?-source=J/A+AS/114/247). Search the quadratic table for the combination of effective temperature and surface gravity closest to those for your target from the literature, and enter those.

   The values that I have used for my targets are shown in Table C.1.

4. Before running fixed_limb.pro, you need to compile ellipticintegrals.pro:

   ```
   IDL> .r ellipticintegrals
   ```

5. Now run fixed_limb.pro.

   ```
   IDL> .r fixed_limb
   ```

   ```
   IDL> fixed_limb
   ```

   The program will prompt you to enter:

   - The input filename. Enter the file that you told apertest.pro to use as an output (e.g., hatp14.ascii).
   - The output filename for a plot with the output lightcurve. I usually use a filename like hatp14.ps.
   - The output filename for a text file which will contain the parameters of the fit. I usually use a filename like hatp14.txt
   - The semimajor axis of the planet from the literature, in AU.
   - The period of the planet from the literature, in days.

   This program will fit the lightcurve with the analytic expressions of Mandel & Agol, 2002, ApJ, 580, L171. It will also plot the fit lightcurve to the screen.

6. You can now obtain errors on the fit parameters. Compile and run error_fixed_limb.pro:

   ```
   IDL> .r error_fixed_limb
   ```

   ```
   IDL> error_fixed_limb
   ```

The program will prompt you for which parameter you want the error on: planetary radius (rp), stellar radius (rs), inclination (incl), or the transit centroid (t1). t2, t3, &c. are the transit centroids for additional transits if you are fitting more than one transit; ignore these for now.

7. Congratulations! You have now produced a normalized, fitted lightcurve from VVO data!

   Note: fixed_limb also creates a file called residuals.sav, which is an IDL save file containing the data, lightcurve fit, and residuals to the fit.

8. You may need to tweak the numbers in the plot statement near the end of fixed_limb.pro in order to get the plot of the residuals to appear in an appropriate location.

C.5.1 Fitting Multiple Transits

fixed_limb.pro can fit up to six transits at once (at this time error_fixed_limb.pro can only handle four transits, but should be able to be modified to work with more).

In order to fit multiple transits, open the output files from apertest.pro for each transit. Copy the contents of each file one after the other into a new text file and save it. Run fixed_limb.pro as above and enter your new file as the input data file name.

Note that fixed_limb.pro will run significantly more slowly with multiple transits.

C.6 Creating an $O - C$ Diagram

1. Now that you have the centroid for your transit, you can create an $O - C$ diagram to look for transit timing variations.

2. Copy ominusc.pro[2] from /Volumes/Groups/westep/transit_programs/analysis_programs to your data directory.

3. Now you need a data file for the transit centroid information. Data files for many of the observed systems are available in the above-mentioned directory. If one of these is for your system, copy it to your data directory. If not, you will need to create a new file in your data directory. Create it using emacs; I usually use a filename like

   ```
   >emacs hatp14times.txt &
   ```

4. Now fill out the data in the file. It should have five columns: transit time (include the full Julian date, e.g. 24555416.72777), the time standard (either HJD or BJD), the error on the transit time in the minus and plus directions, and the reference for the data (enter VVO if it is your own data). Enter your data; VVO data are in HJD.

5. A listing of the literature data on transits can be found at the Exoplanet Transit Database (ETD; http://var2.astro.cz/ETD/index.php). Select your planet from the list on the left-hand side of the page. When the page for this planet loads, scroll down to bottom of the page, where there is a list of observed transits. Follow the links to the papers for the literature

[2] You may also need to copy jdutc2jdtbd.pro, utc2bjd.pro, hjd2bjd.pro and tai_utc.pro.

transits, and enter these into your transit data file. It is critical to pay attention to whether these times are in HJD or BJD! Even if you are using a data file for a system that has already been observed, it is a good idea to check to see if any new transits have been published since the file was last updated.

6. Open ominusc.pro:

   `>emacs ominusc.pro &`

7. You now need to enter a number of values for your planet near the start of the program:

   - The coordinates of the system in the lines labeled `ra` and `dec` .
   - The name of your transit data file on the line starting `namein` .
   - The zero-time for the planetary ephemeris on the line labeled `tco` .
   - If this zero-time is in HJD, uncomment the line reading `tco=hjd2bjd(tco,ra,dec)` .
   - Enter the error on the zero time on the line starting `tcoerr` .
   - Enter the period of the planet, in days, on the line starting `P` .
   - Enter the error on the period of the planet, in days, on the line starting `Perr` .

8. Scroll down to the plot statement about halfway through the program. A few lines above this, change the output plot filename to whatever you want the plot to be called.

9. In the plot statement itself, change the `xrange` to a value that will cover all of your data.

10. Save the file, and run ominusc.pro:

```
IDL> .r ominusc

IDL> ominusc
```

11. Look at the plot that this has produced. If it looks wrong (e.g., all of the points lie far from the $O - C = 0$ line, check to make sure that you have entered which transits are in HJD and which are in BJD correctly, etc.

C.7 How to Do Other Things

C.7.1 Data Formatted for TAP and ETD

1. If you want to create a data file formatted for the Transit Analysis Package (TAP; Gazak et al. 2011, arXiv:1102.1036) or the Exoplanet Transit Database (ETD; http://var2.astro.cz/ETD/protocol.php), open apertest.pro:

```
>emacs apertest.pro &
```

2. Scroll down to the end of the file. In the if statement within the final for loop, comment out the last print statement with a ; and uncomment all of the other lines in within the if statement.

3. Just before the for loop, select a new name for the output file, e.g., hatp14etd.ascii.

4. In IDL, run apertest.pro:

```
IDL> .r apertest

IDL> apertest
```

5. Follow the instructions for either TAP or ETD to load and fit the data.

C.7.2 Renaming Many Files

If the observers failed to name the .fits files with the proper format, the files will have to be renamed in order for reduceI and the analysis packages to recognize them. If the files are simply missing the prefix obj, use the following procedure on the command line:

1. Make a list of all of the files:

   ```
   >ls starname*.fit > junk
   ```

   where starname is the that the files currently have, e.g., hatp14.

2. Now use the awk command to create a script to rename the files, adding "obj" to the start of each name:

   ```
   >awk '{print "mv " $1 " obj"$1}' junk > junk2
   ```

3. Now run the script:

   ```
   >source junk2
   ```

If there is a different problem with the formatting of the filenames, you should be able to modify the above procedure to deal with it.

C.7.3 Installing the reduceI script

1. Download the reduceI script to your IRAF directory, or another directory of your choice::

   ```
   >cd /Volumes/Groups/westep/transit_programs/reduction_programs
   ```

```
>cp reduceI.cl ~/iraf/
```

For example, for my IRAF directory.

2. `cd` to your IRAF directory.

```
>cd ~/iraf/
```

3. Open the login.cl file in your IRAF directory:

```
>emacs login.cl &
```

4. Scroll down to the bottom of file, and before the last line ('keep') but after everything else add the following line, substituting the full file path for your reduceI script for mine:

```
task reduceI=/Network/Servers/vvofiles.astro.wesleyan.edu
/Volumes/e/Home/mcjohnson/iraf/reduceI.cl
```

5. Save and exit login.cl. Start IRAF and load the necessary packages, and reduceI should work.

C.7.4 Viewing consecutive images in ds9

1. `cd` to the directory where the images you wish to view are located

2. List the names of all the image files ('FILES') to a file ('file')

```
>ls FILES > file
```

For example, to list the names of all the files beginning with 'obj' into a file called '_LIST' type:

```
>ls obj* > _LIST
```

3. `cd` into your IRAF directory & start IRAF in an xgterm (see Section 3 for details)

4. Then `cd` into the directory with your image files and open ds9:

   ```
   ecl> !ds9 &
   ```

5. Now open the first item in the list of images names in ds9

   ```
   ecl> imexamine @_LIST
   ```

6. While the cursor is over the image window in ds9 press "n" to go to the next image in the list and "p" to go to the previous one. With this you can also do successive uses of 'imexamine' (the use of 'imexamine' is explained more in Section 4).

Bibliography

Agol, E., Steffen, J., Sari, R., & Clarkson, W. 2005, *MNRAS*, 359, 567

Allen, C. W. 1973, Astrophysical Quantities

Andersen, G. 2006, The Telescope: Its History, Technology, and Future (Princeton University Press)

Ballard, S., Fabrycky, D., Fressin, F., Charbonneau, D., Desert, J.-M., Torres, G., Marcy, G., Burke, C. J., Isaacson, H., Henze, C., Steffen, J. H., Ciardi, D. R., Howell, S. B., Cochran, W. D., Endl, M., Bryson, S. T., Rowe, J. F., Holman, M. J., Lissauer, J. J., Jenkins, J. M., Still, M., Ford, E. B., Christiansen, J. L., Middour, C. K., Haas, M. R., Li, J., Hall, J. R., McCauliff, S., Batalha, N. M., Koch, D. G., & Borucki, W. J. 2011, *ApJ*, 743, 200

Birney, D.S., Gonzalez, G., and Oesper, D. 2006, Observational Astronomy, 2nd edn. (Cambridge University Press)

Carroll, B. W., & Ostlie, D. A. 2006, An Introduction to Modern Astrophysics

Charbonneau, D., Brown, T. M., Latham, D. W., & Mayor, M. 2000, *ApJL*, 529, L45

Charbonneau, D., Brown, T. M., Noyes, R. W., & Gilliland, R. L. 2002, *ApJ*, 568, 377

Chromey, F. R. 2010, To Measure the Sky

Collier Cameron, A., Guenther, E., Smalley, B., McDonald, I., Hebb, L., Andersen, J., Augusteijn, T., Barros, S. C. C., Brown, D. J. A., Cochran, W. D., Endl, M., Fossey, S. J., Hartmann, M., Maxted, P. F. L., Pollacco, D., Skillen, I., Telting, J., Waldmann, I. P., & West, R. G. 2010, *MNRAS*, 407, 507

Damiani, C., & Lanza, A. F. 2011, *A&A*, 535, A116

DeVorkin, D., ed. 2002, Beyond Earth: Mapping the Universe (Smithsonian Institution)

Fahy, T. P. 1987, Richard Scott Perkin and The Perkin-Elmer Corporation (Perkin-Elmer Print Shop)

Ford, E. B., Rowe, J. F., Fabrycky, D. C., Carter, J. A., Holman, M. J., Lissauer, J. J., Ragozzine, D., Steffen, J. H., Batalha, N. M., Borucki, W. J., Bryson, S., Caldwell, D. A., Dunham, E. W., Gautier, III, T. N., Jenkins, J. M., Koch, D. G., Li, J., Lucas, P., Marcy, G. W., McCauliff, S., Mullally, F. R., Quintana, E., Still, M., Tenenbaum, P., Thompson, S. E., & Twicken, J. D. 2011, *ApJS*, 197, 2

Freeman, S. 2005, Biological Science (Pearson Prentice Hall)

Fukui, A., Narita, N., Tristram, P. J., Sumi, T., Abe, F., Itow, Y., Sullivan, D. J., Bond, I. A., Hirano, T., Tamura, M., Bennett, D. P., Furusawa, K., Hayashi, F., Hearnshaw, J. B., Hosaka, S., Kamiya, K., Kobara, S., Korpela, A., Kilmartin, P. M., Lin, W., Ling, C. H., Makita, S., Masuda, K., Matsubara, Y., Miyake, N., Muraki, Y., Nagaya, M., Nishimoto, K., Ohnishi, K., Omori, K., Perrott, Y., Rattenbury, N., Saito, T., Skuljan, L., Suzuki, D., Sweatman, W. L., & Wada, K. 2011, *PASJ*, 63, 287

Gaudi, B. S., & Winn, J. N. 2007, *ApJ*, 655, 550

Hecht, E. 2001, Optics 4th edition

Herrero, E., Morales, J. C., Ribas, I., & Naves, R. 2011, *A&A*, 526, L10

Holman, M. J., Fabrycky, D. C., Ragozzine, D., Ford, E. B., Steffen, J. H., Welsh, W. F., Lissauer, J. J., Latham, D. W., Marcy, G. W., Walkowicz, L. M., Batalha, N. M., Jenkins, J. M., Rowe, J. F., Cochran, W. D., Fressin, F., Torres, G., Buchhave, L. A., Sasselov, D. D., Borucki, W. J., Koch, D. G., Basri, G., Brown, T. M., Caldwell, D. A., Charbonneau, D., Dunham, E. W., Gautier, T. N., Geary, J. C., Gilliland, R. L., Haas, M. R., Howell, S. B., Ciardi, D. R., Endl, M., Fischer, D., Fürész, G., Hartman, J. D., Isaacson, H., Johnson, J. A., MacQueen, P. J., Moorhead, A. V., Morehead, R. C., & Orosz, J. A. 2010, Science, 330, 51

Holman, M. J., & Murray, N. W. 2005, Science, 307, 1288

Horne, J. H., & Baliunas, S. L. 1986, *ApJ*, 302, 757

Johnson, M. 2011, Wesleyan Honors Thesis

Kalas, P., Graham, J. R., Chiang, E., Fitzgerald, M. P., Clampin, M., Kite, E. S., Stapelfeldt, K., Marois, C., & Krist, J. 2008, Science, 322, 1345

Kipping, D. M. 2009, *MNRAS*, 392, 181

Koch, D. G., Borucki, W. J., Basri, G., Batalha, N. M., Brown, T. M., Caldwell, D., Christensen-Dalsgaard, J., Cochran, W. D., DeVore, E., Dunham, E. W., Gautier, III, T. N., Geary, J. C., Gilliland, R. L., Gould, A., Jenkins, J., Kondo, Y., Latham, D. W., Lissauer, J. J., Marcy, G., Monet, D., Sasselov,

D., Boss, A., Brownlee, D., Caldwell, J., Dupree, A. K., Howell, S. B., Kjeldsen, H., Meibom, S., Morrison, D., Owen, T., Reitsema, H., Tarter, J., Bryson, S. T., Dotson, J. L., Gazis, P., Haas, M. R., Kolodziejczak, J., Rowe, J. F., Van Cleve, J. E., Allen, C., Chandrasekaran, H., Clarke, B. D., Li, J., Quintana, E. V., Tenenbaum, P., Twicken, J. D., & Wu, H. 2010, *ApJL*, 713, L79

Konon, J. 2008, Wesleyan Masters Thesis

Leiner, E. 2010, Wesleyan Honors Thesis

Levy, D. H., & O'Byrne, J., eds. 2002, Practical Skywatching (Fog City Press)

Lissauer, J. J., Fabrycky, D. C., Ford, E. B., Borucki, W. J., Fressin, F., Marcy, G. W., Orosz, J. A., Rowe, J. F., Torres, G., Welsh, W. F., Batalha, N. M., Bryson, S. T., Buchhave, L. A., Caldwell, D. A., Carter, J. A., Charbonneau, D., Christiansen, J. L., Cochran, W. D., Desert, J.-M., Dunham, E. W., Fanelli, M. N., Fortney, J. J., Gautier, III, T. N., Geary, J. C., Gilliland, R. L., Haas, M. R., Hall, J. R., Holman, M. J., Koch, D. G., Latham, D. W., Lopez, E., McCauliff, S., Miller, N., Morehead, R. C., Quintana, E. V., Ragozzine, D., Sasselov, D., Short, D. R., & Steffen, J. H. 2011, *Nature*, 470, 53

Maciejewski, G., Dimitrov, D., Neuhäuser, R., Niedzielski, A., Raetz, S., Ginski, C., Adam, C., Marka, C., Moualla, M., & Mugrauer, M. 2010, *MNRAS*, 407, 2625

Maciejewski, G., Dimitrov, D., Neuhäuser, R., Tetzlaff, N., Niedzielski, A., Raetz, S., Chen, W. P., Walter, F., Marka, C., Baar, S., Krejcová, T., Budaj, J., Krushevska, V., Tachihara, K., Takahashi, H., & Mugrauer, M. 2011, *MNRAS*, 411, 1204

Mandel, K., & Agol, E. 2002, *ApJL*, 580, L171

Marois, C., Macintosh, B., Barman, T., Zuckerman, B., Song, I., Patience, J., Lafrenière, D., & Doyon, R. 2008, Science, 322, 1348

Mayor, M., & Queloz, D. 1995, *Nature*, 378, 355

Pont, F., Gilliland, R. L., Moutou, C., Charbonneau, D., Bouchy, F., Brown, T. M., Mayor, M., Queloz, D., Santos, N., & Udry, S. 2007, *A&A*, 476, 1347

Redfield, S., Endl, M., Cochran, W. D., & Koesterke, L. 2008, *ApJL*, 673, L87

Richmond, M. 1990, in Proc. Electronics Oriented Astronomy Seminar 3, ed. J. Sanford (Costa Mesa: OCA Publications), 68

Scargle, J. D. 1982, *ApJ*, 263, 835

Schneider, J., Dedieu, C., Le Sidaner, P., Savalle, R., & Zolotukhin, I. 2011, *A&A*, 532, A79

Seager, S. 2011, Exoplanets

Smith, A. M. S., Anderson, D. R., Skillen, I., Collier Cameron, A., & Smalley, B. 2011, *MNRAS*, 416, 2096

Smith, G. E. 2011, Journal of Applied Physics, 109, 102421

Struve, O. 1952, The Observatory, 72, 199

Szabó, G. M., Pál, A., Derekas, A., Simon, A. E., Szalai, T., & Kiss, L. L. 2012, *MNRAS*, 421, L122

Taylor, J. R. 1997, Introduction to Error Analysis, 2nd Ed. (cloth) (University Science Books)

Werner, M. W., Roellig, T. L., Low, F. J., Rieke, G. H., Rieke, M., Hoffmann, W. F., Young, E., Houck, J. R., Brandl, B., Fazio, G. G., Hora, J. L., Gehrz, R. D., Helou, G., Soifer, B. T., Stauffer, J., Keene, J., Eisenhardt, P., Gallagher, D., Gautier, T. N., Irace, W., Lawrence, C. R., Simmons, L., Van Cleve, J. E., Jura, M., Wright, E. L., & Cruikshank, D. P. 2004, *ApJS*, 154, 1

Wolszczan, A., & Frail, D. A. 1992, *Nature*, 355, 145